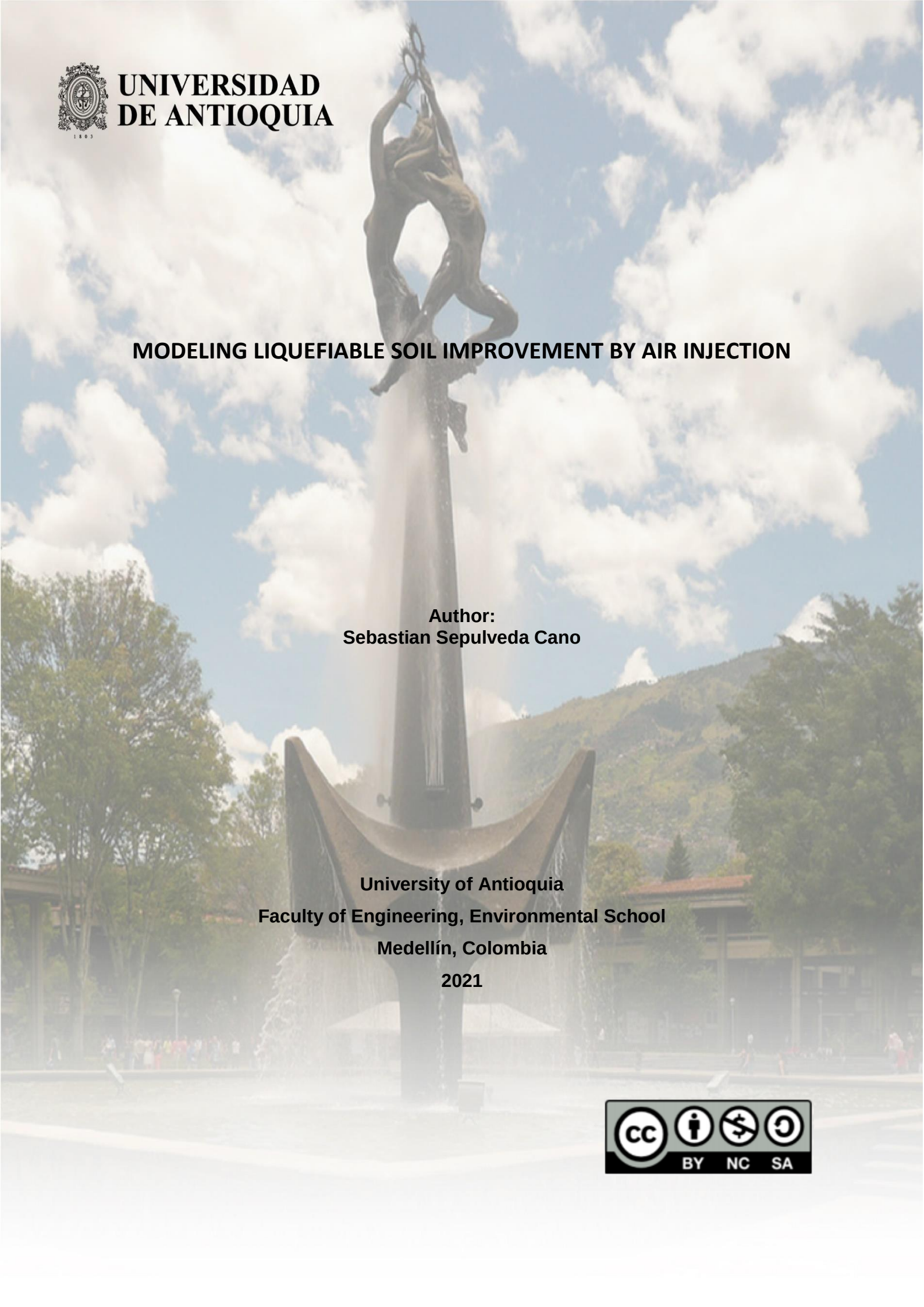

UNIVERSIDAD DE ANTIOQUIA

MODELING LIQUEFIABLE SOIL IMPROVEMENT BY AIR INJECTION

Author:
Sebastian Sepulveda Cano

University of Antioquia
Faculty of Engineering, Environmental School
Medellín, Colombia

2021

MODELING LIQUEFIABLE SOIL IMPROVEMENT BY AIR INJECTION

Sebastian Sepulveda Cano

A Dissertation Presented To The Department of Civil Engineering at the Environmental School in partial fulfillment of the requirements for the degree of
Master in Engineering

Advisors:
Carlos Alberto Vega Posada. Civil engineer. PhD
Edwin Fabian Garcia Aristizabal. Civil engineer. PhD

in the field of:
Geotechnical Engineering
Research Group:
Infrastructure Research Group (GII)

University of Antioquia
Faculty of Engineering, Environmental School
Medellin, Colombia
2021

ACKNOWLEDGMENTS

Without the help and encouragement of the people included on this page, I would not have been able to develop this work. Their support came at different stages of the past years, in many different ways, and directly and indirectly. It is with my deepest gratitude that I write these comments.

I want to express my gratitude to the University of Antioquia, for allowing me to perform my master's degree in Engineering. I am indebted with the University of Antioquia. I appreciate with all my heart for giving me the opportunity to be a professor and enjoy it every minute. I can say that it is one of the most beautiful experience I have ever lived.

My honest and humble gratitude goes to my advisors Professor Carlos Vega and Professor Edwin Garcia for their direction, assistance and supervision in all aspects throughout of this research work. Their vast knowledge and capacities have been a source of inspiration to me.

My colleagues have been an indispensable part during the past years. This page is now being written because they were here with me every day, providing confidence and encouragement during the hardest of times. It is difficult to mention all of them, my sincere and deepest gratitude goes to the following people: Eisinhower Rincon, Yurany Gomez, Diego Valle, Laura Ortiz, Julian Galvez, Valentina Rivera, Oscar Rios, Juan Castro, Manuel Perez, Edisson Castaño, Monica Oquendo, Gustavo Diosa, Carolina Valencia, Juan Montealegre, Estefania Restrepo, and Andres Gonzalez.

I want to express my heartfelt gratitude and respect to my friends Edwar Macias, Leidy Montoya, Kevin Perez, and Manuel Guzman, for sharing with me the years of experience in engineering research they have. Their recommendations and instructions have considerably molded this research. Their unconditional support continuously motivated me and substantially have influenced me as human a being.

Thank you John, for teaching me that it is necessary to dream, but with the condition of believing in our dreams. To examine real-life carefully, to confront our observation with our thoughts, and to perform our fantasy scrupulously. That dose of reality that I receive from you has helped me in that complicated process of forming me as a human a being.

This is a small tribute. It is a small part of what I have built in an incomplete life. This work is dedicated to some extraordinary people, sincere, honest, impartial friends, real friends, and loyal as few. To some people that life will leave the best, at least I believe it, and it is my desire. For them, this gray of life overturned in a few words gathered in a document. This humble present is only a part of the much I owe you. As Carl Sagan said to Annie I say to you "In the vastness of space and the immensity of time, it is my joy to share a planet and an epoch with you". Thank you for illuminating my life with your Friendship. For you, Ruth, Pacho and Maria, with special love and admiration from someone who loves you very much.

Medellin, November 2018, Sebastian Sepulveda Cano

Saw you riding on a moon cloud,

Saw you walking on a whirlpool,

From the corner of my eye,

I saw you.

Bardens, Latimer, Andy Ward, Doug Ferguson.

ABSTRACT

Soil improvement techniques are needed when dealing with sandy, saturated soils susceptible to liquefaction and flow. However, when large areas of soil must be improved, government and private entities limit the use of these techniques because, in the majority of cases, they are too expensive and unaffordable. Therefore, there is a need for inexpensive and reliable emerging methods to improve liquefaction susceptible soils at a reasonable cost.

Among the scientific community, it has been discussed the opportunity and efficacy of using of partial induction of the saturation degree as a method for improving liquefiable soils. One technique to desaturate the soil is by injecting gas bubbles into the soil structure. One of the main concerns of this technique is that the research community has some skepticism on whether or not the injected gas bubbles can remain trapped and stay long enough in the soil voids without dissolving into the groundwater.

Academic interest on this topic is widespread, and resources have been invested in the study of desaturation as a soil improvement technique. As a result, different techniques for introducing gas bubbles into the soil structure have been proposed and tested. Among these techniques are: a) soil desaturation by air injection, b) water electrolysis, c) the implementation of chemicals, for example, the sodium perborate, d) compacted sand piles and e) the application of microbiological methods, for example, the microbial denitrification. The objective of this research is to study and focuses on the desaturation by injection, initially proposed by Okamura Mitsu.

Understanding that there is the possibility of implementing the air injection as a method of liquefiable soil improvement. Moreover, considering that air infiltration in saturated soils and partially desaturation generation are complicated processes, the study of the methods of air infiltration into the soil is made necessary by coupled methodologies of injection-infiltration that reflect variations of state variables over time. Additionally, numerically examination will be developed to study the changes of the non-wetting phase and the wetting phase saturation degree of the soil improved by air injection since this parameter is critical in liquefaction studies and minor variations thereof will have significant effects on the soil resistance to liquefaction.

A parametric analysis will be done, containing the most important hydraulic features that regulate the behavior of partially saturated soils (characteristic soil-water and permeability function), injectability of air in the soil, pressures required during injection, injection duration and desaturation radio. In this Study, the material parameters that actively control soil desaturation process by injecting air will be defined.

1 INTRODUCTION

1.1 PROBLEM STATEMENT

Liquefaction is a phenomenon that has effects on the soil during an earthquake, and in history has caused damage to structures and human losses [1], [2]. Liquefaction is a condition in which non-cohesive soil (e.g., gravels, sands, and silts with very low plasticity) with high moisture content, loses its shear resistance and behaves similarly a viscous fluid due to an increase in the hydraulic gradient that generates high pressures in the water present among the grains [3]. Historically, it is recognized that the typical damages that liquefaction generates to the structures are: bearing failure, severe differential settlement, lateral stretching (from lateral spreading), and racking or twisting of the structures. Nowadays, when the soil is classified as susceptible to liquefaction, it is necessary to develop a treatment for its improvement. Accurate information on available liquefaction soil improvement methods is provided by Seed et al. [4]. These corrective measures are applied in soils susceptible to liquefaction improvement; however, due to their execution costs, they are only applied to projects involving essential structures [5]. It is recognized, that most of the soil improvement methods use mechanical energy and human-made materials, both requiring large amounts of energy due to the production of materials and the construction process realized on site. Therefore, there is a manifest necessity to develop cost-effective liquefaction mitigation methods that can be easily used for new and existing structures [6]–[8].

The scientific community has discussed the possibility and effectiveness of applying a saturation degree-partial induction as a technique to improve liquefiable soils [9], [10]. For this, different techniques have been proposed and tested to introduce gas bubbles into the soil obtaining promising results, because gas in voids increases the liquefaction resistance decreasing the volumetric modulus and increasing the compressibility of the fluid (non-wetting and wetting phase mixture) inside the pores. When the soil is subjected to cyclic loads, gas absorbs the excess of generated pore pressure by reducing its volume [11]. Since the volumetric water module is four times larger than the air volumetric modulus, the modulus of the fluid will decrease dramatically with the addition of a minimal volume of air [12]. Besides, several methods have been proposed to generate bubbles in the liquefiable soils. These methods include air injection [9], water electrolysis [8], chemical reactions [13] and microbiological processes [14], among others, such as dewatering, lowering of the groundwater table through continuous pumping [15], and a microbubble injection method [15]. Bubble generation methods offer an alternative, less invasive in comparison to other methods commonly implemented, cost-effective (especially for large areas), and practical when soil improvement is considered difficult since it can affect permissible load capacity of the surface foundations during the desaturation procedure [16], [17].

Therefore, the purpose of this work is to present a summary on the background of liquefiable soil improvement methods through the generation of gas bubbles, due to the necessity to promote the application of new methodologies for soil improvement and, at the same time, to identify and collect enough technical references on this subject. This work also emphasizes practical aspects of soil improvement methodologies, by the generation of gas bubbles in order to include considerations on geotechnical properties of treated soils. Additionally, mathematical inspection of the soil improved by air injection is realized to characterize the changes in the wetting and non-wetting phase saturation degree. It is done since, the saturation degree of both phases is a relevant parameter in liquefaction phenomena, and slight changes thereof will have substantial effects on the soil cyclic shear resistance or the soil resistance to liquefaction. A parametric analysis is done, evaluating the most important hydraulic features that control the behavior of partially saturated soils (characteristic

soil-water and permeability function), pressures for non-wetting phase required during injection, injection duration, injection rates, and effective desaturation radio. In this Study, the material parameters that actively control soil desaturation process by injecting air will be defined.

1.2 RESEARCH OBJECTIVES

1.2.1 GENERAL OBJECTIVE

Modeling a case of soil desaturation with finite elements, through air injection in a coupled model of infiltration.

1.2.2 SPECIFIC OBJECTIVES

The specific research objectives of this study may be synthetized as follows:

- To analyze a two-dimensional gas infiltration process in a saturated homogenous soil.
- To perform parametric and comparative analysis of the effects of injection pressures, soil-water characteristics and permeability parameters on the soil desaturation process, on changes in the soil pore pressure.
- To examine the effectiveness of air injection as an improvement technique within a soil area susceptible to liquefaction, through the analysis and description of the results obtained in the model of the injection and air infiltration process.
- To make a theoretical study, through mathematical modeling using the finite element method, of the experimental features of inducing a partial saturation degree in liquefiable soils that are observed by studying some scale models and results from the literature in laboratory experimentation.

In order to achieve the above objectives, a research study was assumed to recognize and understand, the fundamental behavior and mechanisms that govern the multiphase flow. In particular, essentials of the biphasic flow that govern the flow of the injected air through a saturated porous media were studied. The research was divided into two separate parts, a comprehensive literature review, and a numerical modeling study. The first one, the literature review, was conceived to make it possible to understand the essentials of the phenomena, the behavior of air injected into a porous medium under scale in a laboratory, and under in –situ or realistic field conditions. In the numerical study, the lite (free) configuration of the software flexPDE [18] was adopted, it is a commercially available toolkit that provides a state of the art in numerical partial differential equations solution methods and mechanized code-writing competences for the study of various technical topics. The finite element method approach solves the non-wetting phase pressure, p_{nw}, and the non-wetting phase saturation degree, Se_{nw}, equations concurrently, rather than sequentially. The code implemented in the numerical study was generated during this research, based on the proposed mechanisms of biphasic flow documented during the literature review of the study.

The essential research component is developed from the physic and mathematical definition of the maximum and minimum injection pressure of the non-wetting phase for a given system. The non-wetting phase injection pressure can be calculated with an expression that includes the hydrostatic pressure directly above to the non-wetting phase injector component and adds the capillary resistance component. Concluding the first part of the research study and given the results to the base questions, defined to understand the phenomena, the next step was the size prediction of the effective radius of the air injected plumes. With the fundamental information collected through observations in the literature review, a model was proposed, and it calculates the geometric features

of air injection plumes at a transitory state. The code is established on a series of simplifying assumptions concerning the behavior of the air flow from the injector through the saturated porous medium. These simplifying assumptions were supported on perceived phenomena, and eventually to reduce a more complex multiphase flow model to a relatively simplified model that solves the conservation of mass problem. The code yields to an initial approximation to the extension of the air injection plume, in an assumed soil below, and in an indicated operational conditions. A small group of soil parameters is the input of the model to calculate the approximation to the size of the plume, typically all of the input parameters are commonly measured as requirements of normative in subsoil explorations, to define design conditions in a project. The code was finally implemented in the parametric analysis to the prediction of the effect of changing soil and injection characteristics on the geometry of air injection plumes.

1.3 ORGANIZATION OF THESIS

This work is separated into five chapters.

Chapter 1 is the introductory chapter and defines the relevance of the research, the problem statement, objectives and order of the research. The general research contains two parts, a comprehensive literature review of desaturation as liquefaction countermeasure and, and numerical modeling research of the partial saturation induction.

Chapter 2 shows an overview of existing theoretical and experimental information related to air-water flow applied to liquefiable soil improvement. The comprised facts in this chapter extended to several fields of science directed toward engineering, and summarize data from several disciplines concerning air-liquid flow. This chapter contains a brief coverage of the fundamental concepts of multiphase flow through porous media and gas-liquid biphasic flow, together with state of the art in air injection research.

Chapter 3 introduces the multiphase flow in porous media model described in detail (the mathematical model, mass-momentum conservation equations, hydraulic properties of unsaturated soils and the boundary conditions) and the implementation developed during this research.

Chapter 4 describes the problem definition, a conceptual model of air expansion is presented and the boundary conditions associated with the phenomena. Also describes the results of the numerical study. Simulations were developed with verified results from some of the experiments in-situ and in the laboratory showed in the literature, and reproduced results previously generated by other researchers using published models of air injection to improve liquefiable soils. A discussion of the results is also developed in this chapter.

Chapter 5 presents the conclusions of this research along with a list of remarks, limitations, knowledge gaps, and recommendations for future research.

2 BACKGROUND AND STATE OF ART

2.1 PARTIALLY SATURATED SOILS

The mechanic response of partially saturated soils is more complicated than fully saturated soils, and it is related with their three-phase microstructure that includes the skeleton (solid phase), pore fluid (wetting phase), and gas (non-wetting phase) [18], as shown in Figure 1.

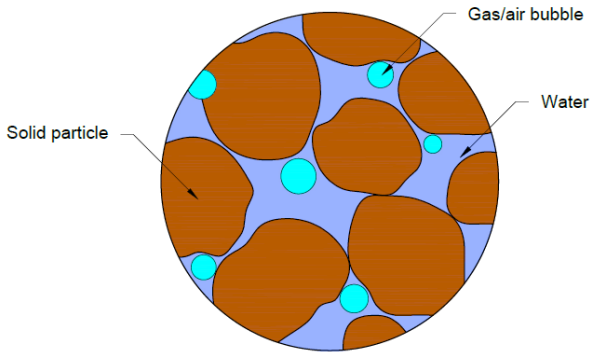

Figure 1 Scheme of a partially saturated soil, modified from Gokyer [19]

The responses of partially saturated soils may be different, according to the wetting phase saturation degree. The volumetric content of the non-wetting phase associated with the pore space or the solid phase, lead to different kinds of mechanisms in the microstructure of the three phasic material. Then, several wetting phase saturation degrees in the partially saturated media generates various mechanical responses in the soil structure. There have been several academics studying the mechanical responses of a diverse kind of partially saturated soils [20].

Specifically, Fredlund and Rahardjo [18] separated the partially saturated soils in three categories as a function of the wetting phase saturation degree. The first category is a partially saturated soil with a wetting phase saturation degree smaller than 80%. In this category, the non-wetting phase is continuous, and menisci of the wetting phase in pores adhere to the soil skeleton. The second category is a partially saturated soil with the wetting phase saturation degree from 80% to 90%. In this category, there is a transition zone where both the non-wetting phase and the wetting phase are continuous. Furthermore, the wetting phase is also continuous with occluded bubbles. The third category is a partially saturated soil with the saturation degree higher than 90%. In this category, all the non-wetting phase is in occluded form, and the wetting phase in pores is continuous.

In addition, to the three categories previously defined, Pietruszczak and Pande [21] indicated that there is an additional category of partially saturated soil named gassy soil. In this category of partially saturated soil, the non-wetting phase is discontinuous, and it is generated by discrete occluded bubbles that are entrapped into the pore spaces of the three-phase material. Moreover, it was also stated that in this kind of material structure, the non-wetting phase is generated by means of the decomposition of organic matter. Finally, the non-wetting phase bubbles developed in this biologic and chemical process come to be higher than the average particle size, and it consequently produces some pressure against the solid phase. It is also stated that gassy soils are mainly detected in marine sediments as studied by Grozic et al. [22]–[25].

Furthermore, Wheeler [26] specified that due to in gassy soils the non-wetting phase bubbles are higher than the common pore spaces, the bubbles cannot be defined as occluded bubbles within the wetting phase. Prominently, Gokyer [19] stated that the non-wetting phase bubbles produced in the wetting phase partial saturation degree induction by the chemical method technique, are smaller than the void space because the non-wetting phase generation is finite, and restricted by the time interval of the sodium percarbonate chemical reaction. It is important to recognize that a partially saturated soil, generated by the wetting phase partial saturation degree induction, is not included in any of the categories previously defined, where occluded non-wetting phase bubbles are entrapped in pore space of the soil skeleton with smaller dimensions than the pore space. The influence of these non-wetting phase bubbles on the three-phase material is a modification of the compressibility of the wetting phase, which is an advantage of the method concerning liquefaction resistance improvement as Okamura et al. [11] concluded.

However, the previously defined categories of partially saturated soils are different from the wetting phase partial saturation degree induction, and it is because all classes appear typically in the region where capillary pressure or matric suction acts, and this region is described above the water table. The capillary pressure is defined usually as the difference between the non-wetting phase pressure and the wetting phase pressure. Thus, almost every time the non-wetting phase is continuous in the capillary zone, and the capillary pressure acts as a negative pressure in the pore space for these categories of partially saturated soils. The categories of partially saturated soils are characterized by the soil-water characteristic curve, which indicates the relation between the capillary pressure of the soil structure, and the wetting phase saturation degree [27], as shown in Figure 2.

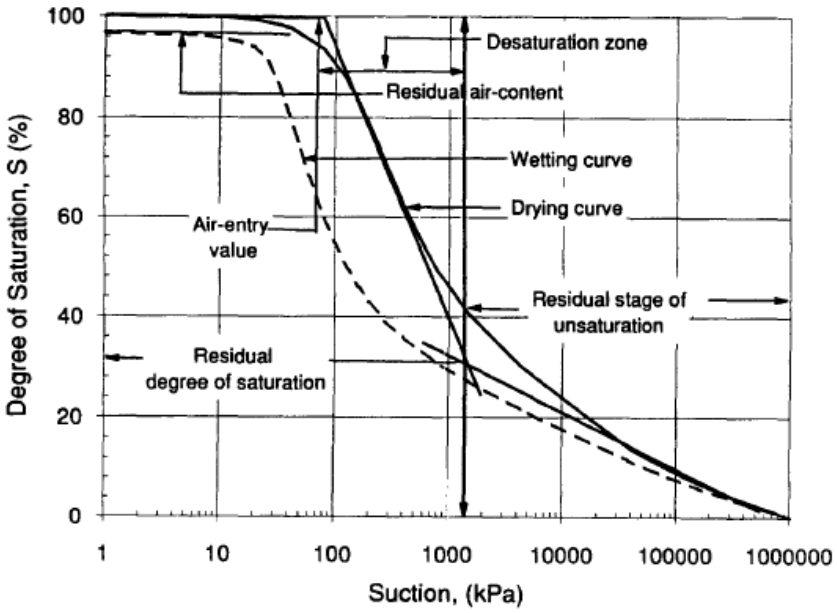

Figure 2 A typical soil-water characteristic curve with various stages of desaturation [27]

Nevertheless, in the application of the wetting phase partial saturation degree induction, desaturation is generated below the water table, mainly, where the pore water pressure is positive. Additionally, the non-wetting phase bubbles are occluded, are smaller than the pore space, and the wetting phase is continuous in the pore space. Consequently, in the wetting phase partial saturation induction degree category of partially saturated soils, wetting phase pressures are above atmospheric pressure, as Pietruszczak and Pande [21] specified. The pressure of non-wetting phase bubbles in a pore space to the wetting phase pressure is related through Kelvin's capillary model equation Fredlund and Rahardjo [18], as follows:

$$(u_a - u_w) = \frac{2T_s}{R_s} \quad (1)$$

Where u_a is the non-wetting phase pressure, u_w is the wetting phase pressure; T_s is the surface tension, and R_s is the radius of curvature. Notably, for occluded non-wetting phase bubbles, Fredlund and Rahardjo [18], and Bishop and Eldin [28] proposed to neglect the effect of surface tension. At this point, for the category of partially saturated soils generated by the wetting phase partial saturation degree induction, the non-wetting phase pressure in the pore space is supposed to be equal to the wetting phase pressure which is above atmospheric pressure regularly at any time. Eseller-Bayat et al. [13] and Gokyer [19] showed some measures of wetting phase pressures in laboratory experiments conducted to show the behavior of the wetting phase partial saturation degree induction technique and were related to the suggested by Fredlund and Rahardjo [18], and Bishop and Eldin [28]. The validity of this simplification in-situ for the wetting phase partial saturation degree induction technique can be examined in the next works.

2.2 CASES STUDIES AND OBSERVATIONS OF BUILDING RESPONSE

When an earthquake occurs, liquefaction phenomena could be developed in loose, fully wetting phase saturated cohesionless soils, as sands that have low plasticity. Typically, liquefaction phenomena is recognized as the instant during the excess pore wetting phase pressures reach the initial vertical effective stress or overburden the effective stress at a defined depth. Usually, liquefaction phenomena it is separated into two main groups. The first one is called the flow liquefaction, and it occurs when the associated static shear stress is high in comparison with the post-liquefaction shear strength. The second one is called the cyclic mobility, and it occurs when the static shear stress is low in comparison with the shear strength of the liquefied soil [29]. The following paragraphs present a summary of case histories of liquefaction generated damage to structures that have been perceived.

In the last decades, earthquakes have frequently presented damage to infrastructure associated with soil liquefaction phenomena. Different buildings like bridges, underground storage tanks, pipelines, roads, dams, and slopes (natural or anthropic) have been impacted by the incidence of liquefaction phenomena [30]. These circumstances led to the progress in the development of countermeasures to reduce liquefaction susceptibility of soils, and consequently the effects on buildings. Mitigation methods have been employed in situ to improve soil's susceptibility to liquefaction, or to reduce the resultant deformations during phenomena. Nevertheless, the responses of mitigation concerning building behavior and possible damage may still be significant, and are not well studied.

Liquefaction associated with earthquakes has produced significant damage to structures in past seismic activity. Extreme settlements and much inclination, bearing capacity failure, lose of the moment strength connections, and column supports of structures founded with shallow elements are typical failure types that have been detected. These liquefaction impacts on the behavior of buildings throughout historic cases are exposed next, initiating with damage detected in the 1965 Niigata (Japan) earthquake.

On June 14th of 1964, a 7.6 magnitude earthquake produced soil liquefaction around vast areas of the Niigata city in Japan. Almost all the buildings affected with considerable damage were two to four levels structures. Indeed, nearly 300 reinforced concrete structures were damaged as a result of liquefaction phenomena [31]. Specifically, in the same study researchers explained that affected

structures were the ones located in the slopes or hills. Furthermore, essential fissures in columns, beams, and walls were perceived as a result of approximately 3.8 m settlements.

While the 8.3 magnitude Tokachi-oki earthquake in 1968 (on May 16th), buildings supported on loose sandy soils, for example office structures and depots, experienced intensive seismic liquefaction damage. Consequently, settlements equal to 40 cm were detected [32]. Ashford et al.[33] stated that more recently, in 2003, a new earthquake of 8.0 magnitude impacted the same zone. Seven buildings (houses) were impacted as a result of liquefaction phenomena, with significant settlements and inclination approximately to 2.5 degrees. On the other hand, no apparent structural damage was detected in primary importance buildings (for instance, power stations and hospitals) supported on improved soils with compaction methods [32]. It offers some experience or confirmation of the potential of soil improvement with compaction. In 2003, the same zone was impacted by one more earthquake, notably, without having any signal of liquefaction phenomena in the zone shake by the 1968 earthquake. These places were improved with compaction methods after the 1968 earthquake occurred [34].

In 1989 (on October 17th), the San Francisco Bay region was shaken by the 6.9 magnitude Loma Prieta earthquake. Essentially, settlements and inclination were perceived in structures supported on loose sandy (filled) soils, and particularly in the same zone that was reported liquefaction phenomena and extensive ground strain with the 1906 (on April 18th) 7.9 magnitude San Francisco earthquake [35]. Furthermore, it was evidenced some damage in structural and non-structural elements in residencies [36]. On the other hand, some compacted fills had reasonably good behavior during shaking, presenting limited liquefaction impacts [35], [37]. One year after, in 1994, the 6.7 magnitude Northridge earthquake was reported as one of the greatest expensive earthquakes in the history of the United States [38]. Mainly affecting some newly constructed steel moment frame structures, additionally as occurred in the 1989 Loma Prieta earthquake, some buildings were impacted by liquefaction phenomena.

In the 7.8 magnitude Philippines earthquake occurred in the year 1990 (on July 16th), Dagupan city was hit. Almost all of the affected structures (primarily constructed with reinforced concrete) were two to four levels supported on shallow foundations on sandy soil profiles. In general, the settlements perceived oscillating from approximately 25 to 125 cm, and inclination of about 10º was informed in some buildings. It is important to clarify that the settlements and inclination were closely linked to the proportions of the buildings and their support system [39], [40]. On the other hand and later, the damage was also related in some magnitude to the confining pressure and shear stresses of the buildings [41]. Furthermore, Tokimatsu et al. [41] some of the affectations were related to structure-soil-structure interaction impacts.

In 1995 (on January 17th) the 6.9 magnitude Kobe (Japan) earthquake generated massive liquefaction geotechnical phenomena. Principally, the impacts were very close to the area of Port and Rokko Island, a zone with mudstone (fill) profiles of about 16 to 20m. The center of the two islands subsided approximately 50 cm, and structural damage was critical [42]. Several edifications like office structures were destroyed with this earthquake. Nevertheless, the most representative damage associated with the liquefaction phenomena was on the older bridges that were destroyed by high lateral forces product of lateral spreading effect [42]. Moreover, the efficacy of soil improvement techniques to prevent liquefaction phenomena was once more estimated. Buildings supported on soil improved by compaction methods, employing densification or vibration, showed settlements of approximately 2 to 3 cm. Consequently, no substantial differential settlement was observed in the improved areas. Nevertheless, some buildings showed severe damage because the

improvement (densification) did not cover to enough depth or lateral amplitude. Two cases were informed on the Rokko Island north, where the improved ground beneath two big tanks did not protect the buildings from suffering large settlements around 62 to 44 cm, correspondingly [43].

Some years later, in 1999 (on August 17th) the 7.4 magnitude Kocaeli earthquake shacked the city of Adapazari. Considerable structure damage and loss of human lives take place in this episode. As the area of the Adapazari city was erected above moderately thin deposit profiles of silt and silty sand, several buildings were subjected to liquefaction phenomena [44]–[46]. Over 60% of two and more story buildings were impacted and experienced partial or total failure [47]. Furthermore, differential settlement larger than 150 mm, and bearing capacity problems considerably affected buildings of four to six levels [48]. Edification settlement was characterized to be strongly related to the contact pressure, and the height/width aspect proportion of structures was also a factor that importantly influenced the inclination degree [44]. On the other hand, liquefaction phenomena were directly related to flexural hinging, and shear-bending damage at the end of the columns. Furthermore, soft story mechanism was recognized in buildings [47].

In the 7.6 to 7.7 magnitude Chi-Chi (Taiwan) earthquake occurred in the year 1999 (On September 21th), impacts of liquefaction phenomena were perceived on the area of the Taiwan west coast. Consequently, liquefaction phenomena produced settlements that were informed at remote sites, principally at Yuan Lin city, in which large settlement of the structure supports was significant [49]. Nevertheless, critical structural affectations were not detected. This event helped to estimate the response of zones with and without soil liquefaction mitigation. Dynamic compaction was implemented at a specific location in the Chang- Hwa Coastal Industrial zone. The efficacy of this soil improvement method was validated by estimating the liquefaction potential previous and subsequent earthquake. Ground settlement associated with this improved zone, after the shake, was about 3 cm. Oppositely, ground settled about 33 to 45 cm at locations in the same zone, but without soil liquefaction mitigation [50].

In 2010 (on January 12th) a 7.0 magnitude disastrous earthquake shacked the city of Port-au-Prince (Haiti). Some anthropic fills and well-graded combinations of sands and gravels in the areas near dock suffered widespread liquefaction phenomena, and consequently, induced failures [51]. Additionally, some separated incidents of structure damage generated by liquefaction phenomena were reported. Notably, a three-level edification collapsed as a result of support complete bearing capacity failure and structural failure [52].

Also in 2010 (on September 4th), the 7.1 magnitude Darfield earthquake hit the south of New Zealand island. Soil liquefaction phenomena produced substantial structural damage. Particularly, two-level reinforced concrete structures founded on spread footings were impacted and suffered general damage associated with lateral spreading below the support [53]. Generally, damage associated with the liquefaction phenomena was intensive in the joints among beam and columns [54]. One year later in 2011 (on February 22th), the 6.2 magnitude earthquake shacked the city of Christchurch (New Zealand). Liquefaction phenomena generated 1.0 to 2.0 m settlements, and inclination of structures was more than 2 degrees. It occasioned some structural damage in small to medium height edifications. The excess pore pressure forces produced ground bulk upward, and foundations inclination [55].

The 9.0 magnitude Tohoku (Japan) earthquake took place in 2011 (On March 11th), and generated a significant amount of soil liquefaction phenomena impacts, principally in the Urayasu City situated in the Tokyo coastal area. Great irreversible structures inclination of approximately 3 degrees and buildings (reinforced concrete structures) on shallow foundations with settlements near 70 cm were

perceived. Cox et al. [33] informed a specific incident, in which liquefaction phenomena induced settlements were approximate of 30 cm. It is important to clarify that the structure settled an extra of 40 cm concerning the ground surface, generating an entire settlement of 70 cm. Therefore, it was demonstrated the necessity to take into account the impacts of soil-structure interaction on analysis of foundation settlements associated to the liquefaction phenomena. Even though liquefaction phenomena produced significant damage, in some of the buildings, where inclination and settlements occurred, no structural damage was perceived. Tokimatsu et al. [56] concluded that the type of foundation implemented in this zone limit the differential settlement excess, and therefore the structural damage associated with the phenomena. Usually, foundations in this area are composed of dense reinforced concrete of approximately 20 cm mats and tie beams system, which was sufficiently rigid to evade differential settlement during the reduction in the distortion of the structural system [33].

Lateral spreading and ground settlement associated with liquefaction phenomena were detected in the 7.6 magnitude in Samara (Costa Rica) earthquake in 2012 (on September 5th), and in both the 6.1, and eight days after the 6.0 magnitude Cephalonia (Greece) earthquakes in 2014 (on January 26 and February 3). In Cephalonia earthquakes, a few insulated liquefaction-induced settlements in buildings were perceived, and some reported damage on roads. While the Samara event, a reinforced concrete building founded in nine square concrete stilts developed settlements around 50 to 75 cm after support ground liquefied [57]. Furthermore, one level reinforced concrete structure during the Cephalonia event settled and rotated about 1 degree, but with the absence of structural damaged [58].

In 2016 (On April 16th), the 7.8 Muisne earthquake shacked the coast of Ecuador. Consequently, some office buildings settled in the bay of the mid-sized city of Manta [59], that is situated above loose silty sand layers and low plasticity zone [60]. Although some structural and non-structural damage were informed at particular sites, significant damage or collapse of buildings was not perceived. The extension of liquefied ground and associated lateral spreading approximately 50 cm generated some damage in buildings placed in Calceta city [60]. Furthermore, some non-structural elements as brick dividing walls of a steel coliseum were injured in the same zone [59].

On the other hand, and in the same week, Kumamoto City (Japan) was surprised by one strong 6.2 magnitude earthquake on April 14th, and two intense aftershocks on April 15, and on April 16, both of 6.0 and 7.0 magnitude, respectively. Even though the urban area was constructed on loose saturated sandy soils, the effects of liquefaction phenomena were remarkably limited [61]. Furthermore, some shallow liquefaction was perceived on the south of the Kumamoto artificial island. Additionally, settlements of 15 to 20 cm associated with liquefaction phenomena, and post-liquefaction settlements of approximately 60 cm at particular sites were experienced.

Summarizing, these informed case studies through previous seismic events exposed the significance of the strong association among soil motion features, soil characteristics, support behavior, and potential damage to structures associated with liquefaction phenomena. Nevertheless, liquefaction phenomena case studies do not give enough data related to the effects of ground liquefaction phenomena, soil improvement methods, and the impact in damage to the structural and non-structural schemes of the building. Developing a continuous compilation of adequately reported case studies is necessary. Furthermore, it is essential to obtain better-quality field information to decrease the incertitude associated with future case studies interpretation. These works, have to be complemented by the continuous research of refined techniques for predicting liquefaction phenomena induced settlements. They are accompanied with procedures that consider uncertainties

meticulously (such as, foundation and structural response on liquefiable soils and mitigation techniques) and laboratory scale models in well-controlled environments.

The liquefaction phenomena have been associated with the generation of massive damage to diverse categories of buildings in the course of preceding earthquake shocks. Nevertheless, the response of structures founded on liquefiable materials, and the efficiency of liquefaction soil improvement procedures on the whole behavior of soil-foundation-structure schemes are misunderstood. Not including soil-foundation-structure interaction in present-day design, and estimation processes can distort predictions of the response of the structure on the ground liquefaction. These facts may lead buildings to preserve a substantial associated risk concerning economy and life-safety, which may be aggravated when soil improvement is not valued or reflected in the design. Therefore, it is essential to estimate liquefaction impacts for structures, for example, tilt, settlement, and structural damage, from a soil-foundation-structure interaction approach.

2.3 WHAT IS THE MAXIMUM DEPTH LIQUEFACTION CAN OCCUR?

How deep can liquefaction phenomena in unconsolidated soils occur? Can sandy materials, or layers of sand inside deposits of shale or clay liquefy at highly depths as 100m and more. Moreover, if this kind of depths would be essential to develop an adequate amount of densification to generate large-scale depressions, for instance, Reelfoot lake as is presented by Stewart and Knox [62]. Can cyclic forces associated with earthquakes be enough to momentarily surpass the overburden pressures related to these specific high depths?

In the literature about this topic there looks to be limited or no considered or reported comments of liquefaction phenomena in depths of 30 m and upper [63]–[66]. Florin and Ivanov [67] stated that liquefaction phenomena that even cover the associated highly loose sands, are almost inconceivable for overburdens related to confinements of 15 m and higher.

In accordance to Youd personal communication in 1994, in his background and practical knowledge, the deepest recognized cases of seismically induced liquefaction were in the Snow Lake and Portage situated in Alaska, during the Anchorage seismic event in 1964 at depths of approximately 30 m. As stated by Ishihara [68], the peak ground accelerations magnitudes must overcome 0.5 g, and liquefaction phenomena would have to occur at depths smaller than 10 m for impacts to be perceived at the ground surface. Alternatively, laboratory investigations and the particular knowledge of the researchers field Stewart & Knox [69] specified it differently.

In laboratory experimentation made by Bishop et al.[68], liquefaction phenomena were examined during considerable confining pressures of approximately 7 to 70kg/cm^2 . This laboratory analysis match with overburden pressures associated with depths oscillating between 30 to 300 m, respectively. Even though it was scaled laboratory experimentation and not an analysis of in situ ground impacts from a seismic event, liquefaction phenomena were stated as probable with the defined overburden pressures. The laboratory experimentation confirmed what can be presumed, that the larger the overburden pressure at defined depth the larger the number of stress cycles or the more extensive the stresses required to produce liquefaction phenomena.

An exemplary diagram made by Seed & Idriss of depth versus shear stress required to induce liquefaction phenomena is well documented in [64], [65], [70]. It can be observed, from the diagram, that for a defined depth, it exist an associated stress that has to be overcome with the pore water pressure to start the liquefaction phenomena. It is not an intrinsic limit to the depth at it is probably the liquefaction by this diagram. Whereas Seed and colleagues do not give the impression to have in consideration the liquefaction phenomena out of the range of the 30 m depths, their analysis and

models of liquefaction phenomena against depth do not exclude liquefaction phenomena induction deeper than defined. Furthermore, Dobry et al. [66] stated a depth-liquefaction potential equation. Once more, similar to the diagram defined by Seed & Idriss, it did not exist an associated threshold to the maximum depth of liquefaction in this formulation. Concerning Prakash [63], as almost immediately as liquefaction takes place, the consolidation phenomena begin. Consolidation results in surface settlement, which is followed by the close packing of sand particles. Furthermore, Prakash perceived that the total magnitude of subsidence at the ground surface it is strongly related to the time that the soil stays as a viscous fluid.

The remarked interest of academics and consultants around liquefaction phenomena is associated with engineering structures as buildings, highways, dams, among others. In case that liquefaction phenomena take place at a specific depth or at ground surface, the subsequent sink and additional disturbances of the soil surface can generate critical damage on structures. As almost of this resulting damage is an effect of liquefaction phenomena at depths beneath 30 m or shallow depths, it is expected that available engineering documents studying liquefaction phenomena at greater depths were challenging to find [62].

Published geologic reports associated with liquefaction phenomena are unusual, including references in geomorphology journals. On the other hand, the influence of seismically induced liquefaction effects on the continuous molding of topography by earthquakes or the morphoseismology is a reasonably new subdivision of geomorphology [62]. Though geologic reports like the civil engineer ones, do not analyze liquefaction phenomena at depths higher than 30 m, it analyze high magnitude pore water pressures at depths of 300 m and more, overcoming the stiffness produced by overburden pressures and go beyond for the induction of liquefaction phenomena [71]–[74]. These excessive magnitudes of pore water pressures are studied in oil wells at thousands of meters depths under the ground surface and are denoted as geo-pressures.

Finally, liquefaction phenomena potential in soils at depths of 12 meters or more is recognized, generally, as reasonably low, connected to overburden effect [75]–[79]. Furthermore, it can be mentioned that sometimes in soil deposits originated without anthropic intervention there is usually no necessity to consider liquefaction phenomena under depths ranging from 15 to 18 m, if structures are founded with shallow supports. Consequently, some causes are defined as follows:

- Typically, for profiles with depths around 12 m and more of non-susceptible to liquefy stratums the associated settlements of the deepest liquefiable stratums are not going to generate sinking near to the surface [76], [80].
- Depths associated with the Holocene deposits, which are generally susceptible to liquefaction phenomena are unusually under 15 to 18m depths order. Throughout, Holocene deposits characterize almost the total of the natural deposits that are liquefiable. Some cases are reported and shown unusual events of Pleistocene deposits that are sufficiently loose to be liquefiable. It is important to clarify that it is problematic to discover any case histories of Neogene or older deposits that are liquefiable [81]–[83].
- Deep natural deposits are encountered commonly highly densified, and this is the reason why Neogene sediments are not typically liquefaction susceptible [83].
- In addition, in some tailings dams upstream with poorly planned filling speeds, problems associated with coarse granular layers with low density could be manifested at greater depths. If at high depths inside tailings is water, the phenomenon of liquefaction could be generated, or maybe strain softening and cyclic mobility phenomena [84]–[86].

2.4 THE LIQUEFACTION RESISTANCE EFFECT OF GAS ON SOILS

The Undrained response of partially saturated coarse-grained soils as sands has been a topic of abundant attention in the last decades [87]–[90]. Initially, researchers developed studies showing the necessity to achieve 100% of saturation degree in laboratory samples, with the purpose of evading overrating the undrained shear resistance in triaxial experimentation [87]–[92]. Martin et al. [87], performed cyclic experimentation on entirely and partially saturated sand samples. They found that for a reduction of 1% in the saturation degree of an entirely saturated sample, 28% of water pressure in the pores was reduced by cycle. Chaney [89] and Yoshimi et al. [92] determined that the susceptibility to liquefy fully saturated sands decreases by half with a 10% reduction in the saturation degree. Xia and Hu [91] showed that liquefaction resistance increased by more than 30% when the saturation degree was reduced to 97.8%. It was demonstrated that small amounts of trapped air could increase liquefaction resistance remarkably.

In the latest years, the aim of examination has moved towards the study the partial induction of the soil saturation degree and its influence on susceptibility to liquefaction [23]–[25], [93]–[120]. Some of the most significant studies are discussed as follow. Grozic et al. [24] indicated that, in undrained compression, coarse-grained soils as loose sands showed a change in the response from softening to hardening by deformation after the saturation degree was lowered to values less than 90%. On the other hand, from cyclic triaxial tests with a variable saturation degree from 75% to 99%, it was found that the existence of gas improved dynamic resistance from 200% to 300%, compared to fully saturated samples. Also, Rad et al. [115] found that coarse-grained soil as sand with the presence of non-soluble non-wetting phase is more resistant than the one with the presence of soluble non-wetting phase. Using the mathematical model formulated by Grozic et al. [23], it was concluded that undrained shear resistance of gaseous soil improved with a decrease in the wetting phase saturation degree. Also, Ishihara et al. [116] demonstrated that the volumetric stiffness of fluids is strongly dependent to the existence of the non-wetting phase, and a minor volume of non-wetting phase can considerably change the fluid pressure reaction inside the pores to the process of loading, the magnitude of Skempton's B constant, magnitude of the P wave, and resistance to liquefy. Skempton's B is the proportion of the rise of the wetting phase pressure over the pores to the effective pressure associated with the confinement. It is a connection among the wetting phase saturation degree and the Skempton's B, and there is typically necessary to generate a B magnitude higher than 0.95 in triaxial experimentation to achieve complete wetting phase saturation of the specimen. Consequently, the decrease of the Skempton's B is the decrease of the wetting phase saturation degree, and it corresponds to a rise of the liquefaction strength of the saturated soil [121]. In cyclic tests, reported by Yang et al.[98], a significant increase in the ratio of cyclic stresses resulted from a reduction in a small percentage of the saturation degree of the initially saturated sand. As well as Bouferra et al. [104], showed that a small reduction in the saturation degree could result in a significant increase in the liquefaction resistance. Furthermore, Tsukamoto et al. [94] demonstrated that a diminution in the wetting phase saturation degree by up to 90%, rises the liquefaction resistance twice compared to entirely saturated samples. According to Yang et al. [96], for a decrease of wetting phase saturation degree by 1%, there is a decrease in the ratio of the excess of wetting phase pressure acting over the pores from 0.6 to 0.15 in pure horizontal cyclic loading.

2.5 METHODS TO INDUCE PARTIAL SATURATION DEGREE

The following discussion topics in this document have been identified within the methods proposed by different authors around the world. It is important to clarify that these methods have been

chosen to be covered in this background since they are considered to be based on well-established mathematical and physical concepts.

2.5.1 Air injection

In recent years, partial desaturation of soil by air injection has gained attention as an innovative technique to decrease liquefaction susceptibility of soils. Research programs, such as numerical models, scale models and in-situ tests, have been carried out about air injection [122]. The saturation degree was investigated after performing air injections by extracting frozen samples ranged, and finally, values of the saturation degree ranged between 70 and 91% [123]. Cyclic shear experimentation was performed under in-situ confinement conditions, and the impacts of desaturation on shear strength and undrained cyclic deformation were studied, finding that shear strength can increase by about 50% with desaturation. However, deformation characteristics are not improved if the soil structure does not change from a loose to dense state [124].

On the other hand, after stopping air injection in the soil, samples were recovered by the freezing method to measure the saturation degree. Results ranged between 88.4 - 98.4% and 65.0 - 88.0% in two studied strata [122]. Okamura and Teraoka [125], found that if the saturation degree after air injection is below that 90%, soil desaturation will remain for a long period, indicating that liquefaction resistance of air-injected soils is higher than the 100% saturated soils. During the last decades, the saturation degree and improvement of liquefiable soils has been investigated and related [9]–[11], [126]–[128]. It has been found that the lower the saturation degree, the higher the liquefaction resistance [94]. Decreases in the saturation degree by air injection have significant effects on the increase in the liquefaction resistance for depths greater than 2.0 m [125]. In cyclic tests, it was shown that with a decrease of 10% in the saturation degree, liquefaction resistance was doubled [129].

In order to study the duration of the effect of desaturation, three zones that were under a desaturation phenomenon before were investigated. Specifically, frozen samples from 4, 8 and 26 years ago were obtained from each place, and laboratory tests demonstrated that for the zone improved 26 years ago, air bubbles still existed inside the ground. None of the samples from the three sites had more than 90% of the saturation degree [130]. In a similar study made by Okamura and Teraoka [125], it was shown that the wetting phase saturation degree of soils after some years was not considerably higher related to the measured in the soil shortly after being injected with air, and increases of 10% were observed for saturation level, which indicates the longevity of air bubbles injected, and it is inferred that achieving degrees of saturation below 90% with air injection would generate durable desaturation conditions [125]. The possibility of air injection implementation is seen as a liquefaction mitigation technique since air injection desaturates the soil and longevity of air within the soil is typically shown for more than ten years [17], [123], [131].

In addition, Zeybek and Madabhushib [132] studied the durability of air bubbles in samples under hydrostatic conditions, at low and high pore pressure, vertical upward and downward flow, variable pore pressure and lateral shaking. They found that some of the air bubbles trapped in the partially saturated soils lost their function under these conditions, increasing the saturation degree of the samples. Moreover, some of the air bubbles generated with the degree of partial saturation induction lost their purpose in some of the tested flow conditions, causing an increase in the saturation degree of the samples. However, it should be noted that the magnitude of the increments was generally, minimal. It was shown for the short term that under hydrostatic conditions in two sand column tests, the average increase in the saturation degree was 1.4 and 2%, respectively.

On the other hand, it was observed that for the long term, the average saturation degree of the same samples increased after100 days by 2.1 and 2.55%, respectively. Additionally, in the study of durability under hydraulic flow condition carried out during 30 hours, changes in the saturation degree were observed to occur mainly in the first hours of the experiment and then remained almost unchanged. Revealing that the volume of occluded air bubbles entrained by the flow of water through the soil matrix was minimal and that most of the air bubbles were trapped in the soil pores. The results obtained even support those ones shown by Eseller-bayat et al. [13].

The air injection method proposed by Okamura and Teraoka [125] is a not-complicated and cost-effective alternative to improve liquefiable soils. The technique fundamentally desaturates soil and generates an increase in the liquefaction resistance. With this method, it is only necessary the insertion of a tube in soils susceptible to liquefaction and to inject air under pressure from the injector. An example of the technique is shown in Figure 3. There is experimental evidence that evaluates changes in the liquefaction resistance generated by air injection. Therefore, rates, magnitudes, and distribution of desaturation have been measured. Some models are those evaluated in shaking tables [133]–[135], centrifugal [9], [16], [128], [136]–[138] and in field [122]. These models have been implemented to investigate, define and evaluate the state of desaturated zones by air injection processes. With this experimental basis, it is possible to identify the advance of the air front, and additionally, to demonstrate that the area of influence and distribution of the saturation degree are affected by the type of soil, stratification, injected air pressure, and injection depth [139]. Zeybek and Madabhushib [132] studied the durability of air bubbles trapped under cyclic loads (with the application of lateral excitation to the samples). When the partially saturated samples were subjected to cyclic loads, they found that the saturation degree increased by 0.64% and 0.41% for higher and lower accelerations respectively.

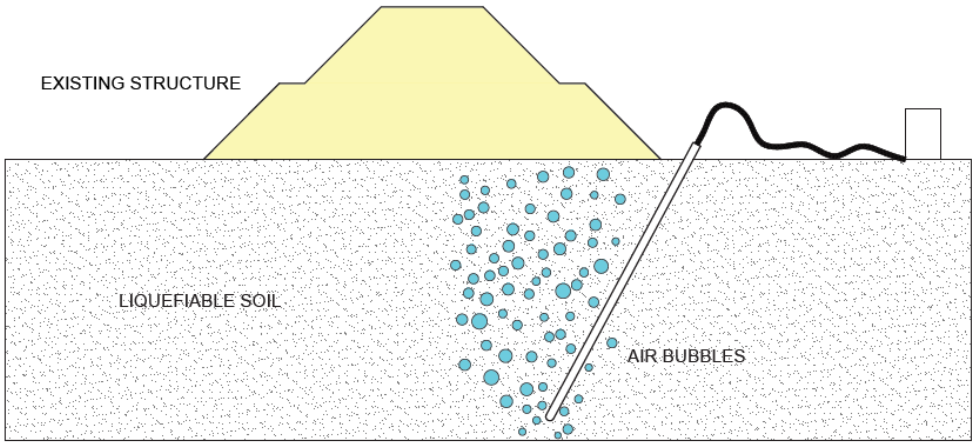

Figure 3 Desaturation by air injection, modified from Okamura and Teraoka [127].

Also, Zeybek and Madabhushib [132] investigated the settlement of improved soil by air injection when it is subjected to dynamic loads. In this study, scenarios with and without surface foundations were presented under the combined effects of various field conditions such as hydrostatic pressure, the increase of fluid pressure and cyclic load. The analyzed data revealed that, although the previously improved soil was exposed to most of the field mentioned above scenarios, air injection was effective in reducing liquefaction-induced settlements, in tests without surface foundation. However, when the tests were made in the same soil injected with air, in the case of the surface foundation, a remarkably large settlement was observed. It is recognized that this is not consistent with the experimental findings of Marasini and Okamura [17]; in Marasini and Okamura [140]

research, greatly instrumented dynamic centrifuge experiments were performed, studying the impact of air injection over relatively light structures. It was indicated that the results were out of the expected, and the importance of investigating the balance among the trapped air bubbles and the pore pressure due to the fluid inside the voids was emphasized. The study was carried out because the movement of air bubbles in the ground is possible if the pressure of the soil or water is significantly reduced.

On the other hand, the numerical simulation of the dynamic response of partially saturated sands has not been thoroughly studied. Some of the work done is mentioned as follows. Mitsuji [141] simulated the partial saturation degree with the decrease of the volumetric modulus of the fluid within the pores, thus obtaining the dynamic response of the partially saturated sand through one-dimensional analysis of the effective stresses. It was found in this study that the velocity, displacements, and shear strain of the soil decreased due to the impact of the reduction in the wetting phase saturation degree. Gao et al. [142], studied the dynamic response of partially saturated soils and the impacts of the volumetric modulus of the fluid in the pores, in the development of excess pore pressure with different initial conditions in the saturation degree. The study was developed through the generation of a numerical model that includes the Biot's theory [143], [144] for the two-phase mixture. Similar studies were performed by Yashima et al. [145], where the effects of the compressibility of the fluid in the pores were observed due to the existence of a degree of partial saturation through a three-dimensional dynamical examination founded on Biot's theory [143], [144]. According to the authors, in order to simulate the 1995 Hyogoken-Nambu earthquake in the zone of Port Island, the excess of pore pressure and acceleration were measured as responses to dynamic loads, obtaining reasonably good results comparable to historical ones.

Recently, Marasini and Okamura [140], presented the results of a numerical work founded on a complete group of experimental records from four centrifuge models, from Ehime University, which were simulated using cyclic elastoplastic numerical model, with the nonlinear theory of kinematic hardening included , based on effective stress analysis called LIQCA-2D and proposed by Oka et al. [146], [147]. They simulated sand with a saturation degree of approximately 85%, by decreasing the volumetric modulus of the fluid in the pores. As a result of the simulations, it was possible to duplicate the excess of pore pressure accurately, and the structural settling and deformation of the foundation soils perceived in the centrifuge experiments. This study established that the dynamic response of the desaturated soil is effectively predicted by decreasing the volumetric modulus of the fluid in the pores, and the generation of the partial saturation degree of the soil works to mitigate the settlement of moderately light structures, such as structures with one or maximum two plants when the soil is subjected to dynamic loads.

In addition, mathematical models and numerical simulations have been developed to study and predict the performance of multiphase flow in soils [148]–[165]. Notably, McCray [149] carried out a research on the background of existing mathematical models that were in charge of describing the behavior of the generation of air bubbles, highlighting the importance of multiphase flow models to characterize the phenomenon induced by air injection, indicating that results depend on the calibration of the model. It was also recognized by Yasuhara, Okamura, and Kochi [139] that models turned around the process of decontamination of coarse-grained soils instead of fine sands and silts, and, that saturation degree in the injected zone was not a relevant parameter.

Also, the desaturation process and simultaneous flow of water and injected air during desaturation process are highly complex phenomena, and it should be noted that air infiltration in saturated soils, desaturation and deformation are concurrent processes (the last two entirely dependent on the

former)[16], [132], [138], [166]. The multiphase flow simulator (TOUGH2) [167] has been implemented to examine the applicability of the soil improvement technique by desaturation. Numerical simulations of multiphase flow show an adjustment over the experimental measurements of the saturation degree and numerical predictions replicate the saturation degree after injection is completed at different air pressures in scale models, and allow to conclude that numerical models predict time and space processes of desaturation in place [139]. In a study done by Okamura et al. [122], numerical results are shown compared qualitatively with images taken by a 3D tomography of an improved soil with air injection and quantitatively with results obtained from samples taken by the freezing method, showing compatibility in the magnitude of desaturation and coherence with the measurements taken directly from soil samples extracted by the freezing method.

In order to measure the radius of influence generated by air injection, a centrifuge test in Okamura et al., [9] was performed on an assembly where the non-wetting phase was injected vertically in a saturated soil model, and the diameter of the desaturated region was found to be 5.0 m for an air injection pressure of 95 kPa. Tomida [168] performed similar tests on a highway embankment with a reasonably high non-wetting phase injection pressure. The researchers found that the effective radius of the desaturated plume from the injector (that is amplified with the non-wetting phase pressure and injection duration), extended 9m in 18 hours of duration of the process. Comparing results with compacted sand piles method that handles spacing between stacks less than 2.5 m and injection pressures of 500 kPa, it is recognized that stack-like elements are conservative since the soil is not only densified by the effect of a more rigid material but also desaturated during the execution of the injection [9]. A method to generate compact sand piles has been widely used to a great extent of Japan's coastal areas with the purpose to mitigate the impacts of liquefaction phenomena on foundation soils and coastal dikes [1]. In general, this soil improvement method does not take into account desaturation due to the injection of air under pressure as a direct or indirect benefit of execution. However, it is shown that soils after being improved, have characteristics of desaturation even though they are below the water table and that this state of desaturation by injection of air under pressure is maintained over time [123]. With samples extracted by the freezing technique at three places where the soil was improved with a vibro-substitution method, soil saturation was found to be low, ranging from 68.8% to 92.6%. It was concluded that due to the amount of air applied during construction of elements of improvement, the intention was not to desaturate soil, but it finally did [9]. In Figure 4, it is indicated schematically the procedure of the sand compacted piles installation used in the sites studied by Okamura et al.,[9].

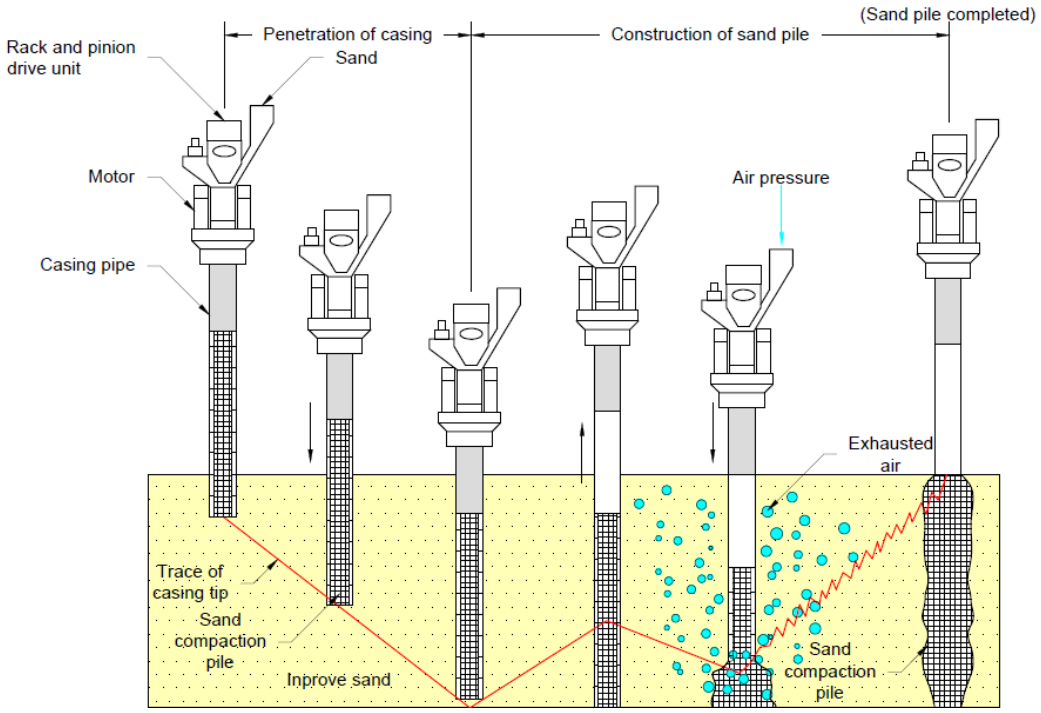

Figure 4 Schematic illustration of sand compacted piles installation procedure, modified from Okamura et al.,[9].

On the other hand, a series of tomographies were performed in an area where the air was injected for desaturation purposes. These indicated that the radius from the injection depth of the desaturated plume, just after stopping the air injection, was approximately 4.0 m for a saturation degree of approximately 60% [122]. Air Injection into the soil is a technique that was developed in the mid-1980s in Germany, to treat saturated soils and groundwater polluted with some volatile organic composites [169]. This technique has been widely used in the field, and there is available information about the approach to improve contaminated soils, such as the work of Lundegard and LaBrecque [170], who carried out field trials to compare methods of measuring the effective soil radius of expansion of non-wetting phase injection. Moreover, non-wetting phase injection into soil can also be used as a technique of improvement of liquefiable soils, besides being executed indirectly in the field during construction of compacted sand piles, it was applied directly by Okamura et al. [122] by implementing an injector tube that was coupled to a flexible pipe through which the non-wetting phase was administered at required pressures. Injection pressure is known to be higher than the sum of hydrostatic pressures (product of hydraulic head at point of injection) and capillary pressures (due to ground), and must be chosen in such way that it does not exceed effective stresses at the point of injection to avoid generating failures and possible cracking of the material [122], [136]. Experimentally, injection pressure at which soil begins to generate cracks corresponds to 80% of effective stresses plus pressure due to the head of water at the injection point [122].

Yasuhara et al. [126] perceived that the higher the non-wetting phase injection pressure, the broader and the uniformity the effective non-wetting phase-entrapped plume that was achieved, which is comparable with the experimental records after Zeybek y Madabhushi [166]. Zeybek and Madabhushi [138] experimentally demonstrated the generation of an excessive settlement of surface foundations during the air injection process because the excessive pressure of the injected air can alter the structure of the soil and can cause cracks and fissures, mostly near of the air injection point. Therefore, it is recognized that although the rise in the air injection pressure is seen as a quick and efficient way of reducing the saturation degree, giving as a result an increase in the

liquefaction resistance, this should be dealt with in detail, particularly in the case of air injection under previously constructed surface foundations. Ogata and Okamura [171] suggested that $(P_{inj})_{max} = P_{hyd} + 0.5\sigma'_v$ gives the maximum theoretical air injection pressure above which the soil skeleton begins to be disturbed, where $(P_{inj})_{max}$, P_{hyd} y σ'_v symbolize the maximum value for the air injection pressure, the hydrostatic pressure at the injection depth and the effective vertical stress at the injection depth, respectively.

Zeybek and Madabhushi [138] perceived that air-generated settlements were unavoidable regardless of the air injection pressure implemented during the process. They related it to the compressible behavior of the partially saturated soils injected with air, and the decrease of the effective effort during the air flow. However, founded on the records of the observations made during the tests shown by Zeybek and Madabhushi [166], the size of the air injection generated settlements can be significantly reduced if: (1) a controlled procedure is maintained throughout the tests (for example, by growing the air pressure in a well-ordered mode and strictly controlling the response of the foundation); (2) the net air injection pressure applied, $(P_{inj})_{net}$, given by $(P_{inj})_{net} = (P_{inj})_{max} - (P_{inj})_{min}$ is ideally lower than 10% of de σ'_v, or it should be ensured that the injection pressure is equal to $(P_{inj})_{net} = (P_{inj})_{max} - (P_{inj})_{min} \leq 0.1\sigma'_v$.

Accordingly, Zeybek and Madabhushi [166], mentioned that air-induced settlements might remain within tolerable values for a field structure in the example of a lower applied net pressure $(P_{inj})_{net}$. It is recognized that Okamura and Noguchi [172] stated that partially saturated soils with uniformly dispersed non-wetting phase bubbles would have equivalent liquefaction resistance as the heterogeneously distributed air bubble soils if sufficient time were allowed for the water within the pores to flow into the air bubbles. However, it is clarified that this finding has not been verified in another document. Thus, the application of a small air pressure can impact the area and the distribution of partially saturated areas, it means that at low injection pressures, it becomes difficult to reach uniformly distributed areas of desaturation, besides, it is clear that the injected air bubbles could have a tendency to flow through preferential flow paths.

From the technique of injecting air into the saturated ground to improve contaminated soil and groundwater, it is known that accurate information about equipment specification and operation can be found in USEPA [173], Wisconsin DNR [174], [175], and Holbrook et al. [176]. Air sparging is an environmental treatment technology that was presented approximately in 1985 Suthersan [177]. The method produces an injection below the water table, with the intention to generate volatilization of contaminants corresponding to solvents or gasoline, volatile organic compounds (VOCs). Furthermore, the method can be used to improve the microbial activity to eliminate less volatile contaminants like diesel or jet fuel. A state of the art of this method shows that the design of the process is mostly empirical and highly dependent on the behavior of in situ test programs, and its evaluation through field monitoring. In general, the method is appropriate for fields with sandy soils having hydraulic conductivities of 10^{-4} or 10^{-3} cm/s or higher, and it is usually implemented at depths less than 10 to 20 m. Representation of a usual air sparging process is depicted in Figure 5.

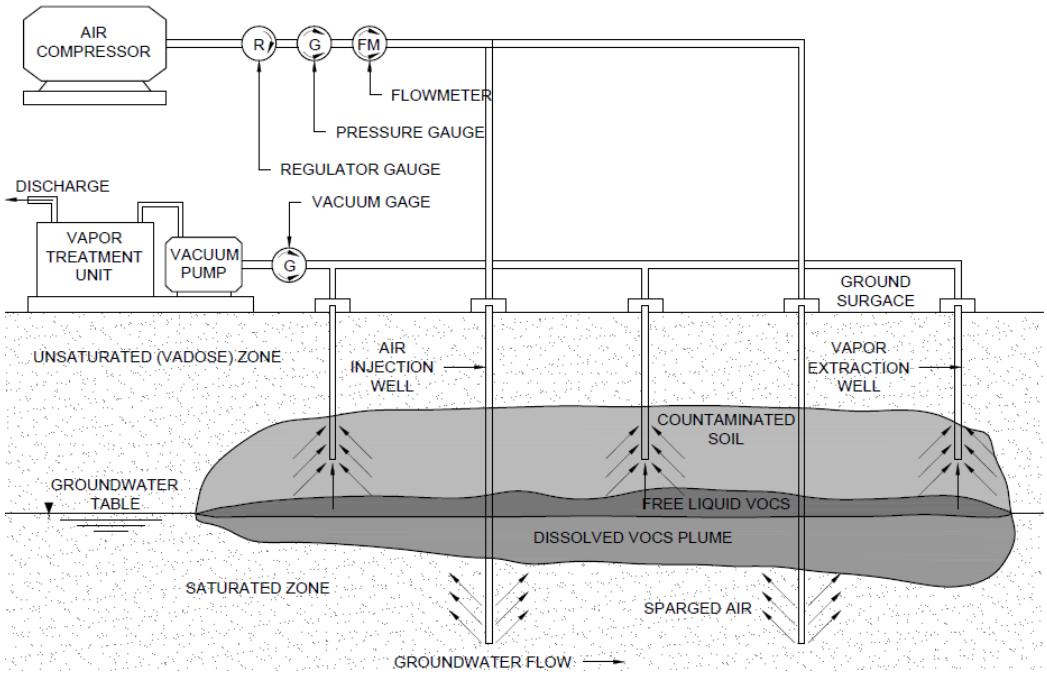

Figure 5 Representation of a usual air sparging operation, modified from Reddy and Adams [169].

Information about air sparging can be implemented as a complement of data shown in the works of Okamura et al. [178], Okamura and Tomida [179] and Tomida [168]. Okamura et al., [178] defined that to build a field system, it is only needed to acquire easy to find materials, and it is not necessary to use any specialized equipment for the design and implementation of the method, those are considered advantages of the air injection technique. In addition, it is recognized that the technique is mechanical in nature, it does not generate pollution, and that the most important factor related to air injection is the radius of influence, which can be restricted by the behavior of air flow in saturated media, i.e., radius and zone of influence dramatically depends on the permeability of soil [178]. Since the influence radius is such an essential factor, accurate measurement is crucial to ensure proper system operation [133], [180]. On the other hand, as an in situ process, it can be implemented with a minimum of disturbance to surface operations, it is efficient and the treatment time would be short in optimum conditions, treatment cost ranges would be significantly lower than those of other treatment technologies, it can be flexible to treat difficult access areas; also, it can be complemented with other technologies to increase breeding efficiency and ultimately it does not involve extraction, treatment, packing or release of groundwater [178], [179].

2.5.2 Electrolysis of water

Partial desaturation of soil by electrolysis of water is a technique to generate decomposition of water (H_2O) into oxygen (O_2) and hydrogen (H_2) gases by a continuous electric current [181]–[183]. It is a technique developed from the knowledge about electrolysis of water and its applications in geotechnical engineering, in order to reduce susceptibility to liquefaction due to the technical feasibility of generating small volumes of non-wetting phase (air) in soils [8].

Furthermore, electrolysis is defined as the ionization of hydrogen and oxygen when an electric current is applied to electrodes in water, and it is developed to trap non-wetting phase molecules in a full wetting phase saturated porous media. Electrolysis was developed as a method to induce partial saturation degree of the wetting phase, introducing gas inside the skeleton pores without the use of a non-wetting phase pressure. The water electrolysis method creates gases (oxygen and hydrogen) in the electrodes (anode and cathode), as is represented next [121]. In the study

performed by Yegian, Eseller, and Alshawabkeh [184], it is shown how a current of 525 mAmp was used for three hours to produce gases in a fully saturated initially sample, obtaining a generation of gases within the sample and a layer of water accumulated above it. The initial saturation degree was 99.7%, after electrolysis it reached 96.3%. Subsequently, it was subjected to a cyclic test, concluding that the maximum pore pressure excess relation did not surpass the value of 0.7 at sample base and 0.43 at the top, i.e., no liquefaction was generated in the sample.

$$At\ the\ cathode: 4H_2O + 4e^- \rightarrow 4OH^- + 2H_2 \uparrow \quad (2)$$

$$At\ the\ anode: H_2O - 4e^- \rightarrow 4H^+ + O_2 \uparrow \quad (3)$$

Yegian, Eseller, and Alshawabkeh [8] develop a series of strain-controlled shaking table tests executed in fully wetting phase saturated and partially wetting phase saturated specimens, both of those prepared by wet pluviation method like Yegian et al. [117] explained. Two spaced 29 cm electrodes (quadrangular meshes of 20cm x 33cm) of mixed metal oxide coated titanium were used for the improvement of the electrolysis productivity. The cathode and the anode were placed at the bottom, and at the top of the model, respectively. The wetting phase saturation degree was recorded by examining the wetting phase level increase in the experimentation box. Finally, the amount of gas produced due to electrolysis was approximately defined by the Faraday's law, as is represented.

$$n(gas) = n(O_2) + n(H_2) = \left(\frac{1}{4}\frac{I}{F} + \frac{1}{2}\frac{1}{F}\right)\Delta t \quad (4)$$

Where n is the moles of the non-wetting phase, I is the electric current applied (525mAmp), F is Faraday's constant $(96.485\ C/mol)$, and Δt is a time interval of the time generation of the current (three hours for the experiment number two). Then mole of non-wetting phase can be changed to volume, as follows:

$$V = \frac{nRT}{P} \quad (5)$$

Knowing that R is ideal gas law constant $(8.314\ Pa\ m^3\ /mol)$; T is temperature (K), and P is absolute gas pressure in Pa $(1\ atm = 101.325\ kPa\ at\ 25°C)$.

Yegian, Eseller, and Alshawabkeh [8] carried out an electrolysis process with a current of $525\ mAmp$ in a fully saturated sample for two tests for periods of 1½ and three h, respectively. The saturation degree, voids relation, and density of the unsaturated sample were defined. As a result, a saturation degree of about 96.3% was obtained. On the other hand, the amount of gas generated within the sample during the process was calculated using Faraday´s mass law and charge equivalence and ideal gases law. It was obtained that the total of gas and volume in 3 h were $0.044\ mol$ and $1.077 cm^3$,

respectively. Setting a 100% efficiency for electrolysis process defines a saturation degree equal to 92.1%, clarifying that efficiency of electrolysis process is usually less than 100%, and no efforts have been invested to knowing more about it so far. The sample was then subjected to a cyclic test, and the maximum pore pressure excess ratios were 0.7 and 0.53 for lower, and upper transducer, respectively. The value of the upper transducer was related to drainage near the free surface of the sample. The test indicated that a reduction in the saturation degree of 99.5 to 96.3% reduces pore excess pressure and for this reduction of 3% in the saturation degree, liquefaction was prevented to begin.

A liquefaction box is developed in order to perform tests under cyclic movement induced on a vibratory table, and after performing the procedure of preparing entirely saturated coarse-grained specimen (sand) in the test container, electrolysis is generated [184]. During the electrolysis method, generation of bubbles inside the sample was perceived through the walls of the assembly, and it was mentioned that the generated bubbles were trapped because it was possible to see an accumulation of free water on the sample that initially was saturated. In turn, on the original sample of saturated sand, no volumetric changes were shown as water was accumulated on the surface, a fact that indicates that electrolysis is generated without perceptible detrimental disturbances in the soil sample [183].

Eseller et al. [183] showed a plan for detection and long-term permanence of gas bubbles in a soil sample to which water electrolysis process was carried out. Experiments were executed by means of a radar (cross-well) to perceive the presence of gas in unsaturated samples, and thus characterize the three-phasic system (sand, water, and gas). This was done in the case of an entirely saturated sample, an unsaturated sample after 24 hours of electrolysis process, and finally 40 hours after completion of the process. Results for the partially saturated sample after 40 hours of completion of electrolysis showed a free water distance of 1.47 cm on the surface of the sample. Also, the saturation degree was 91.5%. A loss of gas is shown over time after the electrolysis process is completed, however, even during the assembly revisions after a week, gas bubbles could still be seen inside. A study of the permanence of gas bubbles in gaps under groundwater flow in both low and high gradients was implemented. For this, constant head flow test facilities were designed. Results indicated that an unrepresentative amount of gas was lost from the upper part of the sample at the beginning of experiments and remained constant even for high gradients. Besides, the saturation degree was measured, indicating an increase from 82.6% to 83.6 %. According to results obtained from these tests, gas bubbles remained within the sample without showing any significant index of possible diffusion.

A column of sand was prepared in Yegian, Eseller, and Alshawabkeh [8] to observe the diffusion of trapped gas after long times. Finally, after 442 days, the wetting phase saturation degree of the coarse-grained (sand) specimen varied from approximately 82.9 to 83.9%. It was also shown that induction of partial saturation in sands in relation to liquefaction resistance and deformations are preferable when the coarse-grained (sand) is of an angular particle than when it is well classified, e.g., Ottawa sand (of rounded particle and uniform gradation).

Industrial application of water electrolysis techniques such as liquefiable soil improvement, numerical modeling, and evaluation of the area of influence of desaturation has not been reported. However, results of recent studies indicate that the technique may be an adequate alternative compared to expensive and invasive generic techniques that can damage the environment. It is recognized that the technique belongs to a young interdisciplinary field and that there are still unknowns that must be taken care of by researchers like the behavior of a sand-water-air mixture in the different initial- field conditions, and exposed to dynamic-cyclic loads; long-term diffusion of non-

wetting phase with a higher overload and a relative small hydraulic gradient; and research in cost-effective in-situ techniques to induce and verify partial saturation in the improved soils.

2.5.3 Microbial method (biogas)

Partial soil desaturation by biogas has been developed for mitigation of susceptibility to soil liquefaction through opportunities and acquired knowledge that has been achieved by interdisciplinary research that converges in microbiology, geochemistry, and civil engineering. Research related to the new discipline called biotechnology in construction is developed in two ways: (1) the biotechnological creation of building materials [185], and (2) the biotechnological construction processes in situ [186], [187]. Mainly, the soil biodesaturation is a method to reduce the wetting phase saturation and, as a consequence, the tendency for the soil to liquefaction by means the generation of in-situ biogas [14], [188], [189]. Bio desaturation is implemented using a physiological cluster of microorganisms called anaerobic nitrate-reducing bacteria (denitrifiers) that generate biogeochemical reactions that develop biogas bubbles in porous media. Some of the implemented denitrifying bacteria and endorsed by the literature are the pseudomonas denitrificans or the paracoccus denitrificans, which decrease the nitrate to nitrogen gas expending, mostly for the reaction, the resource of organic and inorganic electron donors, as the nitrate is an electron acceptor [190]. In summary, the microbial method is implemented by the formation of tiny in-situ gas (N_2) bubbles, using a process of microbial denitrification (i.e., reduction of nitrates NO_3). The nutrients are dissolved in the water and consequently can travel similar to the water in sand [14].

He [191] studied the stress-strength performance and liquefaction susceptibility of biogas desaturated soil through triaxial experimentation. The efficacy of the biogas induction of the wetting saturation degree for the change of soil behavior under dynamic load was tested by means of a laminar box and a shaking table experimental mechanism. A set of experimentations were developed to examine the appropriate circumstances for the generation of denitrifying bacteria and the ideal features for the development of the denitrification process. Three groups of experiments were carried out in the sealed bottles, and developed with three different electron donors like ethanol, sodium acetate, and methanol, respectively, as follows.

$$5C_2H_5OH + 12KNO_3 \rightarrow 10CO_2 + 6N_2 \uparrow + 9H_2O + 12KOH \quad (6)$$

$$5CH_3COONa + 8KNO_3 \rightarrow 10CO_2 + 4N_2 \uparrow + H_2O + 5NaOH + 8KOH \quad (7)$$

$$5CH_3OH + 6KNO_3 \rightarrow 5CO_2 + 3N_2 \uparrow + 7H_2O + 6KOH \quad (8)$$

In the work of He [191], the partial induction of the wetting saturation degree by means of the gas creation reaction was evaluated by means of a small size soil column. The Nitrate (N) concentrations in the specimens were changed starting at 125mg/L and ending at 374mg/L. The reactive process was ended in nearby 3 days, and the reactive process behavior and magnitudes were comparable for all the specimens. The low wetting phase saturation degree that did not generate nitrite aggregation was 82.7% and was sufficient to reduce the liquefaction susceptibility of soil significantly. For specimens constructed with loose sand in the undrained triaxial experiments, the undrained shear strength shows to be greater, while the wetting phase saturation degree come to be lower. When

the Skempton´s B magnitude reduced from approximately 0.95 related to a saturated condition to about 0.3, the undrained shear strength presented a 2.1- time growth in the compression experiments, and a 1.7-times rise in the extension experiments. An instrumented laminar box and a shaking table experimental mechanism were constructed to analyze the liquefaction behavior of biogas partial induction in the wetting phase saturation degree. Experimental results revealed that the liquefaction phenomena were generated for saturated specimens at loose conditions with maximal accelerations of $0.5m/s^2$, and at medium-dense conditions around maximal accelerations of $1.5m/s^2$. Liquefaction phenomena did not develop for biogas application inside any sample with the wetting phase saturation degree around 80% to 95%, assuming similar other situations. Finally, a computer tomography method was implemented to detect the internal pattern and biogas dissemination of the unsaturated soil specimens. For fully saturated soil, the structure of the soil skeleton and pore spaces were reasonably uniform. For partially saturated specimens with the wetting phase degrees of saturation around 88% to97%, were observed some small single non-wetting phase bubbles in the pore spaces. Furthermore, there were a few conglomerated groups of wetting and non-wetting phases generated by the aggregated bubbles in water.

The microbial bioreduction of nitrates by organic compounds in soils susceptible to liquefaction generates a significant amount of nitrogen gas that partially induces the saturation degree and attenuates the generation of excess pore pressure due to cyclic loads [8], [189], [192]–[195]. It is recognized that the liquefaction resistance of the susceptible soils is substantially increased when those are slightly desaturated by the inclusion of gaseous nitrogen produced by the denitrifying bacteria in their voids [188], [189], [193], [196]. The partial induction of the saturation degree through the generation of biogas liquefaction susceptible soils, diminishing the excess pressure of pores and increases the capacity of load and shear resistance of the ground, which benefits the design of foundations and other structures directly [197].

It is clear that dynamic tests should measure liquefaction resistance. However, liquefaction in quasi-static loading settings is significant for the reason that it might be a triggering factor for liquefaction or post-clearance flow failure in some conditions [2]. Notably, He, Chu and Liu [198] showed that for soil desaturation process, a reduction of 100% to 88% was obtained, showing an increase of 24 to 61 kPa in the undrained shear resistance, a behavior of strain hardening for compression tests and a reduction of pore pressure. He and Chu [199]obtained similar results; He, Chu and Xin [200]; in Kavazanjian and O´Donnell [201], and He et al. [202]. He, Chu and Liu [198] also indicated that records acquired from triaxial compression experiments are compared with expressions suggested by Okamura and Soga [11] and Yang et al. [99], explaining the impact of the saturation degree on liquefaction resistance. However, making it clear that the choice of the coefficients will vary depending on whether the test is compression or extension.

Therefore, to study the impact of soil desaturation on its liquefaction susceptibility He, Chu and Ivanov [14] performed 1 g vibration table experiments using a highly instrumented laminar box mechanism. In the assembly, denitrifying bacteria were used to generate bubbles in soil and to reduce the saturation degree of 100% in the sand to the range of 80 to 95%. Results of these tests presented that liquefaction happened in saturated specimens in loose conditions below maximum accelerations and in medium dense states under maximum accelerations of $1.5\ m/s^2$. Nevertheless, no liquefaction occurred for desaturated samples in the same relative density range and under the same input accelerations. It was observed that in most cases, the pore pressure relationships observed were less than 0.5, and settlements and volumetric deformations were considerably small. Facts indicate that biogas technique is effective in decreasing the saturation degree and liquefaction

susceptibility of soils. Comparable effects were achieved by He et al. [202] and Kavazanjian and O´Donnell [201].

Accordingly, Chu [185] developed scale experiments by means of a laminated box and a shaking table to produce dynamic loads in the soil and found out that with only 5% of gas included, the settlements developed in the specimen by the dynamic loads were reduced by 90%. Rebata-Landa and Santamarina [189] induced partial saturation conditions in different soil types (sands, silts, clay soils) by inoculation with Paracoccus denitrificans and a bacterial medium containing nutrients, including nitrates, and demonstrated that the presence of gas bubbles generates a decrease in the measured velocity of the P wave. He et al. [15] exerted shaking table scale models, finding that reducing the saturation degree from 100% to 90% by the biogas method significantly increases the liquefaction resistance. Also, they proved that the more nitrate is annexed to the soil, the lesser the saturation degree. Similar results are shown by He et al. [193], where they used the biological denitrification process to desaturate liquefaction susceptible soils and to show that the volume quantity of gas produced was linearly correlated to the extent of added nitrate, which clearly showed that the saturation degree of the sand could be controlled during the process. In this work, an instrumented laminar box was implemented to study the dynamic behavior of partially saturated specimens. It was shown that the susceptibility to liquefaction decreased (showing that pore pressure excess, volumetric deformation, and differential settlement were lesser than of 100% saturated samples) by reducing the saturation degree of the sample to 95% or less.

Peng and Zhang [203] found that biogas (by Pseudomonas Stutzeri) can be generated when the temperature is between 4 ℃ and 30 ℃ and that the average rate of biogas generation increases along with the temperature. Dynamic tests were performed under an acceleration of 1 m / s^2, and it was observed that the maximum values obtained from pore pressure excess for a sample subjected to partial induction of saturation degree (Sr = 85.2%) were significantly lower than those obtained for samples with a saturation degree of 100%. For the same magnitude of the acceleration, it was obtained that the surface settlements of the samples subject to the partial induction of the saturation degree (Sr = 85.2%) were approximately one third than those obtained in the samples with a saturation degree of the 100%, this after being applied the sine wave 5 times. Moreover, the exponential relation among volumetric strain and average pore water pressure ratio was calculated for full and partially saturated samples. Particularly, the volumetric strain for full saturation sand samples starts to increase at a more accelerating rate than partially saturated samples after the average pore water pressure ratio is upper than 0.2.

Also, a method that combines biogas generation with biocement was developed by Sean O'Donnell [204]. This shows denitrification as a technique for the reduction of the liquefaction executed in a two-stage process, in which desaturation occurs in stage 1 and the precipitation of carbonates occurs in stage 2. P-wave velocity and dialysis bag measurements showed that desaturation developed rapidly after the onset of denitrification (one to three days). Subsequently, direct-shear cyclic tests were performed with different degrees of saturation, and it was shown that only a 3% reduction in the saturation degree resulted in an improvement of more than 40% in the cyclic resistance. The results mentioned before prove that if the production of gas from denitrifying microorganisms induces a degree of partial saturation of 97%, significant decreases in susceptibility to liquefaction are expected. Also, triaxial tests were performed with/without drainage and dynamic direct simple shear on the treated samples and improvements were observed in stiffness, resistance, and dilation with a carbonate content of less than 1%. On the other hand, it was perceived that the effect on the mechanical properties of the soil improved with increasing carbonate, regardless of the initial relative density or the soil type. Similar results from a two-stage process or a method that combines

biogas generation with biocement (using acidovorax sp. DN1) that can enhance the stability of the biogas bubbles in the sand is proposed by Li [205].

In Kavazanjian and O'Donnell [201], cyclic tests showed that decreases in the saturation degree by 1-3% lead to increases of more than 40% in liquefaction resistance. He et al. [202] concluded that the final wetting phase saturation degree is associated to the primary nitrate concentration implemented in the desaturation solution, i.e., the greater the nitrate concentration, the lesser the wetting phase saturation degree. It was found out by tomographies that gaseous phase of unsaturated soil is in the shape of small gas bubble bags that are slightly larger than a grain of sand. A permanence (long-term) problem of the gas bubbles in the improved soil was observed during ascending or horizontal mobilization of water, which is still the most influential characteristic for the field application of the method. In a flow analysis, similar to the one used by Yegian, Eseller and Alshawabkeh [8], it was proved that the gas phase in desaturated soils by biogas was consistent in hydrostatic state, but it turns into unstable under circumstances of constant flow; therefore, precautions must be taken to avoid constant water flow if it is implemented such a desaturation method. This is consistent with the observations of studies made by Li [205] and He [191] that proved that gas bubbles were consistent in hydrostatic conditions. However, gas bubbles in the sand were not consistent below upward, or downward water flows if bio-sealing was not implemented. Also, Sean O'Donnell [204], studied soil columns subjected to continuous flow and demonstrated the applicability of denitrification as a method implemented in two steps for the decrease of susceptibility to liquefaction. Finally, a test by Sean O'Donnell [204] presented that soil columns subjected to continuous flow showed the applicability of denitrification as a method implemented in two steps for liquefaction mitigation under field conditions. The results of the continuous column flow tests indicated that in-situ denitrifying organisms must be bio-stimulated. However, initial nitrate flow and concentrations are fundamental variables in the rate and magnitude of soil improvement through denitrification, because at higher concentrations and higher flow rates both excessive accumulations of nitrite and inhibition can contribute to the development of microbial growth.

An evident problem is recognized in the experiment of the vertical or horizontal water flow on the permanence of the non-wetting phase bubbles in the unsaturated sand. He [191] perceived that for the creation of in-situ biogas by denitrifying bacteria, the nitrogen bubbles were not consistent during ascending or descending water flows with a hydraulic gradient equal to 0.1, and for a sand column assembly of 1 m in length. The bubbles generated in the samples dissipated after 2-4 days, which gradually increased the saturation degree of the mounts up to 100%. In order to develop additional technological solutions to guarantee the permanence(long-term) of sand partially desaturation below groundwater flows, it is proposed to combine the production of in-situ biogas with biosealing due to a small amount of biocement for stabilize the gas bubbles in the soil and generate the partial wetting phase saturation degree induction in the long term. Additional information about mitigation of susceptibility of sand liquefaction by means of the in-situ generation of biogas with biosealing is defined in work done by Li [205].

In addition to economic advantages of the biogas technique in comparison to the commonly used techniques, it is recognized that, since the viscosity of the mixture flow (microbes and nutrients) is low, the mixture can diffuse easily through the soil. Therefore nitrogen (inert gas chemically stable with a density similar to the air) bubbles can be evenly distributed. It is important to mention that generated gas bubbles had a small diameter which makes them difficult to dissolve in water and to flow out from the soil. This technique is energy efficient since no extraordinary energy expenditure mechanism is implemented in the method; it can reduce susceptibility to liquefaction without

altering soil skeleton due to excavations, it means that it generates minimum alterations of the place and can be implemented to existent and susceptible constructions [5], [186], [200], [206]. On the other hand, it is clear that various factors and incomplete reaction processes impact microbial methods are by can produce several toxic materials such as nitrite [14], [189]. Detailed information of limiting factors for microbial denitrification due to high nitrate concentration are mentioned in Van Paassen et al.,[207]. Limiting variables such as pH are mentioned in Saleh-Lakha et al.,[208], temperature effects are included in Stanford et al.,[209] and finally on the presence of oxygen in Saleh-Lakha et al.,[208].

Building materials biotechnologically developed and construction technologies through the application of microbiology have several advantages compared to conventional building materials and processes [210]. Dejong et al.[187] assumed standard of price, method implementation, and success ratio, and community recognition to estimate the potential of diverse biogeochemical methods. Between these methods, biogas obtained a good qualification and acceptance, indicating its high potential in its implementation. In general, biotechnology is used for the manufacture of building supplies due to the low cost of the raw materials, such as those resulting from mining or organic waste [190]; lower costs compared to products resulting from the chemical industry, due to less elaborate and more efficient technologies (less energy consuming) [187]; less toxicity of biomaterials than those resultant from chemical materials [7]; and environmental sustainability of biotechnological production [196]. On the other hand, representative feature for example the low viscosity and the penetration capacity of this solution in the soil [185]; the versatility to define the speed of biochemical reactions by the mixture or characteristics of the biomass or enzyme [7]; the facility with which microbial cells self-multiply during the process[205] has excellent public acceptance related to minor environmental impacts of biotreatment rather than chemical treatment [187]. It should be mentioned that theoretically, a mixture of biotechnology treatments, biogeochemical and mechanical treatments can achieve higher efficiency values than those obtained by a particular category of soil improvement. However, it is clear that so far, a considerable amount of research has not been developed implementing combinations of the different methodologies.

Therefore, it is necessary to study the modeling of biogeochemical processes due to the need for integrating biological and chemical components with modeling methodologies (mechanical and hydraulic). Modeling methodologies that have been formulated in numerical modeling codes applied to geotechnics, and include formulations of finite elements and finite differences endorsed by the scientific community as well as the generation of a mathematical formulation (constitutive model) capable of describing the operation of soils treated with biotechnology. It is recognized that there are severe difficulties related to the modeling of spatial variability (micro-geochemical processes that occur at micrometric scale) of the microbes against the particles that compose the soil skeleton and the choice of an appropriate transition between discrete (represented by the microbes) and continuous (represented by the soil skeleton) scales versus the necessary velocity for the reactions and porosity values to occur, respectively [187].

Despite the above, there is no evidence of the industrial application of biogas as a liquefiable soils improvement technique. Little is known about the longevity of bubbles generated in the soil, numerical modeling, and evaluation of the area of influence of desaturation. However, recent studies indicate that the technique may be an adequate alternative compared to expensive and environmentally invasive generic techniques. The technique belongs to a young interdisciplinary field, and despite the unknowns, this technique must be taken in to account by the researchers. The technique of soil improvement through the generation of biogas requires significant advances in thematic issues related to system heterogeneity, soil phases and porosity, multistage flow and

variety of species. Each one of the topics already mentioned requires research, as both engineering and basic science were developed from their respective disciplines.

2.5.4 Chemical method (chemical reactions)

This technique uses a chemical compound that is the main ingredient of dental product "Efferdent", a compound that mainly reacts producing oxygen gases when contacted with water. This ingredient is called sodium perborate (48% Efferdent), which is a white crystalline powder, that crystallizes as monohydrate or tetrahydrate in water. When sodium perborate monohydrate ($NaBO_3H_2O$) makes a reaction when it comes into contact with water, it produces hydrogen peroxide (H_2O_2), which is a considerable fount of oxygen [13]. It is known that sodium percarbonate can dissolve in water with a defined solubility of 140 g /l at 20 °C. Besides, as a basic solution, it has a pH of 10.5 at a concentration of 1% at 20 °C, and eventually when it is injected into the porous media the pH of the groundwater increases. However, it is known that the pH in the porous media returns to its original level approximately four weeks after the reaction [19]. The sodium percarbonate that was used for the application to generate oxygen gas is commonly used in other applications. For instance, Sodium percarbonate is the primary constituent in the domestic cleaning agents, and it is generally employed because it is environmentally friendly and easy to apply without health and security concerns. Moreover, the injection of sodium percarbonate solution concentration is usually applied in the bioremediation of soils to remove organic contaminants [211]. As a consequence, the reaction of the sodium percarbonate solution through its transport in soil generates non-wetting phase bubbles that stay entrapped in the pore space, and induce the wetting phase partial saturation inside a defined zone, as follows in Figure 6.

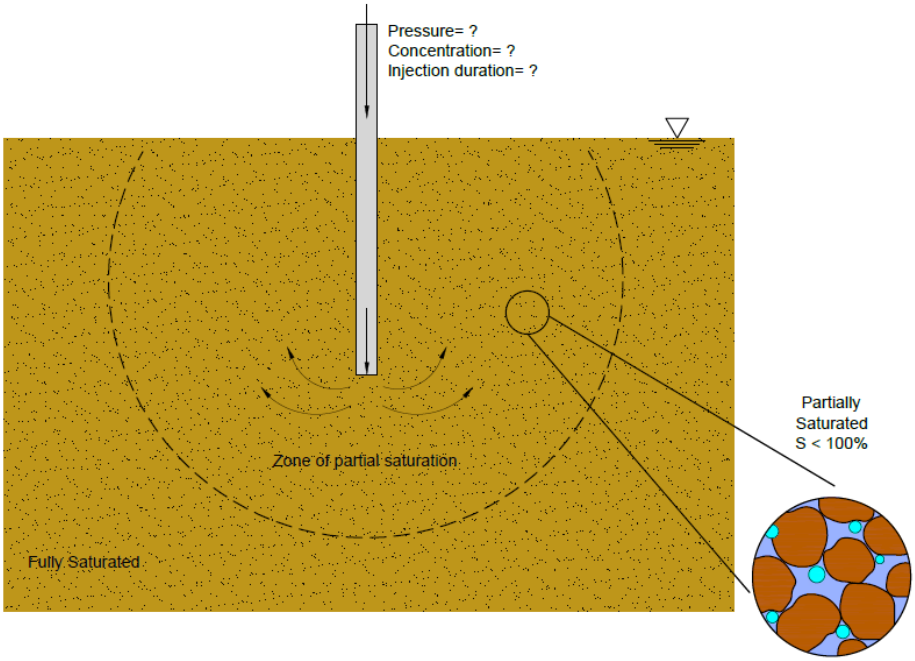

Figure 6 Sketch describing wetting phase induced partial saturation through transport and reactivity, modified from Gokyer [19].

Eseller-Bayat [212] induced different degrees of saturation by the generation of uniformly distributed gas bubbles (confirmed by wave measurements) with dispersed dry sand and Efferdent powder mixtures in predetermined amounts of water and proportions of Efferdent to sand. Also, the consequences of the gas bubble generation in the pore pressure were studied, performing dynamic

tests of simple shear and observing that the excesses of pore pressure generated never reached the initial liquefaction and, on the contrary, reached a maximum value that remained stable under the continuous application of shear strain cycles. In Eseller-Bayat et al. [13], cyclic tests were performed on totally saturated samples generating initial liquefaction. Moreover, samples of partially saturated sand with a saturation degree of less than 90% do not reach initial liquefaction. Similar results were found in Yegian et al. [8] for a saturation degree of 96.3%, and it was also concluded that for a defined wetting phase saturation degree and a particular shear strain amplitude, the higher the relative density, the lesser the maximum pore pressure value. For a particular saturation degree and relative density, the higher the deformation amplitude, the higher the maximum pore pressure.

Besides, desaturation in sands can be prolonged in time even below gradients of pressure (flow) and a cyclic load at the base. Partially saturated samples were evaluated below hydrostatic conditions, vertical flow gradients and horizontal dynamic load at base showed a rise of a smaller amount of than 2% in the saturation degree, representing that a desaturation in sands can be invariably over an extended period, as also established by Okamura et al. [123].

Furthermore, Gokyer [19] investigated the theoretic fundaments of partial induction in the wetting phase saturation degree and developed a numerical approach for simulating the desaturation phenomena in the liquefiable soil, generated by the application of the theory of transport and the reaction of a chemical solution inside the pore spaces. The numerical solution was named SUTRA-Bubble and is founded on a coupled partial differential equations system. The partial differential equation system characterizes a three-dimensional, transient, hydraulic non-linear flow, reactive chemical transport (advective-dispersive) coupled employing algebraic equations for describing the chemical kinetics, oxygen gas generation, and wetting phase saturation degree related decrease. The numerical model SUTRA-Bubble was validated by matching its results with experimental results. Mainly, a set of small and large laboratory scale tests were developed and related to a defined pressure and concentration of sodium percarbonate mixture injection inside a soil sample. Notably, the sodium percarbonate was selected to the application because of its gas generation reaction slow rate in water. The sodium percarbonate dissolves in water and dissociates into sodium and carbonate ions, as well as the hydrogen peroxide, which is the oxygen gas bubbles source, as follows in the related chemical expressions.

$$Na_2CO_3.1.5H_2O_2 \rightarrow in\ water \rightarrow 2Na^{+1} + CO_3{}^{2-} + 1.5H_2O_2(at\ the\ end\ of\ rection) \quad (9)$$

$$1.5H_2O_2 \rightarrow in\ water \rightarrow 1.5H_2O + 0.75O_2(ideal\ conditions - 100\%\ efficiency) \quad (10)$$

The SUTRA-Bubble numerical results of the partial wetting phase saturation degree plume and the wetting phase saturation degree were comparable with the small and large laboratory scale tests results. Furthermore, to design an implementation program or methodology, the numerical model could be implemented for the study and design of in-situ application of the partial wetting phase saturation degree induction. Numerical model can be used for calculating the injection pressure and the time interval of a particular chemical solution concentration to generate the required degree and plume of partial wetting phase saturation degree and concentration of sodium percarbonate. The extension of the plume of the partial wetting phase saturation degree depends on the injection pressure during injection of the solution, and the values of the saturation degree obtained in the

partially saturated zone (the plume) are entirely dependent on the chemical solution concentration. The extension of the plume of the partial wetting phase saturation degree supports the analysis of the definition of the distribution or geometric separation of the injection points in the in-situ application of the method. It is necessary to reach a defined plume of the partial wetting phase saturation degree by means of the injection of a chemical solution concentration, for that reason, the gas generation must be slow enough to allow the injected solution to be transported without bubble clogging in the porous media [19].

Industrial application of chemical reactions techniques such as liquefiable soil improvement and evaluation of the area of influence of desaturation has not been reported yet. However, results of recent studies indicate that the technique may be an adequate alternative compared to expensive and invasive generic techniques that can damage the environment. It is known that the technique belongs to a young interdisciplinary field and that there are still unknowns that must be taken care of by researchers.

2.6 REMARKS, LIMITATIONS AND KNOWLEDGE GAPS

It has been shown that techniques to improve liquefiable soils using partial induction of saturation degree are effective. Due to the implementation of readily available equipment and overall results of methods, partial induction of saturation can offer significant savings compared to the commonly applied methodologies to mitigate liquefaction. Some of the parameters that revolve around methodologies are controlled and would allow a flexible implementation. Also, a given conformation of methods could be proposed as a combined system to improve effects on soil.

Few systems to generate a partial induction of saturation degree have been designed, operated and monitored in the field, under different conditions. On-site performance data would be helpful to identify the advantages and limitations of the techniques, as well as a database to use as a guide for future systems. In order to have an efficient performance, it is essential to carry out a detailed geological and hydrogeological characterization before implementing partial saturation induction methods. Site characterization will also provide valuable information regarding the radius of influence or radius of desaturation.

Partial induction of saturation degree is increasingly being studied due to its low cost and significantly reduced treatment time, compared to the high cost and prolonged treatment time associated with conventional remediation technologies. In general, acceptance of partial induction of saturation degree by regulatory agencies may happen when the subsequent requirements are met: (1) to control the saturation degree ; (2) homogeneity in the distribution of gas generated in the soil pores ; (3) gas bubbles longevity (this requires gases with low solubility, inert chemical features and consistency to remain trapped in the soil); (4) the estimation of the extension of desaturation plume produced by techniques; (5) cost-effectiveness when executed in large areas and small areas.

Desaturation process for liquefaction mitigation is still a relatively new technology, and much more needs to be investigated and learned about how it works and how it can be better applied. Most of the laboratory work done till today includes simplifications that may restrict the applicability of the results to field situations. Additionally, field studies have not been monitored and documented enough to understand soil desaturation processes in depth. Consequently, many of the models developed by researchers so far, include idealistic simplifications or have not been validated with laboratory or field works. Therefore, in order to advance in the state of art of the techniques respect to partial induction of saturation degree, controlled laboratory and in-situ tests should be performed with the purpose to study a wide range of parameters controlled by operators, and specific

parameters depending on in-situ conditions. Finally, a complete evaluation of field systems to develop more realistic mathematical models (responsible for describing and predicting the behavior during desaturation application) should be done.

It should be noted that air infiltration in saturated soils, desaturation and deformation are concurrent processes (the last two entirely dependent on the former). It is necessary to study processes of air infiltration in soils, using coupled infiltration-deformation methods that reflect variations of safety factors over time. The study of air infiltration in saturated soil and corresponding soil response through desaturation, deformations, and faults is a complex behavior since it is controlled by a large number of nonlinear variables associated with hydraulics, constitutive properties of soils and characteristics of the injected air. Being aware of the phenomena nonlinearities occurring in soil and the effect they have on human life, the study of improvement of liquefiable soils with the generation of gas bubbles becomes a subject of great interest and importance. It is necessary to clearly understand how this process of improvement, influences desaturation and deformation of soils, and in consequence, allows to decrease the susceptibility of liquefaction.

3 MULTIPHASE FLOW IN POROUS MEDIA MODEL DESCRIPTION

A mathematical study of multiphase flow in soil is of broad relevance in several disciplines of science and engineering corresponding to hydrology and groundwater flow (infiltration and recharge, by precipitation, irrigation, or artificial recharge), oil and gas reservoirs, gas-liquid contactors, waste management (movement of pollutants with infiltration caused by landfills or fertilizers), biodegradation, and more [213]. Therefore, studies of flow and transport in the partially saturated soil are restricted to the capillary zone above the water table. In this work, just the standard mechanisms of biphasic flow are included, i.e., an incompressible and isothermal biphasic flow in homogeneous porous media with capillary effects. Another physical behavior like compressibility by pressure and phase changes by variations in temperature are not in the objectives of this work but are potential developments of the existing model.

In this work, a mathematical model to simulate biphasic flow in porous media is defined as an alternative to solve a modified Navier-Stokes problem with the usually called Darcy– Forchheimer law [214]. It is resolved the mass conservation of pore fluid problem for the non-wetting and wetting phase, where fluid velocities are stated through a generalization of Darcy´s law, as is presented by Van Dijke et al [215], Horgue et al [213], Ziagos et al [216] and Pinder and Gray [217]. This is because of some fundamental definitions to the mathematical modeling of these phenomena, for example, the phase saturation degree, non-wetting and wetting phase relative permeability functions, capillarity pressure models, and particular types of boundary conditions must be incorporated in the study. Complete states of the art of mathematical approaches scientifically available to resolve this kind of systems of partial differential equations can be found in Aziz and Settari [218], Gerritsen and Durlofsky [219]or Chen et al. [220].

Darcy's law defines the equation of flow in saturated soil. Darcy's law equation also applies for biphasic flow in partially saturated soils Fredlund and Rahardjo [18]. However, in partially saturated soils the permeability coefficient is different as the used for fully saturated soils, because it may be modified through the flow. The governing equations of flow in a partially saturated zone is derived by combining Darcy's velocity equation with mass conservation of the pore fluid Bear [221]. Simulation methods for the flow of fluid in an unsaturated zone are all based on this governing equation.

In the experimental setup for gas and water, gas enters from an injector inside the domain made of water and sand (soil skeleton). The incoming gas (the non-wetting phase) forces the water (the wetting phase) toward the outlet at the top boundary of the domain. At the inlet, the gas pressure is constant in time, and no water exits through the domain bottom. Neither the gas nor the water can pass through the base and the vertical walls. The water and gas pressures at the outlet are equal to zero. The domain has a total height of 30 m and a 30 m width.

3.1 MATHEMATICAL MODEL

3.1.1 Mass-momentum conservation equations

The partial induction in the saturation degree by the air flow through air injection is treated as a biphasic flow problem. The mathematical model is established on Darcy's law for both the non-wetting phase air, nw, and the wetting phase water, w, as demarcated by the following expression:

$$\vec{U}_i = \left[-\frac{k_{int}k_{r,i}}{\mu_i}(\nabla p_i + \rho_i g \nabla D)\right] \qquad i = w, nw \tag{11}$$

Considering a porous medium incompressible biphasic flow, the macro-scale balance equation for each phase i is as follows:

$$\theta\frac{\partial S_i}{\partial t} + \nabla \cdot \vec{U}_i = 0 \qquad i = w, nw \tag{12}$$

Where θ is the total porosity; S_i is the saturation; t is time; k_{int} is the intrinsic permeability of the fluid i (m^2); $k_{r,i}$ is the relative permeability (a function of saturation for a given fluid); μ_i is the fluid's dynamic viscosity $(Pa \cdot s)$; p_i is the fluid pressure (Pa); ρ_i is the fluid density (kg/m^3); g is acceleration of gravity; and D is the coordinate (for example, $x, y,$ or z) of vertical elevation (m), or $D(y)$ is the depth of the reservoir. $\vec{U}_i$ is the phase velocity traveling through the cross-sectional area for pore fluid, that is part of the total area of the porous medium, and it is conditioned to the total porosity θ, and each phase saturation S_i. The driving forces determine the phase velocity for the flow, namely the phase pressure and buoyancy forces, and by the phase mobility, that is the product of the intrinsic permeability k_{int}, relative permeability $k_{r,i}$, and phase viscosity μ_i. Essentially, the permeability is a representative feature of the porous medium that reproduces the ease with a phase flows through the porous medium when it is fully saturated. Additionally, the relative permeability is a reduction factor for the permeability when partial saturation occurs in the porous medium. The concept of relative permeability describes the fact that immiscible fluids tend to interfere with another fluid as they flow through soil. The presence of one fluid in a given pore through which a second fluid is flowing will reduce the permeability of the medium to the second fluid [222]. Relative permeability is therefore closely related to the saturation degree of both phases, as illustrated as follows in Figure 7.

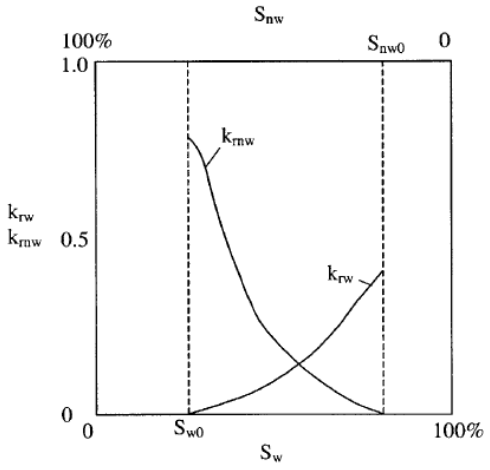

Figure 7 Typical relative permeability curves [223]

As shown in Figure 7, the sum of the two permeabilities is typically smaller than one, implying that there are pores containing fluid that do not contribute to flow [222]. The rapid decrease of $k_{r,w}$, the relative permeability to the wetting phase, indicates that the larger pores (i.e., the higher volume of fluid) is occupied by the non-wetting phase first. As the S_{nw}, increases, the average pore size

saturated by the wetting phase becomes smaller, which also leads to an increase in $k_{r,nw}$, the relative permeability to the non-wetting phase [223]. In this context, the Viscosity affects the ease of phase flow and is defined by the temperature. The driving forces for the flow of a phase through the pore volume are a combination of phase pressure and density gradient as in the term of phase potential $(\boldsymbol{\nabla} p_i + \rho_i g \boldsymbol{\nabla} D)$ that make part of the Darcy equation for each phase. The combined effects of interfacial tension and wettability, capillarity, relative permeability and grain size distribution on biphasic flow through a soil effectively cause the wetting fluid to be preferentially driven into the small pores of the medium, while the non-wetting fluid preferentially flows into the larger pores [222]. Biphasic flow in soil follows separate equations for the wetting phase,w, and nonwetting phase,nw, fluids. Taking into account that an incompressible biphasic flow in a homogeneous and isotropic skeleton, the macro-scale mass balance equation for each phase i with the superficial velocity given by the generalized Darcy's model reads:

$$\theta \frac{\partial S_w}{\partial t} + \boldsymbol{\nabla} \cdot \left[-\frac{k_{int} k_{r,w}}{\mu_w} (\boldsymbol{\nabla} p_w + \rho_w g \boldsymbol{\nabla} D) \right] = 0 \tag{13}$$

$$\theta \frac{\partial S_{nw}}{\partial t} + \boldsymbol{\nabla} \cdot \left[-\frac{k_{int} k_{r,nw}}{\mu_{nw}} (\boldsymbol{\nabla} p_{nw} + \rho_{nw} g \boldsymbol{\nabla} D) \right] = 0 \tag{14}$$

In this work, it is studied the flow of a non-wetting (nw) phase and wetting (w) phase through the soil. The saturation, S_i, varies from 0 to 1. Non-wetting and wetting phase saturations responds to the next expression for biphasic flow in a soil skeleton. Equations are combined with the constitutive relation:

$$S_w + S_{nw} = 1 \tag{15}$$

In relation to the capillary features related to the soil, there is no equilibrium among averaged pressure responses corresponding to the non-wetting and the wetting phase. In traditional biphasic flow in soil method, it is usually defined as macro-scale capillary pressure p_c function of the wetting phase saturation S_w. However, is important to know that sometimes the capillary pressures for coarse-grained materials, as liquefiable sands, are negligible compared to wetting phase pressures, and flow mathematical models can be defined merely considering the advancement of the advective front [224]. The capillary pressure or suction p_c is commonly defined as the difference between the pressure of the non-wetting and wetting phases, then:

$$p_c(S_w) = p_{nw} - p_w \tag{16}$$

The capillary pressure correlation and the saturation relationship eliminates two unknowns of the system and the mass conservation of the pore fluid equations read:

$$-\theta\frac{\partial S_{nw}}{\partial t}+\boldsymbol{\nabla}\cdot\left[-\frac{k_{int}k_{r,w}}{\mu_w}(\boldsymbol{\nabla}(p_{nw}-p_c(S_w))+\rho_w g\boldsymbol{\nabla}D)\right]=0 \quad (17)$$

$$\theta\frac{\partial S_{nw}}{\partial t}+\boldsymbol{\nabla}\cdot\left[-\frac{k_{int}k_{r,nw}}{\mu_{nw}}(\boldsymbol{\nabla}p_{nw}+\rho_{nw}g\boldsymbol{\nabla}D)\right]=0 \quad (18)$$

With p_{nw} and S_{nw} the system variables. The partial differential equation scheme defined by the mass conservation expressions has a lot of non-linearities since the implementation relative permeability functions $k_{r,w}$ and $k_{r,nw}$.

3.1.2 Model formulation

The mass conservation of the pore fluid expressions is written in the form a pressure (the global mass conservation)–saturation system by summing Equations. The system then reads:

$$\boldsymbol{\nabla}\cdot\left[-\frac{k_{int}k_{r,w}}{\mu_w}(\boldsymbol{\nabla}p_{nw}+\rho_w g\boldsymbol{\nabla}D-\boldsymbol{\nabla}p_c(S_w))+-\frac{k_{int}k_{r,nw}}{\mu_{nw}}(\boldsymbol{\nabla}p_{nw}+\rho_{nw}g\boldsymbol{\nabla}D)\right]=0 \quad (19)$$

$$\theta\frac{\partial S_{nw}}{\partial t}+\boldsymbol{\nabla}\cdot\left[-\frac{k_{int}k_{r,nw}}{\mu_{nw}}(\boldsymbol{\nabla}p_{nw}+\rho_{nw}g\boldsymbol{\nabla}D)\right]=0 \quad (20)$$

Furthermore, it is essential to stabilize the non-wetting phase saturation expression (the one with temporal derivative) in the current method by including a stabilizing expression,$\varepsilon\Delta s$, a little artificial diffusion that helps smooth the solution to the equation of balance for the non-wetting phase. (The notation, AΔs, denotes the Laplacian of the non-wetting phase saturation degree). Magnitudes of ε are appropriately small to preserve the fundamental integrity of the presented non-wetting phase saturation degree partial differential equation.

3.1.3 Implemented formulation

To make simpler the formulation of the equations, the phase mobility M_i and the gravitational contribution L_i are included as follows:

$$M_i=\frac{k_{int}k_{r,i}(Se_{w,eff})}{\mu_i} \quad (21)$$

$$L_i=\frac{k_{int}k_{r,i}(Se_{w,eff})}{\mu_i}\rho_i \quad (22)$$

Although, that in the generalized Darcy's law the expression $L_i=M_i\rho_i$ is satisfied, it is appropriate to disaggregate each phase influence respectively. Primarily, it is observed that intricate models including viscous resistance parameters between phases, for example, Raats and Klute [225], and Baveye and Sposito [226] can be functional with this generic approach. Moreover, supposing that the

capillary pressure merely is governed by the saturation degree of the wetting phase, the capillary term ∇_{p_c} can be redefined as:

$$\nabla p_c\left(Se_{w,p_c}\right) = \frac{\partial p_c}{\partial S_w}\nabla S_w \tag{23}$$

A term that allows to reformulating the pressure equation as:

$$\nabla \cdot \left[-\frac{k_{int}k_{r,w}}{\mu_w}\left(\nabla p_{nw} + \rho_w g\nabla D - \frac{\partial p_c}{\partial S_w}\nabla S_w\right) + -\frac{k_{int}k_{r,nw}}{\mu_{nw}}\left(\nabla p_{nw} + \rho_{nw} g\nabla D\right)\right] = 0 \tag{24}$$

Alternatively, admits to redefine the pressure equation as a Poisson-type equation:

$$\nabla \cdot [(M_w + M_{nw})\nabla p_{nw}] = -\nabla \cdot \left[(L_w + L_{nw})g\nabla D - M_w \frac{\partial p_c}{\partial Se_w}\nabla S_w\right] \tag{25}$$

Also, the saturation degree of the non-wetting phase equation as:

$$\theta\frac{\partial S_{nw}}{\partial t} + \nabla \cdot (-M_{nw}\nabla p_{nw} - L_{nw} g\nabla D) = 0 \tag{26}$$

3.1.4 Hydraulic Properties of Unsaturated Soils

3.1.4.1 Relative permeability relationships

Mathematical model includes the concept of effective saturation degree of the wetting phase that is a normalization of the wetting phase saturation degree, then:

$$Se_{w,eff} = \left(\frac{S_w - S_{w,irr}}{1 - S_{nw,irr} - S_{w,irr}}\right) \tag{27}$$

Where $S_{nw,irr}$ and $S_{w,irr}$ are the demarcated irreducible and minimal wetting phase and non-wetting phase saturation degree nw and, correspondingly. In the present model, $k_{r,w}$ and $k_{r,nw}$ are the non-dimensional permeability functions for the wetting and the non-wetting phase, respectively. Typically, $k_{r,w}$ and $k_{r,nw}$ are the function of two of three probable volume and mass features, called, the wetting phase saturation degree, void ratio, and volumetric wetting phase content [227], [228]. The relative permeability function of each phase takes a magnitude in the interval of 0 to 1, including both, and it is determined by the localized wetting phase saturation degree S_w. This model proposes that the existence of additional fluid in the pore spaces of the soil decreases the pore space

accessible, and consequently, diminishes the permeability [217]. In a more complex examination, the permeability is supposed to be modified by the saturation degree and void ratio, but in the present analysis the hydraulic properties relative to the wetting and non-wetting fluid in Van Genuchten [229] retention model are the influence of saturation degree on permeability functions for wetting and non-wetting phase and are assumed as:

$$k_{r,w} = {Se_{w,eff}}^{a}\left[1-\left(1-\left(Se_{w,eff}\right)^{\frac{1}{m}}\right)^{m}\right]^{2} \tag{28}$$

$$k_{r,nw} = \left(1-Se_{w,eff}\right)^{b}\left(1-\left(Se_{w,eff}\right)^{\frac{1}{m}}\right)^{2m} \tag{29}$$

Where a and b are the shape parameter of wetting phase permeability and the shape parameter of non-wetting phase permeability, respectively, and m and n' are the material parameters in the Van Genuchten [229] expressions. Corey [230] stated that two essential topics limit the effectiveness of defining relative permeability relations from the disposition of the pore sizes and $p_c(S_w)$ functions. They are: (1) the resulting definitions that are effective just for S_w a reduced amount of than approximately 0.85, for the reason that the water and retention records does not reproduce the disposition of the pore sizes at saturations near 1.0 ever since phase n is obstructed to flow into every zone of the porous medium at drainage process at this state; (2) the relative permeability functions are defined for an isotropic material. The relative permeabilities are scalar values that do not take into account the anisotropy, and it is because the moisture and retention information does not reproduce the properties in every direction of the porous material.

Additionally, the material connectivity (between pores) fitting parameters, a and b, have to be defined typically when experimental information of the functions of relative permeability are fitted. These material parameters reproduce the influence of the relationship concerning pore sizes and the ease (tortuosity) of the flow paths. Recognizing the information achieved from experiments of wetting phase flow for fifty samples, Mualem [231] stated that $a = 0.5$ generates a right adjust of the information, and this magnitude must be implemented as an original supposition when wetting - phase records are related. Furthermore, it is realistic to suppose that the tortuous trend tracked by a non-wetting phase will be slightly smaller than that tracked by the wetting phase because the non-wetting phase does not have a tendency to follow the solid phase boundary or passing into the smallest pore spaces [217]. Then, the parameter b is estimated to be smaller than the parameter a. For the non-wetting phase (air) - wetting phase (water) system, parameter $b = 0.33$ is suggested as a first supposition. A clear difference of the adjusted parameters from these suggested values is like a warning that shows that the $p_c(S_w)$ function is not an acceptable interpreter of the disposition of the pore sizes [232].

3.1.4.2 Soil-water Characteristic Curve and capillary pressure model

The capillary pressure equation is founded on the concept of effective wetting phase saturation degree. Nevertheless, the macro-scale capillary pressure goes to high values(infinity) when the wetting phase saturation S_w have a tendency to $S_{w,irr}$ (and its derivative when S_w goes to $S_{w,max}$ in the Van Genuchten equations [229]). To the application of the irreducible and maximal saturation in the model, it is defined the effective saturation for capillary pressure Se_{w,p_c} as follows.

$$Se_{w,Pc} = \left(\frac{S_w - Se_{Pc,irr}}{Se_{Pc,max} - Se_{Pc,irr}} \right) \tag{30}$$

The minimal $Se_{Pc,irr}$ is a material parameter that must fulfill:

$$Se_{Pc,irr} < Se_{w,irr} \tag{31}$$

In the Van Genuchten equations, the maximal saturation $Se_{Pc,max}$ must fulfill:

$$Se_{Pc,max} > Se_{w,max} \tag{32}$$

The soil-water characteristic curve is demarcated as the connection among the volumetric wetting phase content or saturation degree and suction of the soil. The mechanics of a capillary zone shows that when the critical capillary pressure is reached for non-wetting phase entry into the porous medium, the non-wetting phase enters the pore space of the medium and the wetting phase saturation degree decreases to generate a partially saturated media. Then, the wetting phase saturation degree in this capillary area is connected to the capillary pressure. This relation is defined empirically by laboratory experiments on various categories of soils. The soil water characteristic curve can be defined as an extent of the water-holding or the storage capacity of the porous media as the volumetric water content fluctuates when it is exposed to different magnitudes of suction. In the formulation, the Van Genuchten [229] expression for the soil water characteristic curve is adopted:

$$Se_{w,Pc} = [1 + (\alpha p_c)^n]^{-m} \tag{33}$$

Finally, the dependence of capillary pressure on the saturation is assumed by the following equation, based on the Van Genuchten equation:

$$p_c(Se_{w,Pc}) = \frac{1}{\alpha} \left(Se_{w,Pc}^{\frac{-1}{m}} - 1 \right)^{1-m} \tag{34}$$

Where m and $n$are material parameters and the expression $m = 1 - 1/n$ is supposed. $p_c(Se_{w,Pc}) = p_{nw} - p_w$ is the suction and $Se_{w,Pc}$ is the effective saturation degree for capillary pressure. Deriving the Equation, the capillary term in the pressure Equation and saturation Equation can be assumed as:

$$\frac{\partial p_c}{\partial Se_w}\left(Se_{w,Pc}\right) = -\frac{1-m}{\alpha m}\left(\left(Se_{w,Pc}\right)^{\frac{-1}{m}} - 1\right)^{-m}\left(Se_{w,Pc}\right)^{-\frac{1+m}{m}} \quad (35)$$

3.1.5 Boundary and initial conditions

Initially, the water follows the hydrostatic distribution, and the gas content is equal to zero inside the domain. Where $\boldsymbol{n}$ is the unit vector normal to the boundary. The boundary conditions allow the water to exit only from the top of the soil column. Because air enters at the column injector and exits in the top boundary, the boundary conditions for the non-wetting phase are:

$$\delta\Omega\, Inlet(Gas\ injector)$$
$$p_{\boldsymbol{nw}} = p_{\boldsymbol{nw0}}(t) = P_{injection} \quad (36)$$
$$Se_{nw} = Se_{nw0}(t) = 1$$

$$Base(Bottom\ wall)$$
$$\boldsymbol{n}.\left[-\frac{k_{int}k_{r,nw}}{\mu_{nw}}(\boldsymbol{\nabla} p_{nw} + \rho_{nw} g \boldsymbol{\nabla} D)\right] = 0 \quad (37)$$

$$\delta\Omega\, Sides(Vertical\ walls) - Tautological\ flux - Horizontal\ flux$$
$$\boldsymbol{n}.\left[-\frac{k_{int}k_{r,nw}}{\mu_{nw}}(\boldsymbol{\nabla} p_{nw} + \rho_{nw} g \boldsymbol{\nabla} D)\right] = -\frac{k_{int}k_{r,nw}}{\mu_{nw}}(\boldsymbol{\nabla} p_{nw} + \rho_{nw} g \boldsymbol{\nabla} D) \quad (38)$$
$$p_{\boldsymbol{nw}} = p_{\boldsymbol{nw0}}(t) = \rho_w g y = Hydrostatic\ pressure$$

$$\delta\Omega\, Top(Outlet) - Tautological\ flux - vertical\ flux$$
$$\boldsymbol{n}.\left[-\frac{k_{int}k_{r,nw}}{\mu_{nw}}(\boldsymbol{\nabla} p_{nw} + \rho_{nw} g \boldsymbol{\nabla} D)\right] = -\frac{k_{int}k_{r,nw}}{\mu_{nw}}(\boldsymbol{\nabla} p_{nw} + \rho_{nw} g \boldsymbol{\nabla} D) \quad (39)$$
$$p_{\boldsymbol{nw}} = p_{\boldsymbol{nw0}}(t) = 0$$

$$\delta\Omega\, Surface$$
$$p_{\boldsymbol{nw}} = p_{\boldsymbol{nw0}}(t = 0) = 0 \quad (40)$$
$$Se_{nw} = Se_{nw0}(t = 0) = 0$$

4 ANALYSIS AND SIMULATION OF GAS INJECTION INTO A SATURATED MATERIAL

The finite element mesh and the defined boundary conditions for the predictions are presented in Figure 8 and Figure 9, respectively. The concentration of grid nodes is great in the existing zone of the expanding non-wetting saturation degree plume and also near to the injector, where the non-wetting phase saturation degree gradient is high (steepest). The domain Ω is defined properly to be the rectangular area, $\Omega = \{(x,y) : 0 \leq x \leq 30m, 0 \leq y \leq 15m\}$.

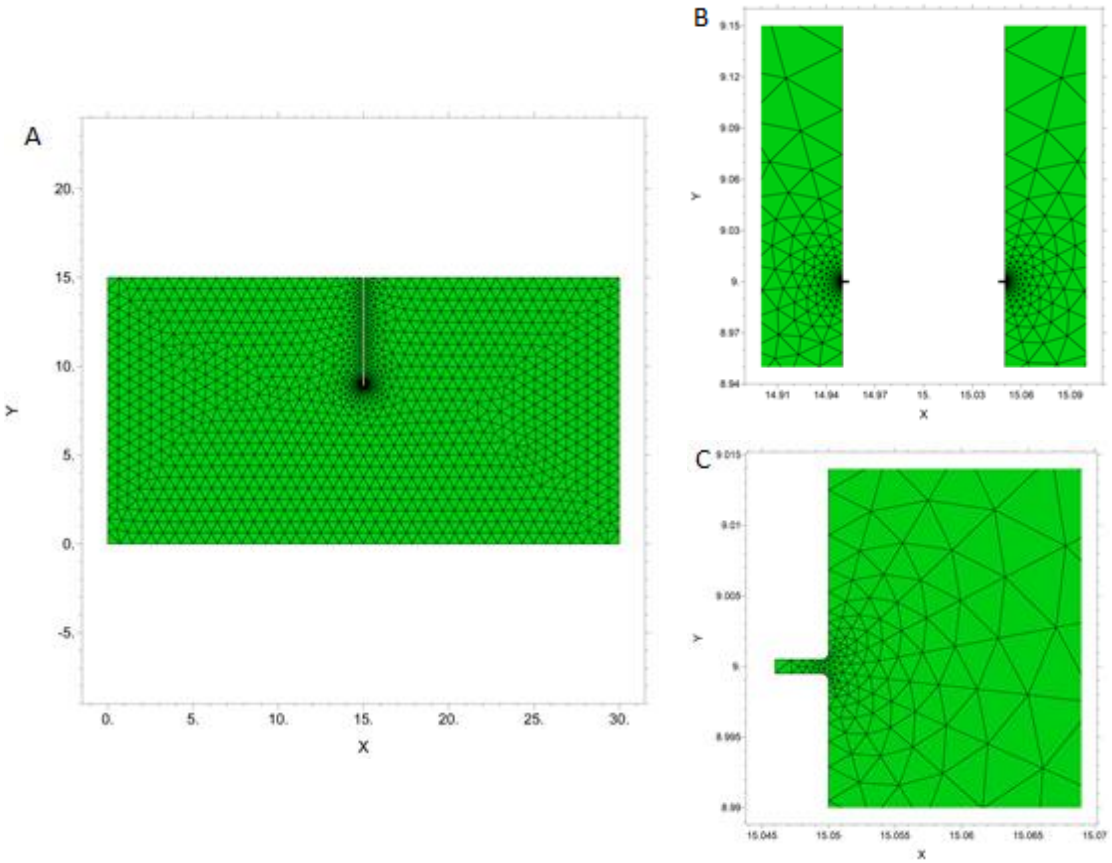

Figure 8 (A) Domain finite element mesh, (B) two symmetrical injector's scheme, and (C) finite element mesh near right injector.

As is shown in Figure 9, a homogeneous soil rectangle with 30 m width and of 15 m depth is implemented in the predictions. A no-flow (undrained) boundary for the non-wetting phase is assigned at the bottom, and non-wetting phase flux is allowed on the lateral sides of the rectangle. Non-wetting phase flux is allowed at a depth of 6 m in the injector (A non-wetting phase well with an effective radius of 0.0005 m), and at the top of the homogeneous soil rectangle. The top of the rectangle is exposed to a non-wetting phase pressure equal to 0 kPa. The injector of 0.001m effective diameter at a depth of 6 m is subjected to variable injection pressure, less than the maximum theoretical air injection pressure in which the soil skeleton begins to be excessively disordered. Injector geometry was defined as constant since Marulanda [224] stated that the injector does not have a significant impact on the features of a non-wetting phase plume as long as the non-wetting phase is injected uniformly over a significant area of flow. The simulations of the injection process start from a fully wetting phase saturated condition where initial non-wetting phase saturation degree is equal to 0.0, and the matric suction p_c is the same along the rectangle and equal to 0 kPa.

At t=0, non-wetting phase begins to flow as a result of the pressure generated at the injector till pressure hydrostatic condition at injection point is exceeded.

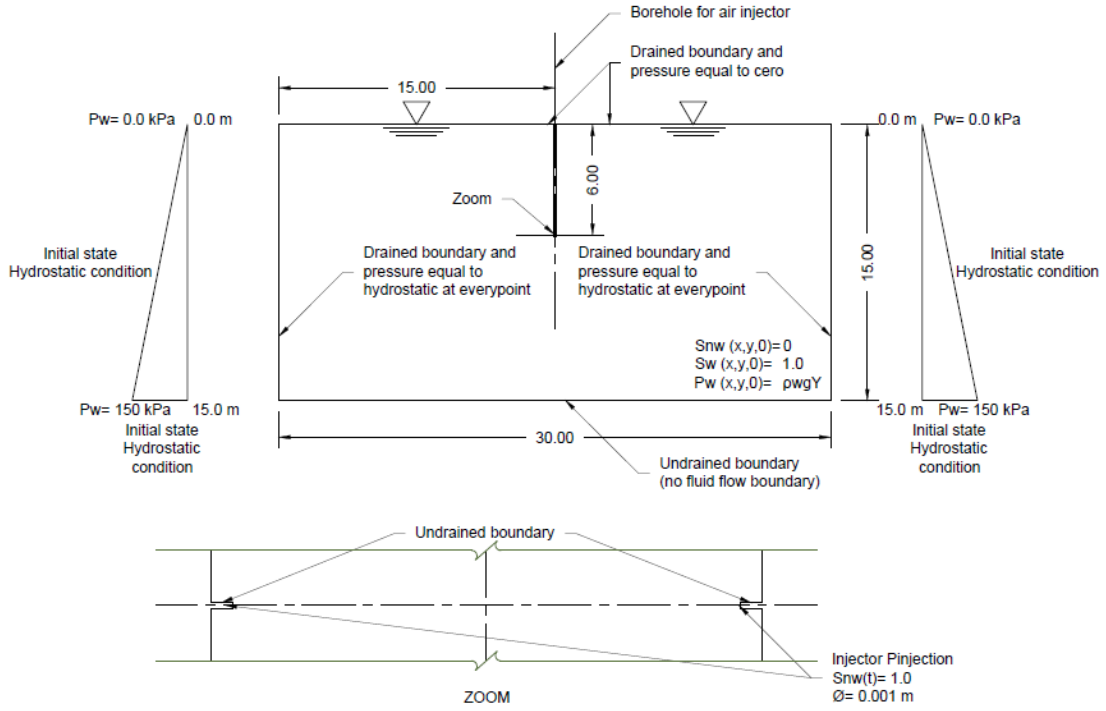

Figure 9 Boundary conditions

In order to observe the impact of the hydraulic features on the equations, diverse magnitudes for the hydraulic parameters (Van Genuchten parameter α, n, the value of wetting phase permeability a, and coefficient of gas permeability b) were implemented in the predictions. Also, different magnitudes of injection pressures were considered to study the biphasic flow in the initially fully wetting phase saturated material system. The parameters for the soil–water characteristic curve (α and n) were selected established on Lu and Likos [20], and they are presented in Table 1 and Table 2 for the first and second group of simulations, respectively. These material parameters define diverse representative soils as sands ($\alpha = 0.10, 0.12,$ and $0.14\ 1/kPa$ and $n = 4.0$ and8.0), and silty sands ($\alpha = 0.07$ and $0.10\ 1/kPa$ and $n = 2.0$ and 4.0).

Table 1 Hydraulic parameters, injection pressures, and permeability used for the first group of simulations.

$\alpha\ (1/kPa)$	n	$S_{w,max}$	a	b	$P_{nw,inj}(kPa)$	$k_{int}(m^2)$
0.07	1.30	**1.00**	0.50	**0.33**	70	**$1.00x10^{-11}$**
0.10	2.00		1.00	0.50	75	
					80	
					85	
0.12	**4.00**		2.00	0.80	**90**	
0.14	8.00		**3.00**	1.00	100	

In the Table 1, underlined quantities are kept invariant while a group of predictions is being generated. For example when group of predictions n is generated (parameter $n = 1.3, 2.0, 4.0,$ and 8.0), parameters $\alpha = 0.10\ 1/\text{kPa}$, $s_{w,max} = 1.0$, $a = 3.0$, $b = 0.33$, $k_{int} = 1.00x10^{-11}m^2$, and $P = 90\text{kPa}$; when group of predictions a is generated $(\text{parameter } a = 0.5, 1.0, 2.0, \text{and } 3.0)$, parameters $\alpha = 0.10\ 1/\text{kPa}$, $n = 4.0$, $b = 0.33$, $s_{w,max} = 1.0$, $k_{int} = 1.00x10^{-11}m^2$, and $P = 90\text{kPa}$.

Table 2 Hydraulic parameters, injection pressures, and permeabilities used for the second group of simulations, different injection pressures for four different soils.

$Soil$	$\alpha\ (1/kPa)$	n	a	b	$P(kPa)$	$k_{int}(m^2)$
1	0.07	2.0	3.00	0.33	70 - 100	$5.55x10^{-12}$
2	0.10	4.0				$1.00x10^{-11}$
3	0.12	6.0				$5.55x10^{-11}$
4	0.14	8.0				$1.00x10^{-10}$

Given the importance of the van Genuchten parameters, a very brief overview of the significance of a and m and some typical values for a group of soils of interest to air sparging will be provided here. Van Genuchten [229] presented a closed-form analytical equation that provides an adequate fit for measured soil water retention curves. The equation provides means of describing the relationship between the capillary pressure, p_c, and the saturation, s_w, of a given soil based on two fitting parameters, α, and n. Due to its simplicity, the Van Genuchten equation has been widely used in the modeling of unsaturated flow. The influence of the hydraulic material parameters implemented in the numerical predictions on the soil–water characteristic curve is shown in Figure 10, as follows:

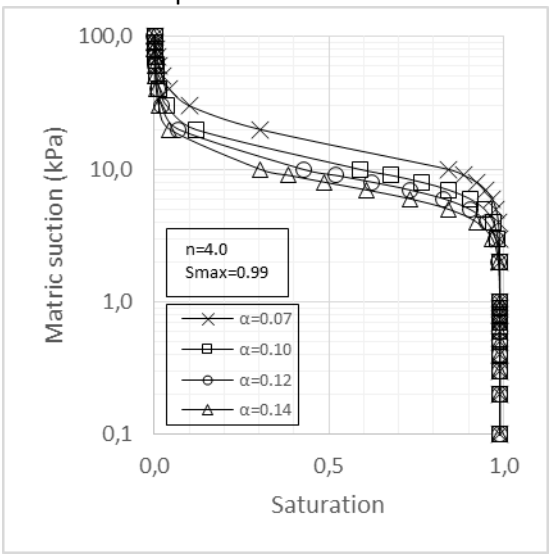

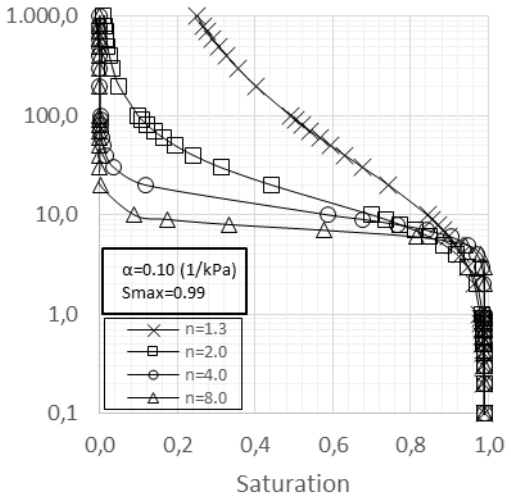

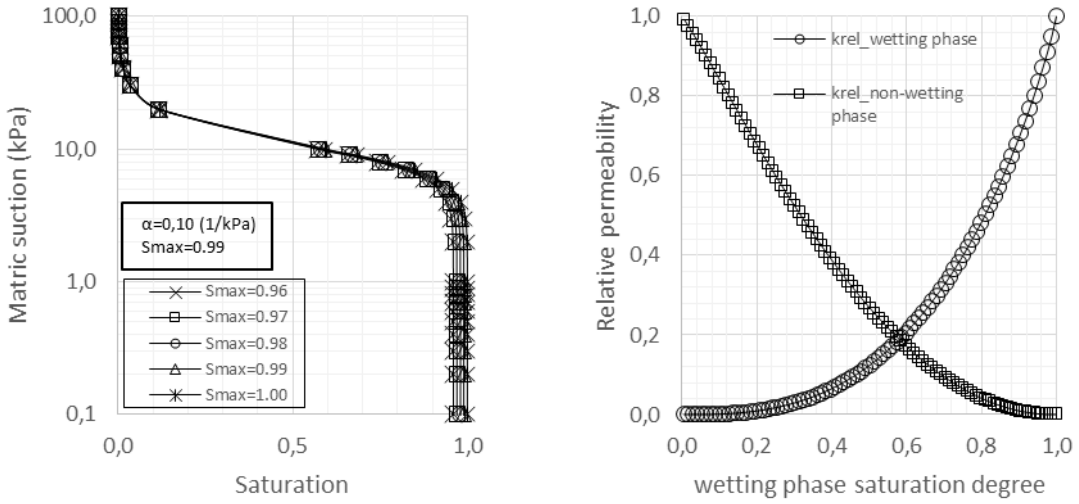

Figure 10 Effect of the hydraulic parameters n, α and $s_{w,max}$ on the soil–water characteristic curve and permeability function.

Figure 10 is a schematic showing the significance of the variations of the Van Genuchten parameters. In Figure 10 the parameter α normalizes all soils to one same relative level. The larger the value of α, the lower the plateau of the soil on the $p_c - s_w$ relationship, and therefore the coarser the soil. The parameter n governs the symmetry of the water retention curve, as illustrated by Figure 10. The n parameter is dimensionless, and its value varies from 0 to 8.5 in sands [20]. The lower the value of n, the higher the tendency of the soil to retain fluids by capillarity [233].

The material parameters essential for the mathematical model presented previously are shown in Table 3. The values in Table 3 associated to the physical properties of fluids come from the multiphase flow work of Hopman et al. [234], and all were related to a constant 20° C temperature, both for air and water. It is important to clarify that for these analysis$Se_{w,irr} = Se_{nw,irr} = Se_{Pc,irr} = Se_{Pc,max} = 0$, since these material parameters are defined from hysteretical processes and are difficult to obtain from literature.

Table 3 Material parameters used in the air-water simulations.

Variable	Expression	Description
ρ_w	$1000\ kg/m^3$	Fluid density, wetting phase
μ_w	$1x10^{-3}\ Pa\ s$	Dynamic viscosity, wetting phase
ρ_{nw}	$1.28\ kg/m^3$	Fluid density, non-wetting phase
μ_{nw}	$1.81x10^{-5}\ Pa\ s$	Dynamic viscosity, non-wetting phase
θ	0.34	Porosity
$S_{w,max}$	1.0	Maximum wetting phase saturation degree
$S_{w,min}$	0.0	Minimum wetting phase saturation degree

It is important to clarify that in this work is developed an isothermal and incompressible two-phase flow with capillary effects analysis. However, in more complex multiphase flow analysis defined in the literature exist a series of connections between non-wetting phase density, non-wetting phase pressure, and temperature. Some of the relationships are:

- Fluctuations of non-wetting phase density if the non-wetting phase pressure increases or decreases with the implementation of Boyle's Law $(if\ p_{nw}\ increases\ \rho_{nw}\ increases, \rho_{nw} \sim p_{nw})$.

- Variations of non-wetting phase density if the temperature increases or decreases with the application of Charle's Law (if temperature(T) increases ρ_{nw} $decreases, \rho_{nw} \sim 1/T$).
- Changes of pressure if the temperature (T) increases or decreases with the inclusion of the Gay-Lussac's Law (if temperature (T) $increases$ p_{nw} $increases, p_{nw} \sim T$).

Putting all three together, are defined as ideal gas laws for moist and dry non-wetting phase, both with the associated molecular weight of non-wetting phases, the gas constant and temperature changing in time. Additionally, the analysis of the multiphase flow in more rigorous approaches requires considering the following processes [235], [236]:

- The advective flow of liquid water.
- Advective and diffusive vapor flow.
- Airflow of the gaseous phase by advection and diffusion.
- The advective flow of air dissolved in water.
- Conductive heat flow in all the phases of the System.
- The flow of heat associated with the flow of the liquid.
- The flow of heat associated with the flow of the gas phase.

From the above processes, the equations of conservation of mass and energy are formulated obtaining a system of differential equations. Also, in this kind of formulation, equilibrium relationships between phases are defined and implemented [235], [236], some of these are shown below:

- The balance between the liquid phase and the vapor phase (Kelvin equation or psychrometric equation), where the vapor pressure is expressed as a function of the temperature, suction, and density of the liquid.
- Thermal equilibrium between the different phases at each point, so that any thermal imbalance between phases dissipates almost instantaneously.
- The balance between the dissolved air and the air of the gas phase.
- The balance between dissolved air and liquid (Henry's Law).
- The balance between air and vapor of the gas phase (Dalton's Law), where the total pressure of the gas is equal to the sum of the partial pressures of the vapor and air.

Within the framework of the mechanics of unsaturated soils, codes have been developed with a rigorous, multiphase flow approach that solves the non-isothermal multiphase flow coupled to deformations of the solid medium. These include: CODE-BRIGHT[237], COMPASS [238]and FADES [235]. But, these complex physical features such as phase changes or compressibility of phases are not in the scope of this thesis but are mentioned as possible further developments of the presented model.

On the other hand, typical results for a first general prediction are presented below. The isocontours generated for this first case of analysis are shown. It is intended to show in some way the important behavior associated with the buoyancy forces, and the gradients of pressure that refer to the injected phase and its tendency to flow.

In Figure 11 is shown an illustration of the plumes for a time history of the non-wetting saturation degree obtained by the simulations, and specifically for the soil number 2 in Table 2, for an injection pressure of $90kPa$. This illustration presents a change of the soil from an initial entirely wetting phase saturated condition ($p_c = 0\,\mathrm{kPa}$) to a partially saturated state, different to the corresponding hydrostatic condition near to the injector. Results for this test example shows the isocontours of the non-wetting phase saturation degree as a function of x and y at t=9OO, 1800, 2700 and 3600 seconds. The model is tracking the non-wetting phase saturation degree front. Because no injected non-wetting phase (air) has yet reached the drained zones, it is established that the volumetric content of moved wetting phase (water) is the same(since equations represent incompressible flow)

to the volumetric content of injected non-wetting phase (air) as is shown for t=9OOs and t=1800s. Also, the non-wetting phase and wetting phase saturation gradients are null at the drained zones at t=9OOs and t=1800, so the group of cells near the drained zone is simply there for determining the particular pressure gradients of wetting phase removal and for relevant features connected to the geometry of that zone. Non-wetting phase, infiltrating into the saturated soil, results in a decrease in saturation. This phenomena, consecutively, leads to alterations in pore water pressure (an increase in capillary pressure), an increase in the shear strength of the material and a decrease in the soil tends to liquefy.

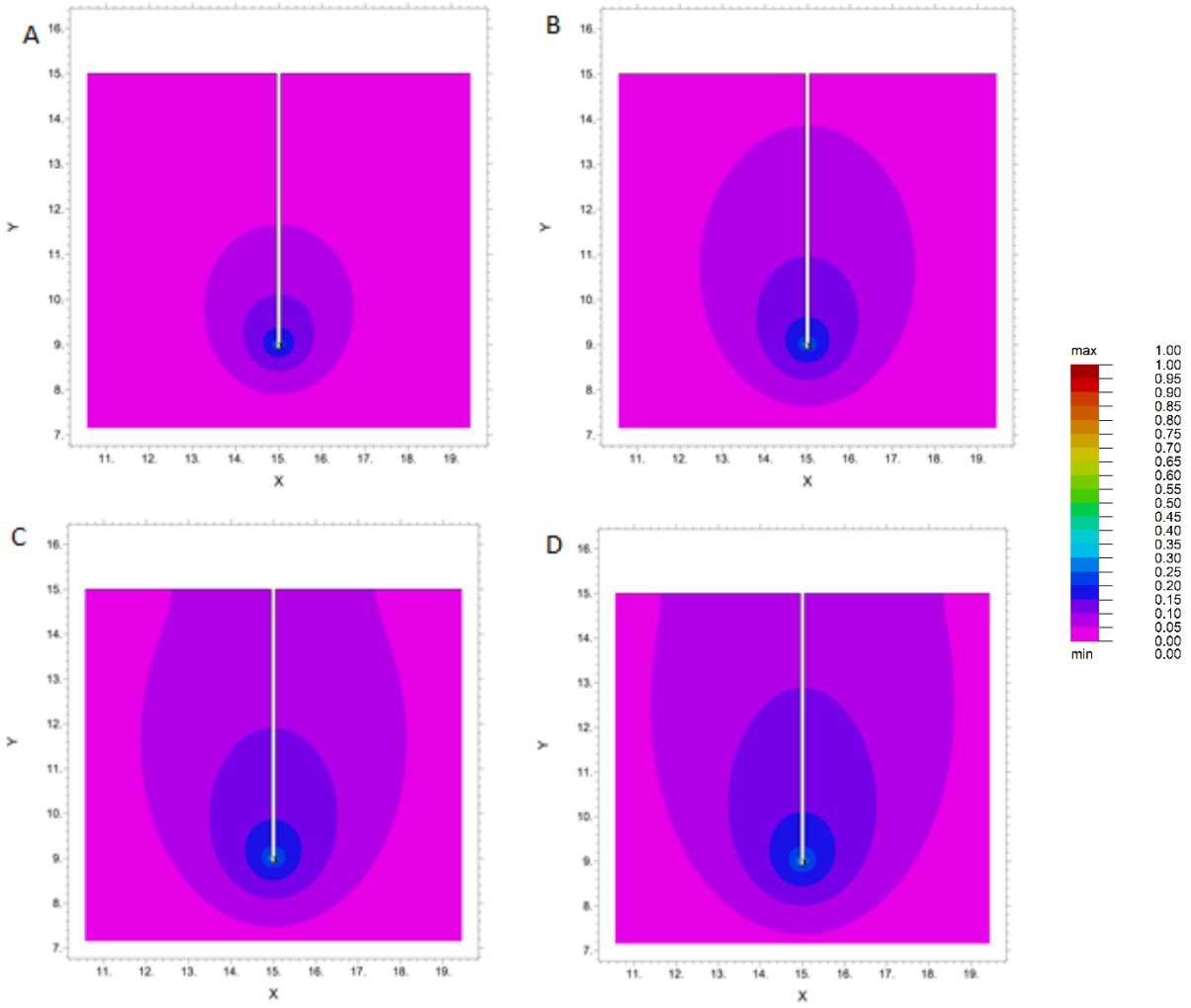

Figure 11 Temporal change in the non-wetting phase degree of saturation induced by air injection. Isocontours of predictions of distributions and magnitudes of desaturated zones for soil number 2, for an injection pressure of $90kPa$, at (A) t=9OOs, (B) t=1800s, (C) t=2700s, and (D) t=3600s. Distance in meters.

In Figure 11 the mechanism driving the upward flow of a non-wetting phase is buoyancy. Buoyancy is typically described as a force acting upward, which occurs with the purpose of return a submerged body to an equilibrium state. The balance is lost when a form of a specified volume, with a different density than that of the surrounding wetting phase, is submerged and moves the wetting phase. The weight of the body is different from that of the equivalent volume of wetting phase displaced. Equilibrium is maintained by the presence of the buoyancy force, which is described by the expression$(\rho_w)(g)(volume)$. Due to the severe contrast among the densities of non-wetting phase and pore wetting phase, a non-wetting phase in the free field will then rise due to the difference

between the magnitudes of the upward buoyancy force F_b and the downward gravity force $F_g$as shown in Figure 12.

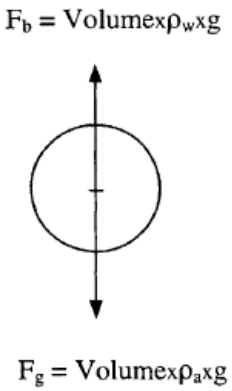

Figure 12 Buoyancy forces acting on a submerged bubble, internal force approach [224]

Marulanda [224] explains that buoyancy forces occur nevertheless of the variety of submerged body (rigid or fluid), but are directly connected to its volume, and consequently will change with variable shapes. Changing volumes are inherent to the behavior of the non-wetting phase, thus leading to varying magnitudes of buoyancy forces. The example of a non-wetting phase bubble clearly describes this behavior. As the non-wetting phase bubble flow in a column of static water, for example, the surrounding hydrostatic fluid pressure reduces with decreasing distance to the phreatic surface. In order to balance the changes in external pressure, the pressure inside the non-wetting phase bubble needs to decrease, and this primary generates expansion of its volume. Buoyancy forces consequently increase, and the non-wetting phase bubble accelerates. It is essential to evaluate the effects of pressure gradients and buoyancy on the flow of injected non-wetting phase through the soil. Clayton [239] schematized some typical forms of the effects of buoyancy on the trends of development of flow during non-wetting phase injection, and it is presented in Figure 13.

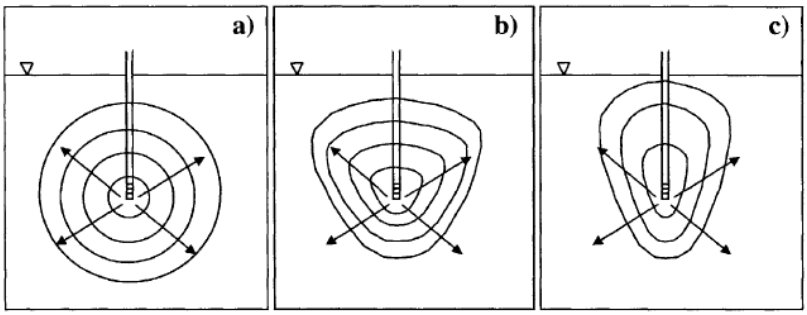

Figure 13 scheme of the differences in the amount of initial non-wetting phase invasion under conditions of a) no buoyancy; b) moderate buoyancy; and c) strong buoyancy [239].

In a homogeneous soil, with isotropic permeability, if the phase injected has the same density as the pore phase, then the buoyancy forces are equal to zero, and the injected phase spreads spherically from the injector, as shown in Figure 13 a). This explanation neglects pressure gradients occurring within the injected phase. As the density difference among the two phases (e.g., air-water systems) come to be larger, buoyancy forces are progressively more important, and non-wetting phase expansion tends to follow a more upward trend as presented in Figure 13 b) and c) [239], as results presented in Figure 11.

In the next segments, the argument proposes to explain a tendency in the biphasic flow behavior of material besides the relation among the simulation results and the theoretical information observed in the literature. Finally, in order to show the potential desaturated plumes of the two-dimensional injection analysis, the results of predictions will be presented, where the impact of the changing capillary pressure is also counted in. It is essential to clarify that isocountors presented in the Figures of the next chapter are generated all with a fixed zoom with a square shape and 8.8m side and left lower edge located in the coordinates x=10.6m and y=7.2m.

4.1 PREDICTION OF A TWO-DIMENSIONAL MULTIPHASE FLOW PROBLEM

4.1.1 First group of results of numerical simulations

4.1.1.1 Effect of injection pressure

The pressure of the non-wetting phase injected and predicted results of effective radius profiles, corresponding to six different injection pressures $\left(P_{nw,inj} = 70, 75, 80, 85, 90\ and\ 100kPa\right)$ and for a non-wetting phase injection time equal to 9OOs, 1800s, 2700s, and 3600s, are shown in Figure 14, respectively. First four injection pressures are less than the injection pressure suggested by Ogata and Okamura [171], for an injector at 6 meters depth, that is approximately equal to $87kPa$ (for a soil with a unitary weight of $\gamma = 19.0\ kN/m^3$). The fifth injection pressure is little higher than recommended by Marulanda [224], Okamura et al. [122], Ogata and Okamura [171], and Zeybek et al. [138], [166]. Moreover, the sixth injection pressure is much higher than the maximum injection pressure recommended in the literature. It is essential to mention that not all the injection pressures added to the parametric analysis correspond to one that will not produce destruction of the internal structure of the soil to be improved.

However, it is decided to analyze these range of injection pressures and the isocontours of non-wetting phase saturation degree with the objective of establishing whether the advance of the desaturation front has a behavior directly proportional to the increase in pressure or if this is done without any particular pattern.

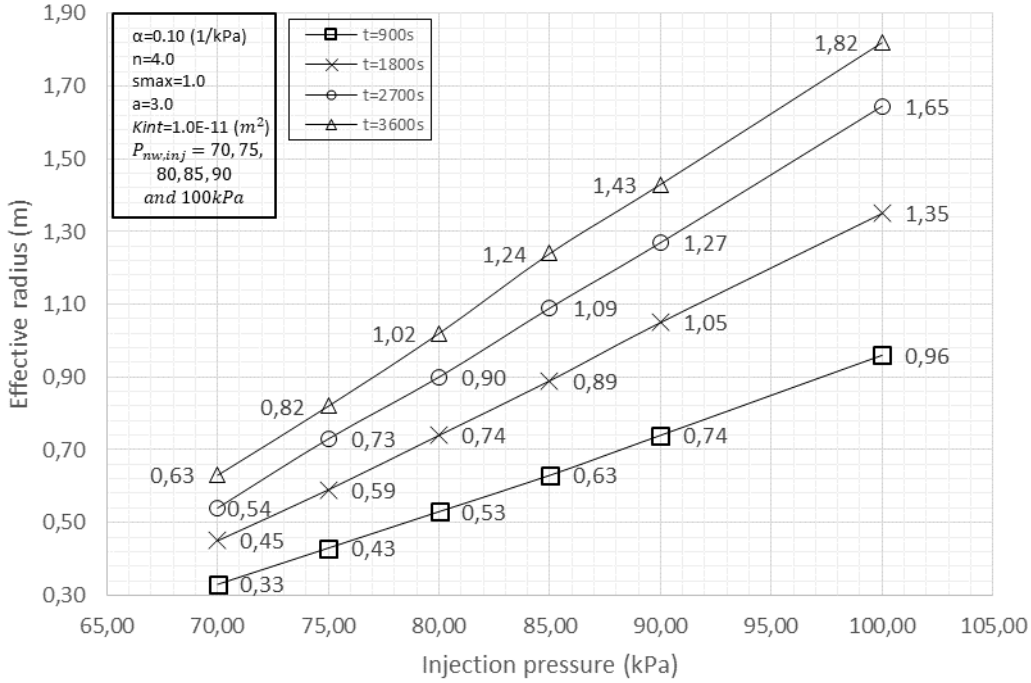

Figure 14 Plume effective radius or advance length, taken from the isocontour corresponding to $S_{nw} = 0.1$, for injection pressures varying from 70 to 100kPa, and injection times equal to 900s, 1800s, 2700s, and 3600s.

It can be perceived from the Figure 14 that the higher the injection pressure, the more the increase of capillary pressure and the higher the effective non-wetting phase saturation degree radius after 9OOs, 1800s, 2700s, and 3600s. Results obtained are similar to the results obtained in-situ through field monitoring on the impact of pressure and injection in a three-dimensional layered soil column by Okamura et al. [178]. Also, these results were confirmed numerically by Yasuhara et al. [126]; who investigated, in coupled conditions, the influence of the injection pressure on the wetting phase fluid pressure and the non-wetting phase saturation degree distributions in a homogeneous soil domain. It is perceived that variations of the injection pressure for fixed permeability values, constant material parameters, and variable injection times generate substantial increases in the advance lengths of the non-wetting phase, and it is perceived that the magnitudes of the penetration radius vary significantly with variations of the injection pressure for fixed times. From the previous, it can be seen that the injection pressure and time are fundamental variables within two-phase flow analysis.

Commented the above and took into account that soil is formed in different phases that involve solid particles, liquids, and gases; it can then be inferred that in addition to the permeability of the soil, other factors such as injection pressure are essential in advance of the non-wetting phase. Since if the method is executed in moderately permeable soils, the advance of the non-wetting phase will be governed mainly by the injection pressure; as can be seen in the results obtained for the first case of analysis in the isocontours shown in Figure 15. In the analysis carried out to define Figure 15, the permeability parameter and hydraulic parameters associated with the material were kept constant, and the injection pressures of the non-wetting phase were varied according to that defined in Table 1.

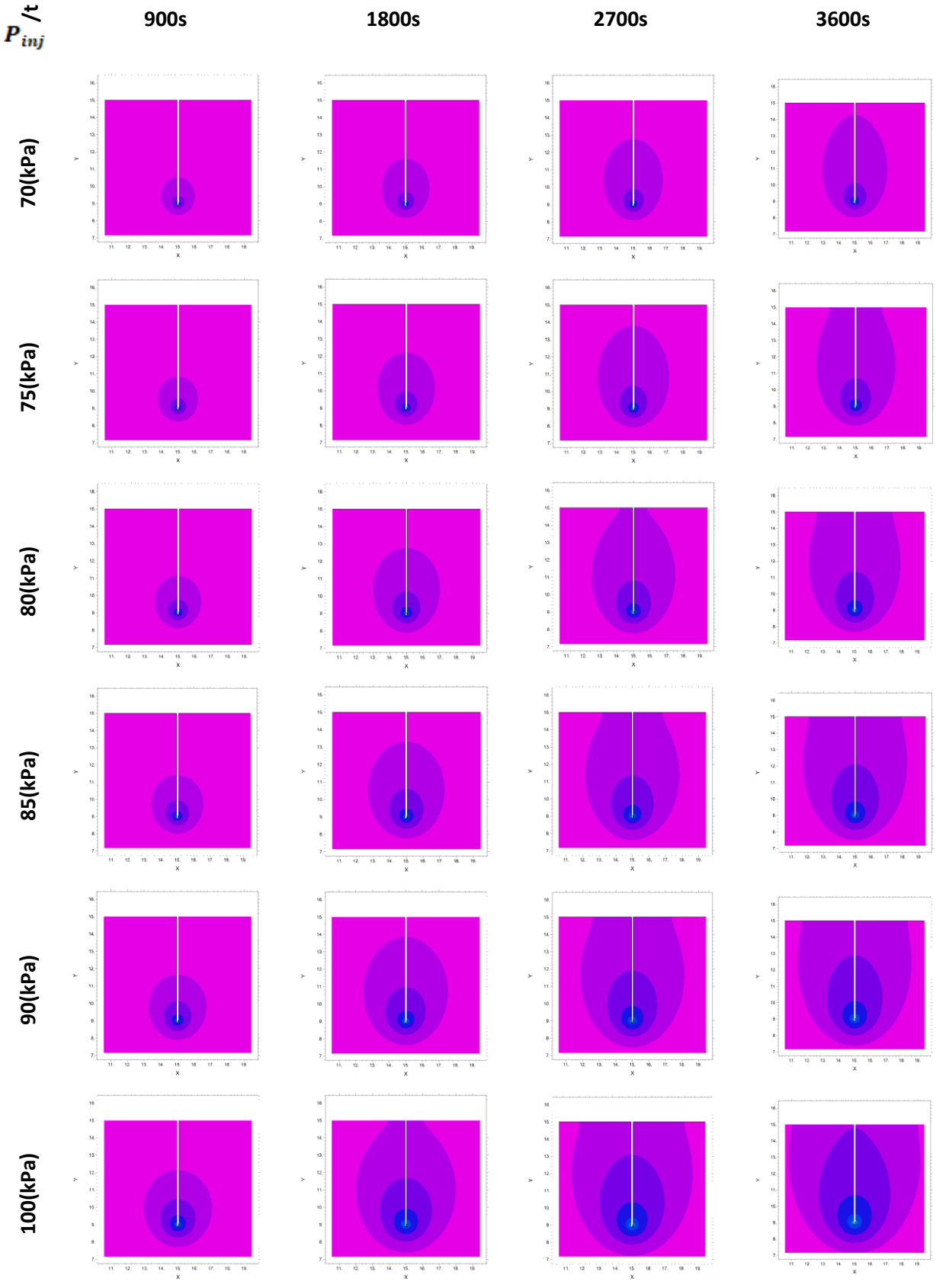
P_{inj} /t
900s
1800s
2700s
3600s
70(kPa)
75(kPa)
80(kPa)
85(kPa)
90(kPa)
100(kPa)

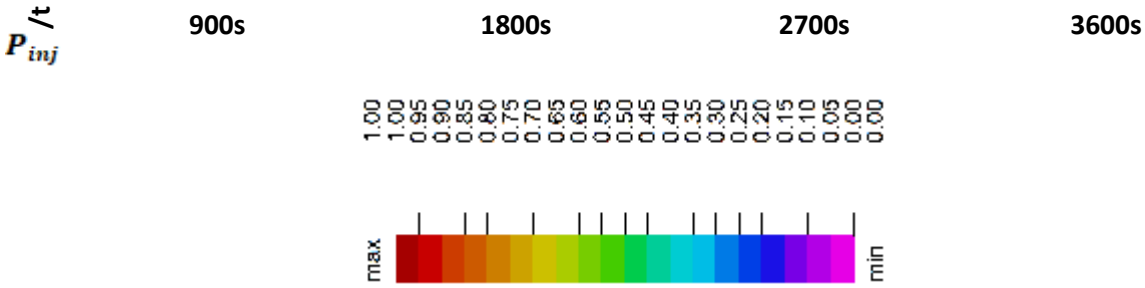

Figure 15 Temporal change in the non-wetting phase degree of saturation induced by air injection .Isocontours-distribution of plume expansion, taken from the corresponding injection pressures $(P_{nw,inj} = 70, 75, 80, 85, 90\ and\ 100kPa)$, and injection times equal to 900s, 1800s, 2700s, and 3600s. Distance in meters.

In Figure 15 the results obtained for this analysis shows the effect of the pressure on the method and the importance of overcoming the hydrostatic pressure at the injection points is also observed to have a more effective gas advance. This fact makes it visible that if the pressure with which the non-wetting phase is injected is greater, the greater the advancement of this in the soil. It is observed that the advance of the expansion plume of the non-wetting phase that is injected occurs mainly in the vertical direction for injection conditions under relatively low pressures and close to the hydrostatic pressure at the injection point. However, under conditions of injection pressure of the non-wetting phase close to the injection pressure recommended by literature and above, it is observed from the isocontours that there is a predominantly vertical advance of the non-wetting phase injected (mainly due to the gravitational forces) and in the other hand a considerable advance in horizontal direction and growing over time. It is expected from the phenomenon that for injection times of 1800s under a constant injection pressure of 100kPa the method begins to generate outputs of the non-wetting phase injected on the surface of the ground to be desaturated. In the same way, it is expected that for injection times of 2700s and 3600s under constant pressure of 80kPa and 75kPa, respectively, it begins to generate non-wetted phase outputs injected on the surface of the ground to be desaturated.

4.1.1.2 Effect of parameter α

The material parameter α is essential in the definition of the soil water characteristic curve since it approximates the inverse of the non-wetting phase entry pressure in the soil water characteristic curve [20]. High magnitudes of the non-wetting phase entry pressure are related to the small pore dimensions, and the small magnitudes of non-wetting phase entry pressures are related to large pore sizes. Therefore, high magnitudes for parameter α characterize coarse- granular soils as sands, and small magnitudes denote fine- granular soils as silts and clays [240]. The impact of diverse magnitudes for material parameter α in the soil water retention characteristic curve is observed in Figure 10. The material parameter α and predicted results of effective radius profiles, corresponding to four diverse magnitudes implemented for parameter α $(\alpha = 0.07, 0.10, 0.12\ and\ 0.14\ 1/kPa)$, to show its effect in the non-wetting phase injection-infiltration problem, and for an non-wetting phase injection time equal to 9OOs, 1800s, 2700s, and 3600s, are shown in Figure 16.

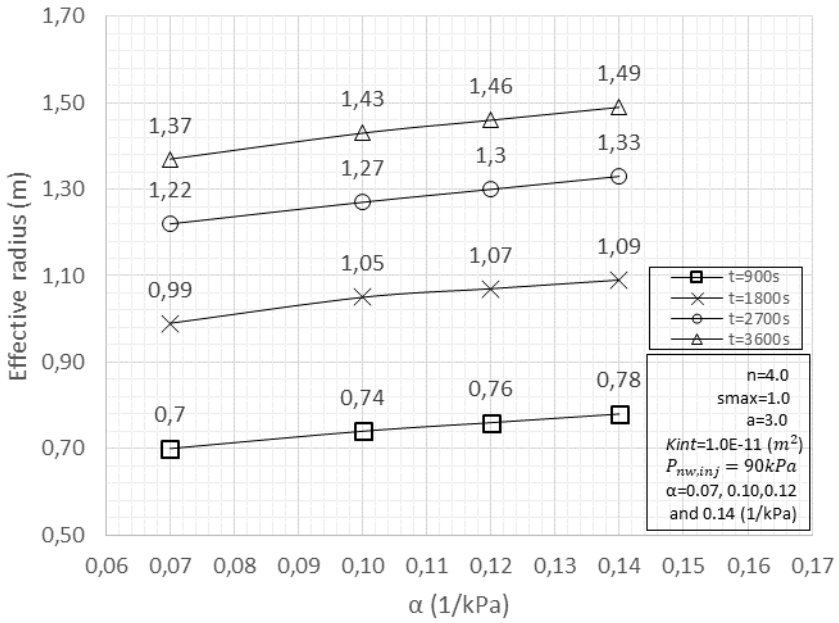

Figure 16 Plume effective radius or advance length, taken from the isocontour corresponding to $S_{nw} = 0.1$, for injection pressure $(P_{nw,inj} = 90\ kPa)$, changing parameter $(\alpha = 0.07, 0.10, 0.12\ and\ 0.14\ 1/kPa)$, and injection times equal to 900s, 1800s, 2700s, and 3600s.

In Figure 16, it can be observed that after parameter α rises, the effective desaturation radius increases for the same time and the same assumed initial capillary pressure and the same material parameter n. The previous results mean that soils with large magnitudes for material parameter α, as soils like sands, are estimated to be a reduced amount of wetting phase saturated than soils with small α values, as soils like silts and clays, at the same capillary pressure and the same non-wetting phase injection time. As a result, for the same injection pressure and permeability at the same time, faster non-wetting phase infiltrations can be expected for coarse-grained soils, as soils like sands, where parameter α is large. Although it is perceived that variations of the parameter α for fixed permeability values, constant injection pressures, and variable injection times generate relatively significant increases in the advance lengths of the non-wetting phase, it is observed that the magnitudes of the penetration radius do not vary significantly with variations of the parameter α for fixed times. From the previous, it can see that the injection time is a fundamental variable within two-phase flow analysis.

Isocontours of predictions of the evolution in the wetting phase saturation degree for the variation of the material parameter α corresponding to four diverse magnitudes α $(\alpha = 0.07, 0.10, 0.12\ and\ 0.14\ 1/kPa)$, employing the ground model and parameters constrained as is explained in the Table 1 is shown in Figure 17

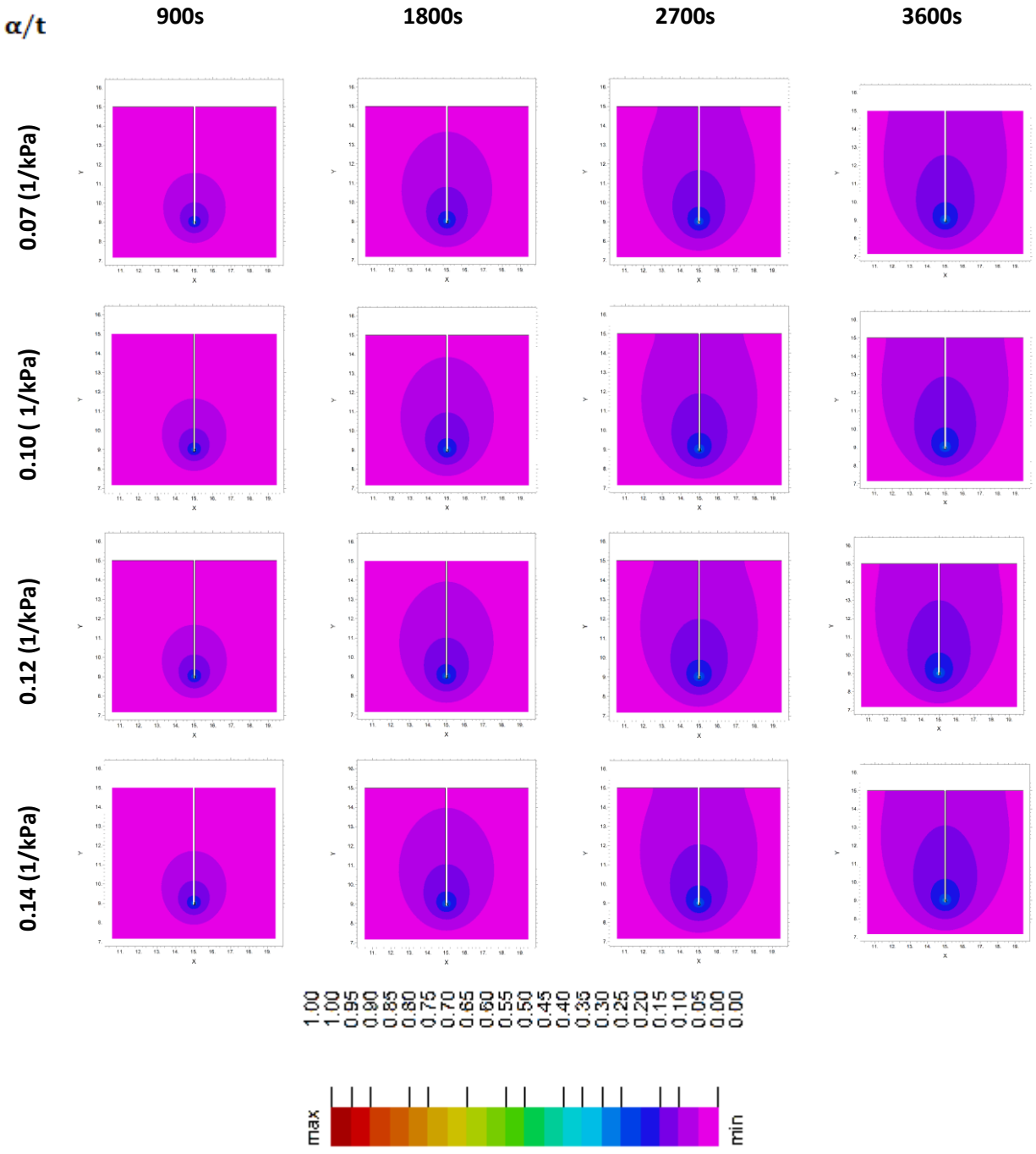

Figure 17 Temporal change in the non-wetting phase degree of saturation induced by air injection. Isocontours-distribution of plume expansion, taken from the corresponding injection pressure $(P_{nw,inj} = 90\ kPa)$,variation of parameter α $(\alpha = 0.07, 0.10, 0.12\ and\ 0.14\ 1/kPa)$ and injection times equal to 900s, 1800s, 2700s, and 3600s. Distance in meters.

In Figure 17 it is observed from the isocontours that the advance of the expansion plume of the non-wetting phase that is injected occurs mainly in the vertical direction (mainly due to the gravitational forces). Variations of the parameter α $(\alpha = 0.07, 0.10, 0.12\ and\ 0.14\ 1/kPa)$ for fixed permeability values, constant injection pressures, and variable injection times generate relatively significant increases under high α values on the advance lengths of the non-wetting phase. It is observed that the shapes of the desaturation plumes do not vary significantly with variations of the parameter α for fixed times. It is expected from the phenomenon that for the diverse values of parameter α and for injection times of 2700s and 3600s under a constant injection pressure of 90kPa the method

begins to generate outputs of the non-wetting phase injected on the surface of the ground to be desaturated for every value of α parameter evaluated.

4.1.1.3 Effect of parameter n

The material parameter n makes an important role in the soil water characteristic curve and the relative permeability functions, for the non-wetting phase and wetting phase, respectively. Furthermore, the material parameter n is recurrently implemented to limit the material parameter m, that is connected to the general proportion of the soil water characteristic curve and is expressed by the relation $m = 1 - 1/n$ [18]. The material parameter n is connected with the pore size distribution of the soil [20]. Then, the particle diameter arrangement of the material has a significant impact on the capillary pressure and the wetting phase saturation degree connection and the biphasic fluid flow. Pinder and Gray [217] stated that for well- sorted materials, materials that have a slight collection of particles, the capillary pressure, and the wetting phase saturation correlation is moderately flat. So, it means that flow process takes place quite abruptly over a small range of suction, but for a well-graded materials, a minor change zone is showed from partially saturated to saturated conditions because flow happens over a high interval of capillary pressures. The impact of diverse magnitudes for material parameter n in the soil water retention characteristic curve is observed in Figure 10. In Figure 10, minor magnitudes for material parameter n denote together, finer soils (i.e., silts and clays) and well-graded soils. In contrast, greater magnitudes represent together, coarser soils (i.e., sands) and well-sorted soils. Figure 18 describes for a constant injection pressure of 90kPa the predicted results of effective desaturation radius profiles, obtained during the infiltration process at times equal to 9OOs, 1800s, 2700s, and 3600s for different values of parameter n $(\mathrm{n} = 1.3, 2.0, 4.0, \text{and } 8.0)$.

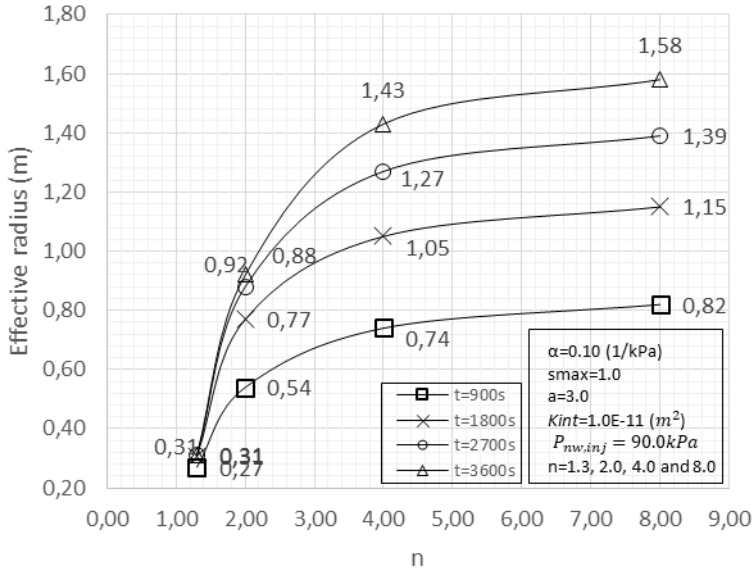

Figure 18 Plume effective radius or advance length, taken from the isocontour corresponding to $S_{nw} = 0.1$, for injection pressure $(P_{nw,inj} = 90\ kPa)$, changing parameter n $(\mathrm{n} = 1.3, 2.0, 4.0\ and\ 8.0)$, and injection times equal to 900s, 1800s, 2700s, and 3600s.

In Figure 18 a non-linear reaction in the profiles is perceived. For minor n magnitudes, the predicted results of effective desaturation radius stay practically invariant, at the same injection pressure, and at any time when n $(n = 1.3)$, but when n increases $(\mathrm{n} = 1.3 \text{ to } 2.0)$ the predicted results of effective desaturation radius start grow rapidly for the same time and with time increases. For larger n values, however, the response is less different or less reversed since predicted results of effective desaturation radius increase slowly when n increases$(\mathrm{n} = 2.0 \text{ to } 4.0)$. A comparable tendency is perceived in the predicted results of effective desaturation radius profiles when n increases

$(\mathrm{n} = 4.0 \text{ to } 8.0)$, in which the predicted results of effective desaturation radius increase slowly but with a tendency to be approximately constant when n increases $(\mathrm{n} = 6.0 \text{ to } 8.0)$. These diverse reactions can be clarified by the primary wetting phase saturation degree $(S_w = 1)$ at the start of the injection process, specifically, $t = 0s$. Additionally, the desaturation proportion is fast for materials with the small n magnitude where the primary saturation disposition along the column is high; as a consequence, the wetting phase pressure inside the pores is high.

Isocontours of predictions of the evolution in the wetting phase saturation degree for the variation of the material parameter n corresponding to four diverse magnitudes$n$ $(\mathrm{n} = 1.3, 2.0, 4.0, \text{and } 8.0)$, employing the ground model and parameters constrained as is explained in the Table 1 is shown in Figure 19.

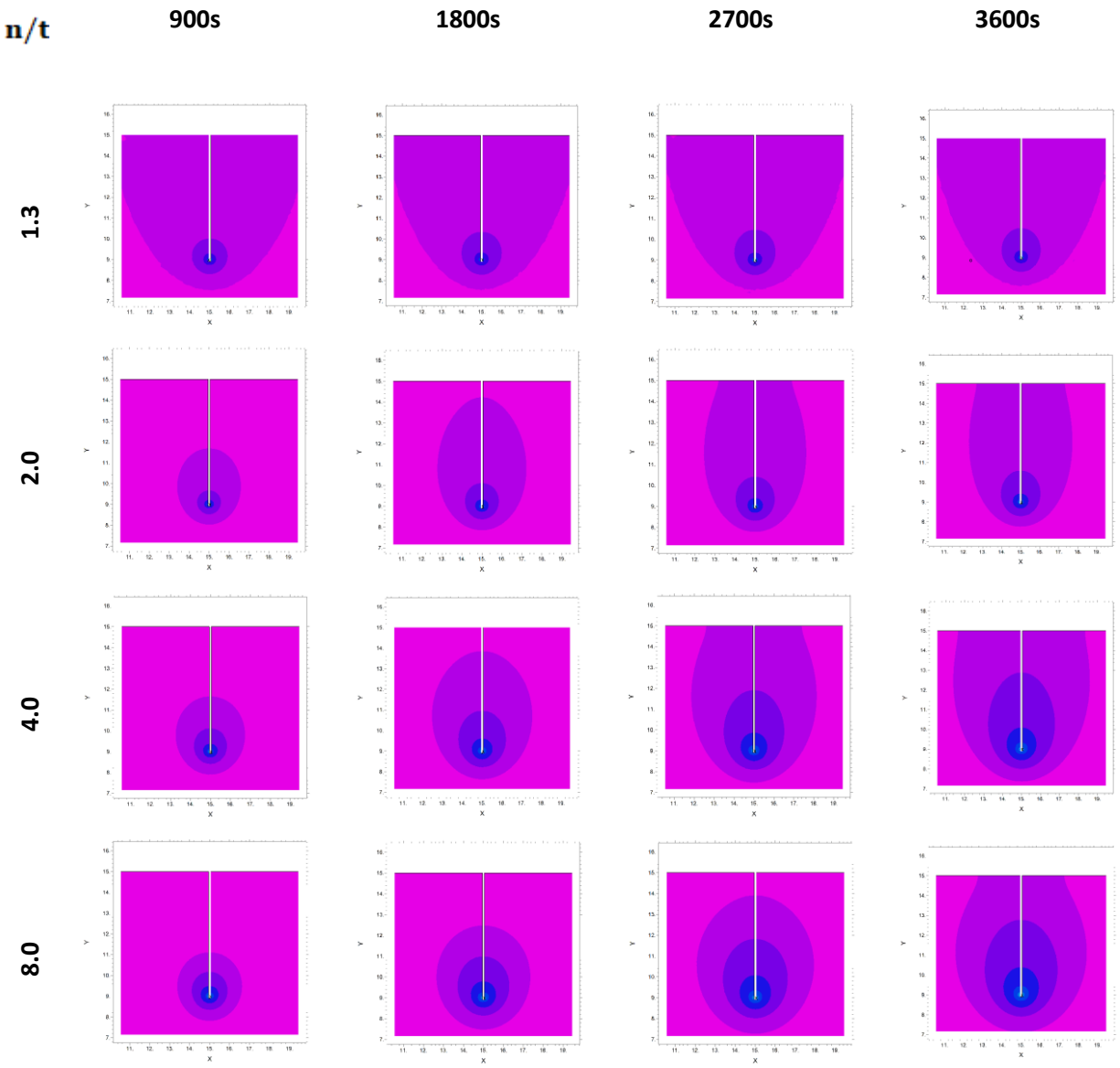

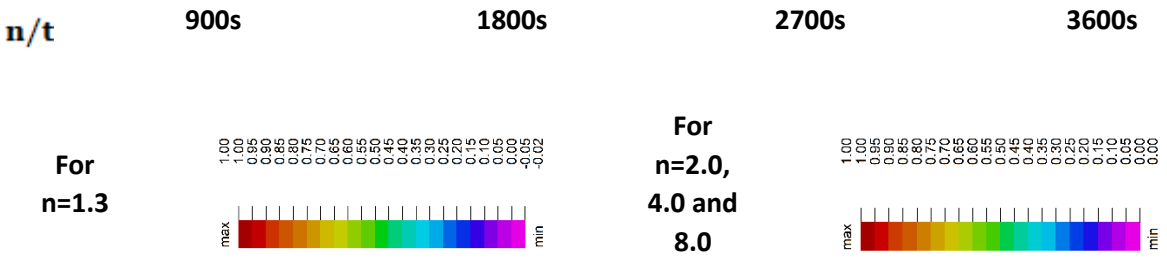

Figure 19 Temporal change in the non-wetting phase degree of saturation induced by air injection. Isocontours-distribution of plume expansion, taken from the corresponding injection pressure $(P_{nw,inj} = 90\ kPa)$,variation of parameter n $(\mathrm{n} = 1.3, 2.0, 4.0\ and\ 8.0)$ and injection times equal to 900s, 1800s, 2700s, and 3600s. Distance in meters.

From Figure 19 several responses are observed on the forms of the desaturation plumes that are defined for each of the injection times and the variation of the associated n parameter. For a value of the material parameter $n = 1.3$, an parabolic plume of desaturation is essentially invariable during a two-hour injection process. For an analysis associated with a $n = 2.0$ and 4.0 material parameter, desaturation plumes of an parabolic shape are observed, which mainly move in the vertical direction, to a lesser extent in the horizontal direction, and increase their influence area with the increase in the material parameter n from 2.0 to 4.0. On the other hand, for a value of the material parameter $n = 8.0$, a form of advancement of the plumes with a less marked parabolic shape is observed and tends mostly to generate a flow of the non-wetting phase that is somewhat symmetrical for injections of up to 1800s in duration. However, for injections from 2700s onward, asymmetric variations of the non-wetting phase and associated with gravitational forces are observed. It is expected from the phenomenon that for injection times of 2700s and 3600s, under a constant injection pressure of 90kPa, from material parameter n=2.0 to 4.0 the method begins to generate outputs of the non-wetting phase injected on the surface of the ground to be desaturated. Particularly for a value of the material parameter $n = 8.0$, under a constant injection pressure of 90kPa and an injection time of 3600s the method begins to generate outputs of the non-wetting phase injected on the surface of the ground to be desaturated

4.1.1.4 Effect of parameter a

The material parameter a is a crucial parameter in the characterization of the relative permeability equation. Greater material parameter a magnitudes generate more rapidly permeability falloff in the partially saturated condition, that is, the example of coarse-grained soils as sands. On the other hand, lesser a magnitudes characterize permeability equations for fine-grained soils as silts and clays. The impact of material parameter a, i.e., $a = 0.5, 1.0, 2.0, and\ 3.0$, in the effective desaturation radius profiles at times equal to 9OOs, 1800s, 2700s, and 3600s, are shown in Figure 20.

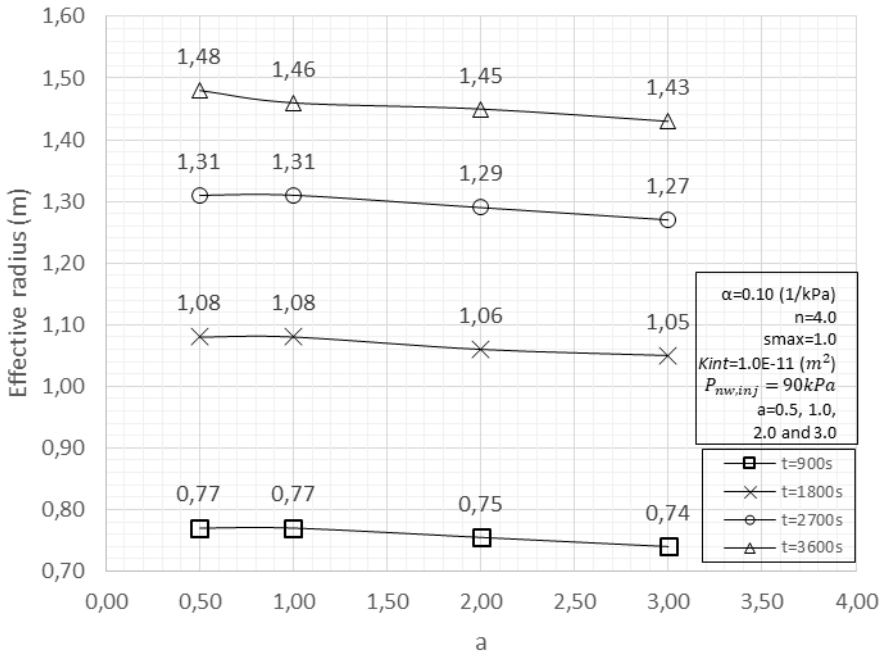

Figure 20 Plume effective radius or advance length, taken from the isocontour corresponding to $S_{nw} = 0.1$, for injection pressure $(P_{nw,inj} = 90\ kPa)$, changing parameter $(\mathrm{a} = 0.5, 1.0, 2.0\ and\ 3.0)$, and injection times equal to 900s, 1800s, 2700s, and 3600s.

As is presented in Figure 20, once material parameter a rises, the effective non-wetting phase saturation degree radius decreases along the column. Although it is perceived that variations of the parameter a for fixed permeability values, constant injection pressures, and variable injection times generate decreases in the advance lengths of the non-wetting phase, it is perceived that the magnitudes of the penetration radius do not vary significantly with variations of the parameter a for fixed times. Additionally, isocontours of predictions of the evolution in the wetting phase saturation degree for the variation of the material parameter n corresponding to four diverse magnitudes $a = 0.5, 1.0, 2.0, and\ 3.0$, employing the ground model and parameters constrained as is explained in the Table 1 is shown in Figure 21.

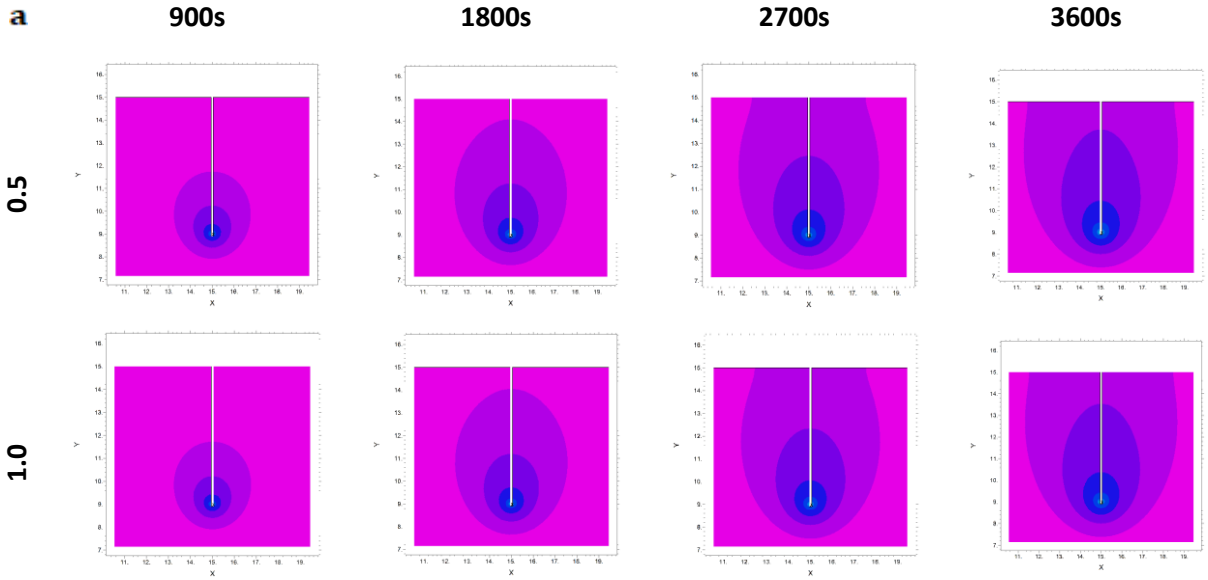

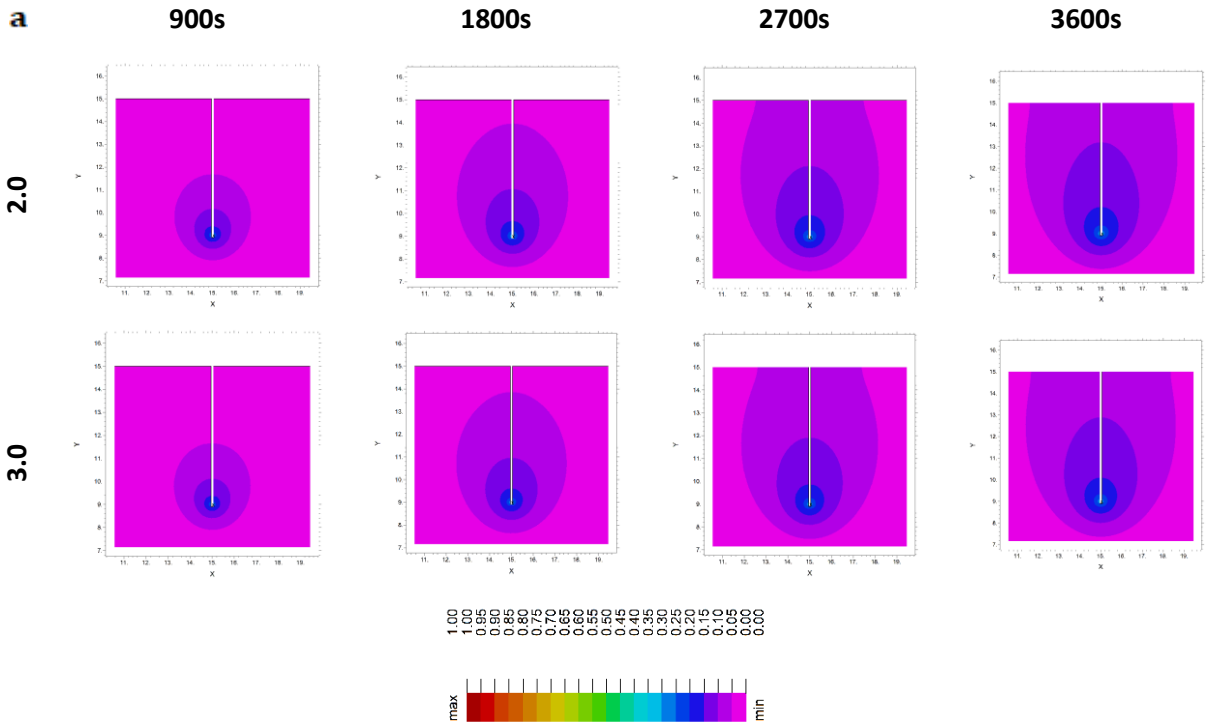

Figure 21 Temporal change in the non-wetting phase degree of saturation induced by air injection. Isocontours-distribution of plume expansion, taken from the corresponding injection pressure $(P_{nw,inj} = 90\ kPa)$,variation of parameter a $(a = 0.5, 1.0, 2.0, and\ 3.0)$ and injection times equal to 900s, 1800s, 2700s, and 3600s. Distance in meters.

In Figure 21 it is observed from the isocontours that the advance of the expansion plume of the non-wetting phase that is injected occurs mainly in the vertical direction (mainly due to the gravitational forces). Variations of the parameter a $(a = 0.5, 1.0, 2.0, and\ 3.0)$ for fixed permeability values, constant injection pressures, and variable injection times generate decreases under high a values on the advance lengths of the non-wetting phase. It is observed that the shapes of the desaturation plumes do not vary significantly with variations of the parameter a for fixed times. It is expected from the phenomenon that for the diverse values of parameter a and for injection times of 2700s and 3600s under a constant injection pressure of 90kPa the method begins to generate outputs of the non-wetting phase injected on the surface of the ground to be desaturated.

4.1.1.5 Effect of parameter b

The material parameter b is related to the representation of the relative permeability expression associated with the non-wetting phase. Larger magnitudes for b produce more rapidly non-wetting phase permeability falloff in the partially saturated state, explicitly, the behavior related to coarse-grained soils, as sands. The effect of material parameter b, for example, $b = 0.33, 0.5, 0.8\ and\ 1.0$ in the desaturation front radius profiles at times equal to 9OOs, 1800s, 2700s, and 3600s, are exposed in Figure 22.

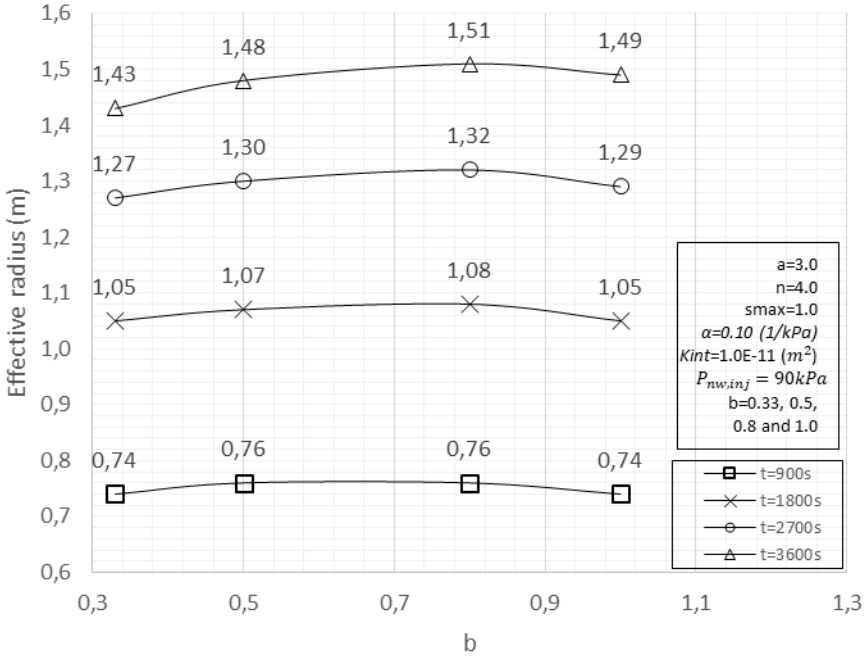

Figure 22 Plume effective radius or advance length, taken from the isocontour corresponding to $S_{nw} = 0.1$, for injection pressure $(P_{nw,inj} = 90\ kPa)$, changing parameter $(\mathrm{b} = 0.33, 0.5, 0.8\ and\ 1.0)$, and injection times equal to 900s, 1800s, 2700s, and 3600s.

As is presented in Figure 22, once material parameter b rises, the effective non-wetting phase saturation degree radius slowly increases along the column, when b increases $(\mathrm{b} = 0.33\ \mathrm{to}\ 0.8)$. Although it is perceived that variations of the parameter b for fixed permeability values, constant injection pressures, and variable injection times generate decreases in the advance lengths of the non-wetting phase when b increases $(\mathrm{b} = 0.8\ \mathrm{to}\ 1.0)$, it is perceived that the magnitudes of the penetration radius do not vary significantly with variations of the parameter b for fixed times. Additionally, isocontours of predictions of the evolution in the wetting phase saturation degree for the variation of the material parameter n corresponding to four diverse magnitudes $b = 0.33, 0.5, 0.8\ and\ 1.0$, employing the ground model and parameters constrained as is explained in the Table 1 is shown in Figure 23.

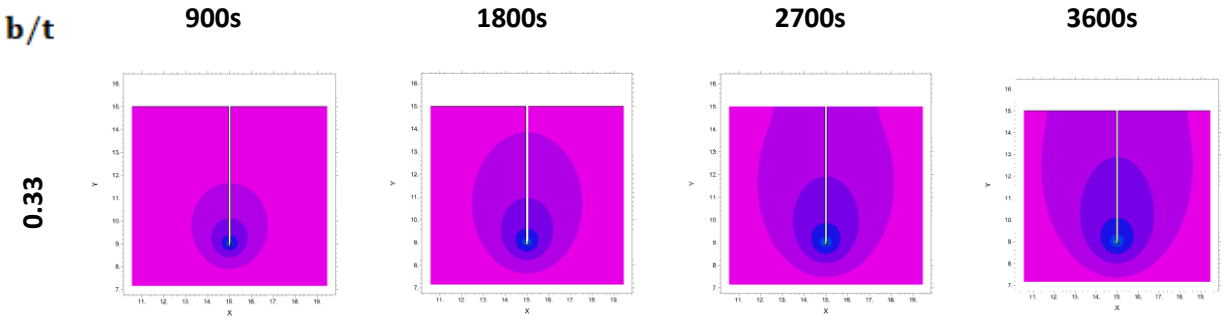

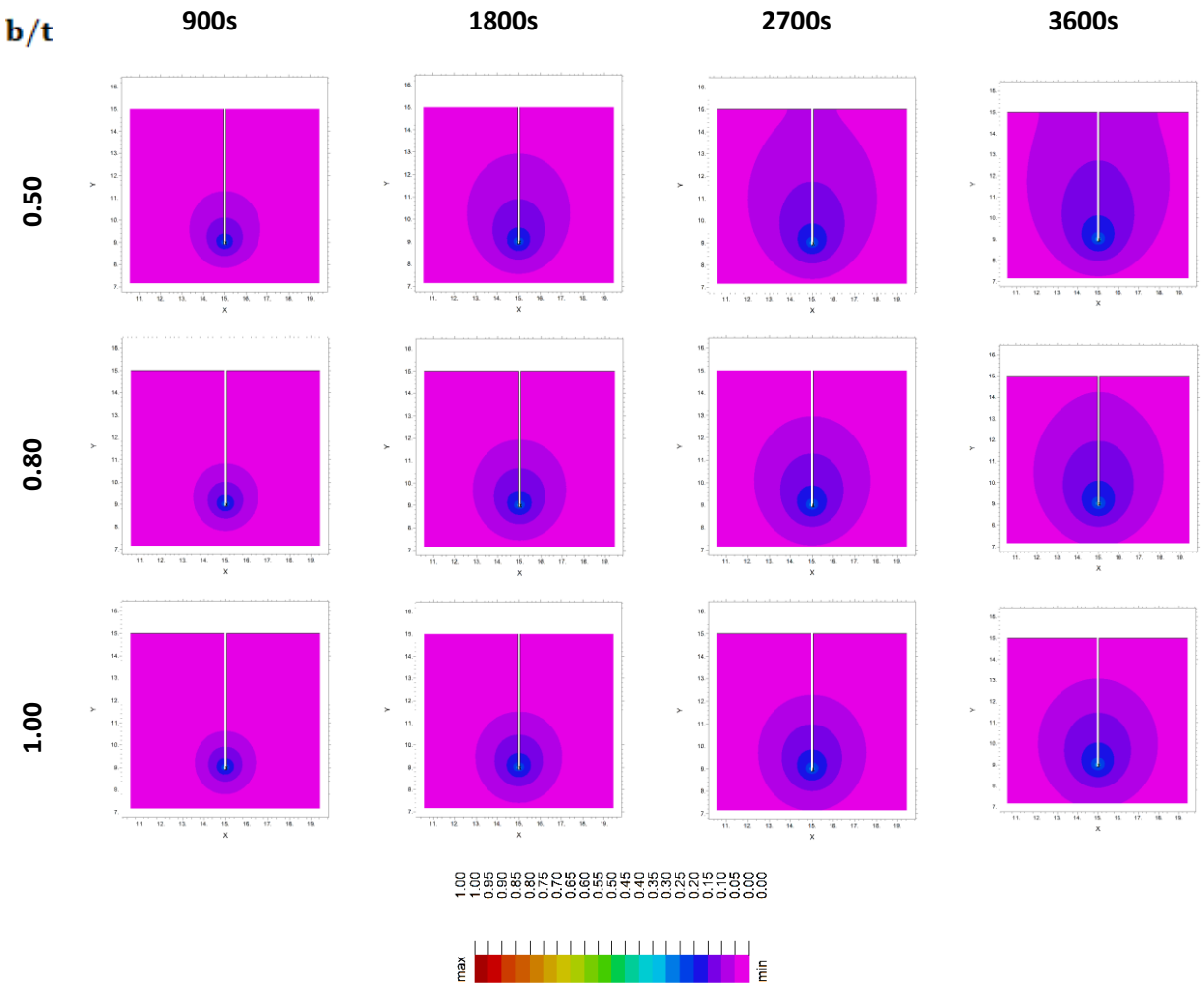

Figure 23 Temporal change in the non-wetting phase degree of saturation induced by air injection. Isocontours-distribution of plume expansion, taken from the corresponding injection pressure $(P_{nw,inj} = 90\ kPa)$,variation of parameter b $(b = 0.33, 0.5, 0.8\ and\ 1.0)$ and injection times equal to 900s, 1800s, 2700s, and 3600s. Distance in meters.

In Figure 23 two different responses of the non-wetting phase injection phenomenon on the expansion of the generated desaturation plumes are obtained. For low values of parameter $b\,(b = 0.33\ and\ 0.5)$, it is perceived that the non-wetting phase travels mainly in the vertical direction and to a lesser extent in the horizontal direction increasing in time. For high values of parameter $b\,(b = 0.8\ and\ 1.0)$, desaturation plumes with less pronounced parabolic forms and a less marked advance of the non-wetting phase in the vertical direction are obtained during times analysis. It is emphasized that for high values of parameter $b\,(b = 0.8\ and\ 1.0)$ no output would be expected on the surface of the soil to be improved from the non-wetting phase injected, even for injection times of 3600s, on the other hand, for low values of the parameter $b\,(b = 0.33\ and\ 0.5)$ would be expected output on the soil surface of the non-wetting phase injected for injection times of 2700s and above.

4.1.1.6 Summary

The effect of the material parameters on the non-wetting phase injection-infiltration process is shown through the magnitudes of the effective desaturation radius profiles at times equal to 9OOs, 1800s, 2700s, and 3600s (see Figure 14 to Figure 20). These figures show that material parameters α and n devise a more significant influence on the proportion of the desaturation process once they are related to parameter a, for the same injection pressure and the same permeability. In the case of

parameter α, the effective non-wetting phase saturation degree radius is greater when α is greater; this is for the reason that greater material parameters α characterize coarser soils (sands). As parameter α decreases, the effective non-wetting phase saturation degree radius is short. Material parameter n expose an interesting influence (nonlinear) on the interval it takes the material to be partially desaturated. Initially, the effective desaturation radius state fundamentally invariant in time when $n = 1.3$, for the same pressure and the same permeability, but when n increases $(\mathrm{n} = 1.3 \text{ to } 2.0)$ the predicted results of effective desaturation radius start grow rapidly for the same time and with time increases. For larger n values, however, the response is less different or less reversed since it has a combined effect, namely, predicted results of effective desaturation radius increase slowly when n increases$(\mathrm{n} = 2.0 \text{ to } 4.0)$. A comparable tendency is perceived in the predicted results of effective desaturation radius profiles when n increases $(\mathrm{n} = 4.0 \text{ to } 8.0)$, in which the predicted results of effective desaturation radius increase slowly but with a tendency to be approximately constant when n increases $(\mathrm{n} = 6.0 \text{ to } 8.0)$. Higher magnitudes for n (sands) implicate a quick conversion among saturated and unsaturated conditions. The material parameters a and b do not have a significant influence on the desaturation proportion for the partially desaturated condition.

The effect of the injection pressure on the two-dimensional biphasic flow analysis is projected by the reactions of the non-wetting phase injection-infiltration process and the effective non-wetting phase saturation degree radius in the soil column near the injector after 9OOs, 1800s, 2700s, and 3600s of injection. The influence of the injection pressure in the generation of the partial induction of the degree of saturation is shown in Figure 14. In this figure, once injection pressure rises, for the same permeability and material parameters the effective non-wetting phase saturation degree radius significantly increases faster. The influence of the injection pressure on the method and the importance of overcoming the hydrostatic pressure at the injection points are also observed to have a more effective non-wetting phase advance, being visible the fact that it is high the injection pressure with which the non-wetting phase is injected, the more significant the advance of this in the soil.

The information presented here predict the influence of the hydraulic parameters in the injection issue founded on the non-wetting phase saturation degree and the effective non-wetting phase saturation degree radius. The material parameters of the soil associated with the biphasic flow presented in Table 1, and Table 3 were changed and kept invariant, respectively, through all the predictions. Even though the material parameters connected to the analysis may not be consequent with various hydraulic parameters showed in literature, they do indicate a tendency that offers valuable evidence on the coupled biphasic flow performance of materials, which is the primary idea of this parametric analysis. Furthermore, the records of the parametric exploration demonstrate the relation of the biphasic flow performance of saturated and partially saturated soil on the hydraulic parameters. In this research, the impact of the hydraulic parameters on the desaturation of the soil due to the injection was considered. In the works to come, it is required some research on the impact of the constitutive parameters of the material, e.g., viscoplastic parameters, by recommended mathematical methods with a multiphase coupled elasto-viscoplastic approach show in literature. It is since the occurrence of the surface deformation, and the strain concentration on these materials and desaturation process have to be discussed mainly concerning the injection pressure, the effective non-wetting phase saturation degree radius, and the wetting phase and non-wetting phase permeability of the material (both subject to changes in void ratio. In the works to come, it is essential for the confirmation of the desaturation methods to perform experiments on injection in saturated-unsaturated materials with whole instrumentation and calibration of the hydraulic and the deformation features.

4.1.2 Second group of results of numerical simulations

The influence of injection pressures on the features of the non-wetting phase flow was, therefore, one of the major motivations of this research. Injection pressure is one of the parameters governing the behavior of the non-wetting phase injected into porous media. It has been suggested that increasing the non-wetting phase injection pressure above the injector, leads to a rise in air channel density, and therefore to a rise in non-wetting phase saturation degree within the boundaries of a non-wetting phase plume [241]–[243]. This presumed influence was quantified, and a systematic study of the effects of increasing non-wetting phase injection pressures is shown in terms of effective desaturation radius. First four injection pressures are less than the injection pressure suggested by Ogata and Okamura [171], for an injector at 6 meters depth, that is approximately equal to $87kPa$ (for a soil with a unitary weight of $\gamma = 19.0\ kN/m^3$). The fifth injection pressure is little higher than recommended by Marulanda [224], Okamura et al. [122] and Zeybek et al. [138], [166] Moreover, the sixth injection pressure is much higher than recommended in the literature. It is important to note that not all the injection pressures added to the parametric analysis correspond to one that will not produce destruction of the internal structure of the soil to be improved.

However, it is decided to analyze these range of injection pressures and the isocontours of non-wetting phase saturation degree with the objective of establishing whether the advance of the desaturation front has a behavior directly proportional to the increase in pressure or if this is done without any particular pattern.

The pressure of the non-wetting phase injected and predicted results of effective radius profiles, corresponding to six different injection pressures $(P_{nw,inj} = 70, 75, 80, 85, 90\ and\ 100kPa)$, for a non-wetting phase injection time equal to 9OOs, 1800s, 2700s, and 3600s and for four different soils presented in Table 2 is shown in Figure 24 to Figure 31, as follows.

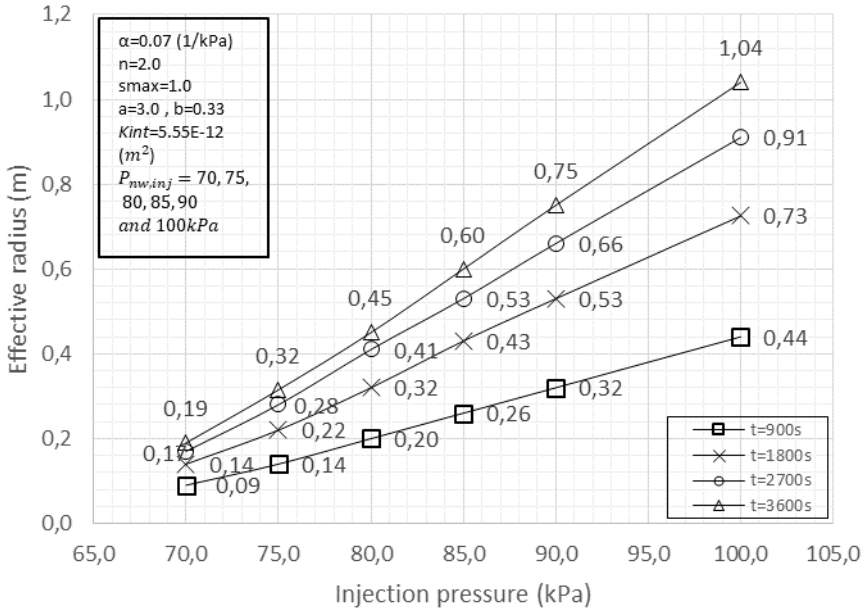

Figure 24 Plume effective radius or advance length, taken from the isocontour corresponding to $S_{nw} = 0.1$, for injection pressures $(P_{nw,inj} = 70, 75, 80, 85, 90\ and\ 100kPa)$, for Soil number 1 in Table 2, and injection times equal to 900s, 1800s, 2700s, and 3600s.

In the Figure 24 the comparison of the non-wetting injection pressures $(P_{nw,inj} = 70, 75, 80, 85, 90\ and\ 100kPa)$ and the effective desaturation degree profiles at the time intervals 900s, 1800s, 2700s and 3600s, for the soil number 1 ($k_{int} = 5.55x10^{-12}m^2$)

presented in the Table 2, are shown. This figure also includes soil parameters. The effective desaturation radius starts increasing slowly for lower injection pressures and is slightly different after the a time interval of 900s, but these difference growths with the rise in the time after the interval of 1800s to 3600s. The larger the effective desaturation radio profiles are obtained for the higher non-wetting phase injection pressure. Comparable conclusions can be achieved from the effective desaturation radius profiles that are shown comparatively in Figure 14. Isocontours of predictions of the evolution in the non-wetting phase saturation degree for the variation of the non-wetting injection pressures $(P_{nw,inj} = 70, 75, 80, 85, 90\ and\ 100kPa)$, for the soil number 1 ($k_{int} = 5.55x10^{-12}m^2$), employing the ground model and parameters constrained as is explained in the Table 2 is shown in Figure 25

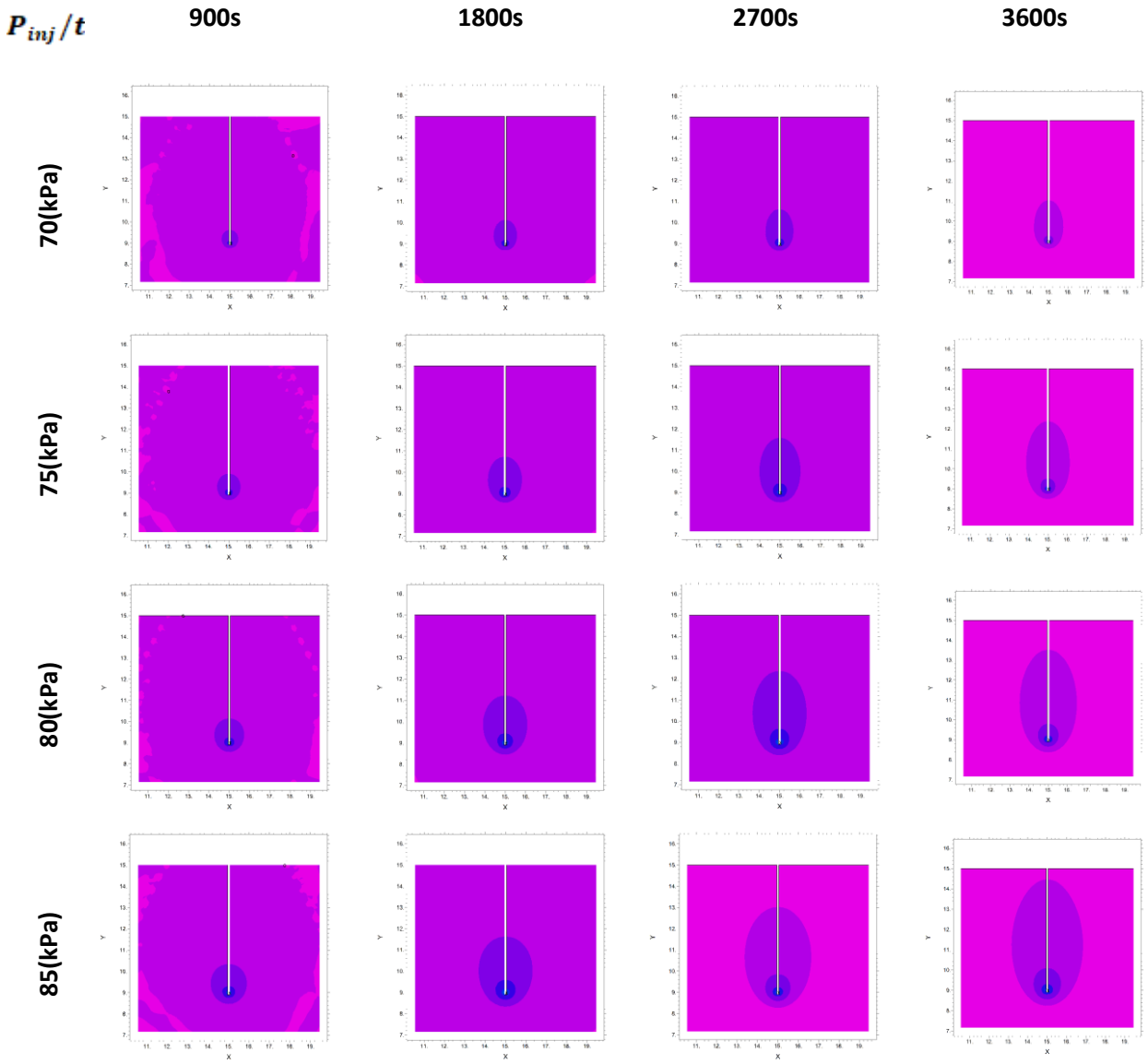

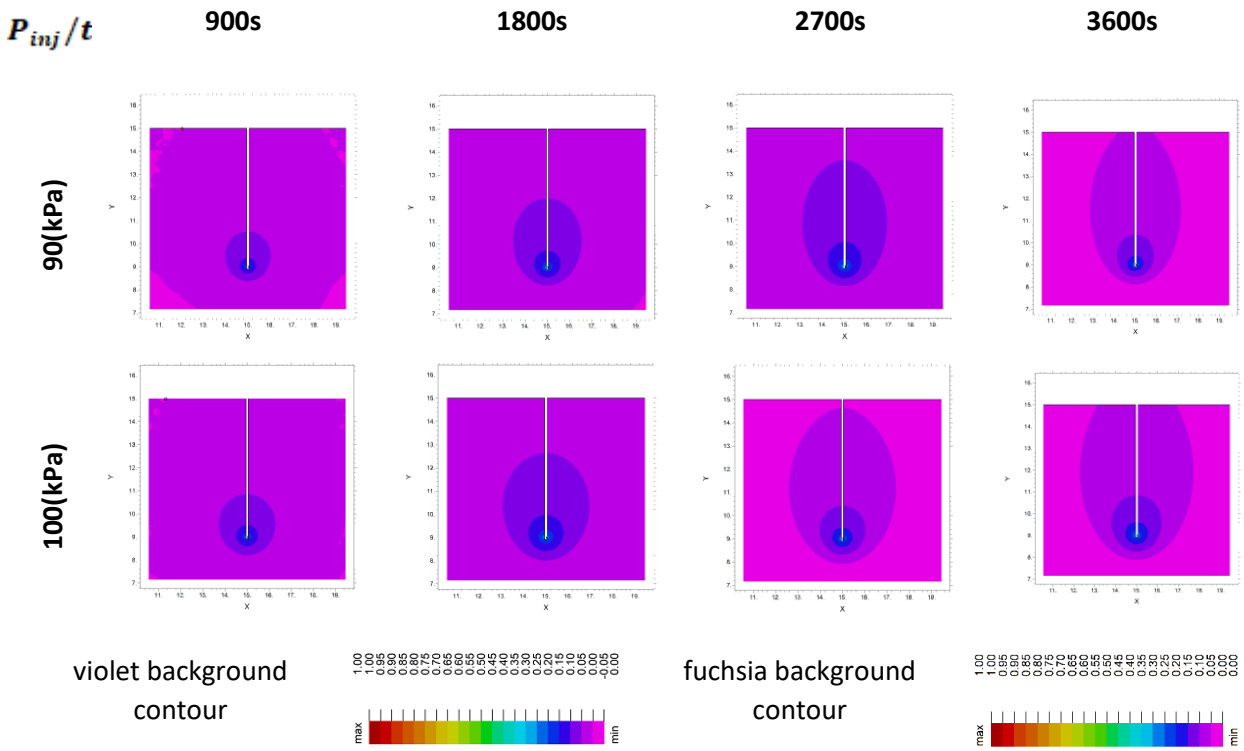

Figure 25 Temporal change in the non-wetting phase degree of saturation induced by air injection .Isocontours-distribution of plume expansion, taken from the corresponding injection pressures $(P_{nw,inj} = 70, 75, 80, 85, 90\ and\ 100kPa)$, for the soil number 1 ($k_{int} = 5.55x10^{-12}m^2$) in Table 2 and injection times equal to 900s, 1800s, 2700s, and 3600s. Distance in meters.

In Figure 25 the results obtained for this analysis shows the effect of the pressure, the intrinsic permeability on the method and the importance of overcoming the hydrostatic pressure at the injection points is also observed to have a more effective gas advance. This fact makes it visible that if the pressure with which the non-wetting phase is injected is greater, the greater the advancement of this in the soil. It is observed that the advance of the expansion plume of the non-wetting phase that is injected occurs primarily in the vertical direction for injection conditions under relatively low pressures and close to the hydrostatic pressure at the injection point. However, under conditions of injection pressure of the non-wetting phase close to the injection pressure recommended by literature and above, it is observed from the isocontours that there is a predominantly vertical advance of the non-wetting phase injected (mainly due to the gravitational forces) and in the other hand a considerable advance in horizontal direction and growing over time. It is expected from the phenomenon that for injection times of 3600s under a constant injection pressure of 90kPa or 100kPa the method begins to generate outputs of the non-wetting phase injected on the surface of the ground to be desaturated.

In the Figure 26 the comparison of the non-wetting injection pressures $(P_{nw,inj} = 70, 75, 80, 85, 90\ and\ 100kPa)$ and the effective desaturation degree profiles at the time intervals 900s, 1800s, 2700s and 3600s, for the soil number 2 ($k_{int} = 1.00x10^{-11}m^2$) presented in the Table 2, are shown.

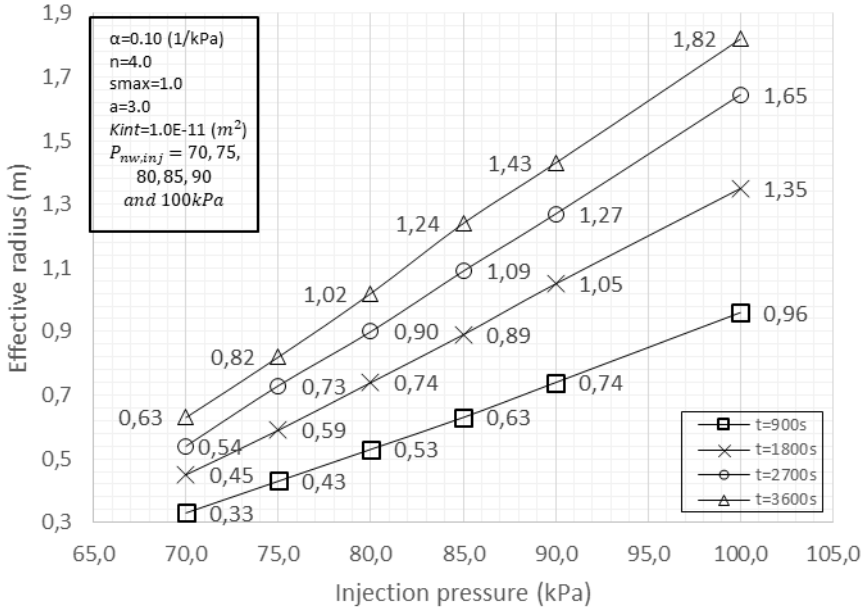

Figure 26 Plume effective radius or advance length, taken from the isocontour corresponding to $S_{nw} = 0.1$, for injection pressures $(P_{nw,inj} = 70, 75, 80, 85, 90\ and\ 100kPa)$, for Soil number 2 inTable 2, and injection times equal to 900s, 1800s, 2700s, and 3600s.

It can be perceived from the Figure 26 that the greater the injection pressure, the additional the increase of matric suction and the higher the effective non-wetting phase saturation degree radius after 9OOs, 1800s, 2700s, and 3600s. It is perceived that variations of the injection pressure for fixed permeability values, constant material parameters, and variable injection times generate substantial increases in the advance lengths of the non-wetting phase, and it is perceived that the magnitudes of the penetration radius vary significantly with variations of the injection pressure for fixed times. From the previous, it can be seen that the injection pressure and time are fundamental variables within two-phase flow analysis.

In the Figure 27 the comparison of the non-wetting injection pressures $(P_{nw,inj} = 70, 75, 80, 85, 90\ and\ 100kPa)$ and the effective desaturation degree profiles at the time intervals 900s, 1800s, 2700s and 3600s, for the soil number 3 ($k_{int} = 5.55x10^{-11}m^2$), presented in the Table 2, are shown.

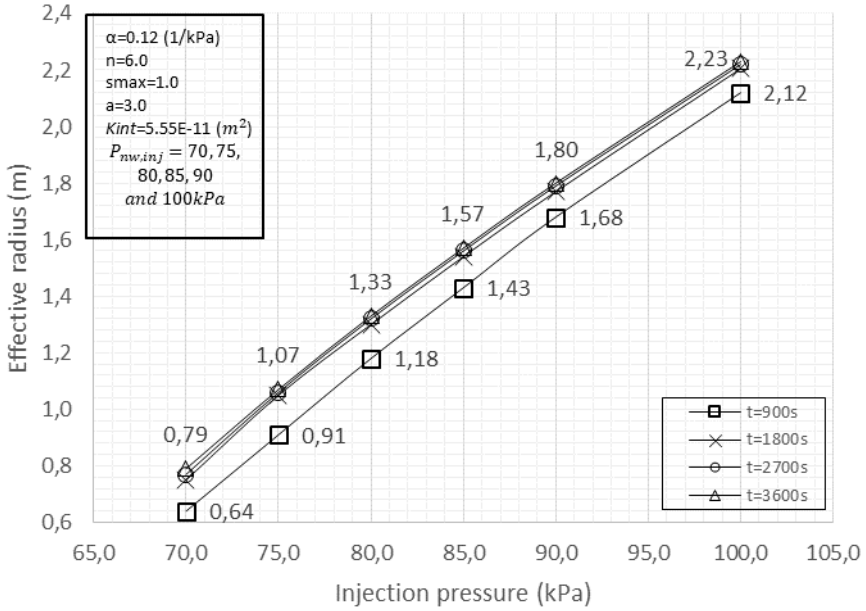

Figure 27 Plume effective radius or advance length, taken from the isocontour corresponding to $S_{nw} = 0.1$, for injection pressures $(P_{nw,inj} = 70, 75, 80, 85, 90\ and\ 100kPa)$, for Soil number 3 in Table 2, and injection times equal to 900s, 1800s, 2700s, and 3600s.

From Figure 27, it is possible to see two different responses in the injected pressures and the effective desaturation radius along the surface. In the cases when the injection pressures after 900s are plotted the effective desaturation radius are clearly defined, since it increases with the increase of injection pressures and during the same time injection. For the cases of injection times of 1800s, 2700s and 3600s the effective desaturation radius increase with considerable pressures during the injection time, but almost at three cases reaching or generating the same non-wetting saturation degree at the surface. Previous can be explained or related to values of high permeabilities that control the injection phenomena. This trend for large permeabilities shows that the non-wetting phase flow in this kind of soils is mainly developed by a vertical gradient generating a defined upward trend in the flow. Isocontours of predictions of the evolution in the non-wetting phase saturation degree for the variation of the non-wetting injection pressures $(P_{nw,inj} = 70, 75, 80, 85, 90\ and\ 100kPa)$, for the soil number 3 ($k_{int} = 5.55x10^{-11}m^2$), employing the ground model and parameters constrained as is explained in the Table 2 is shown in Figure 28.

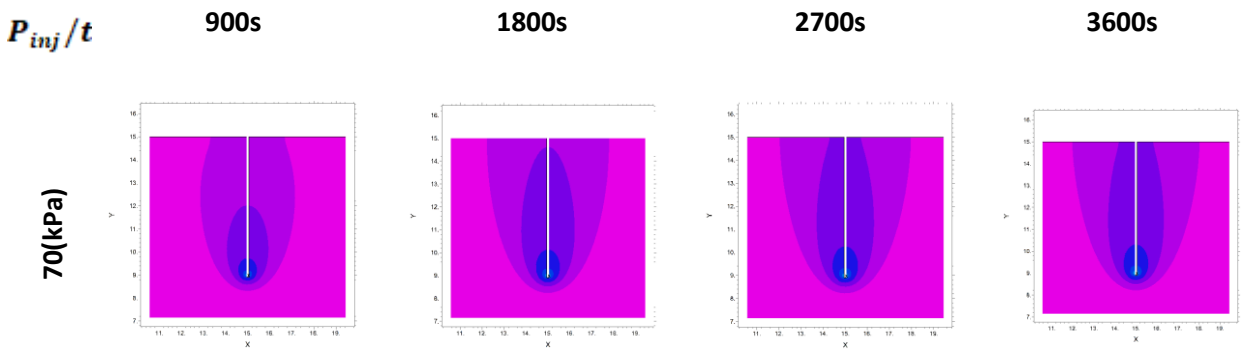

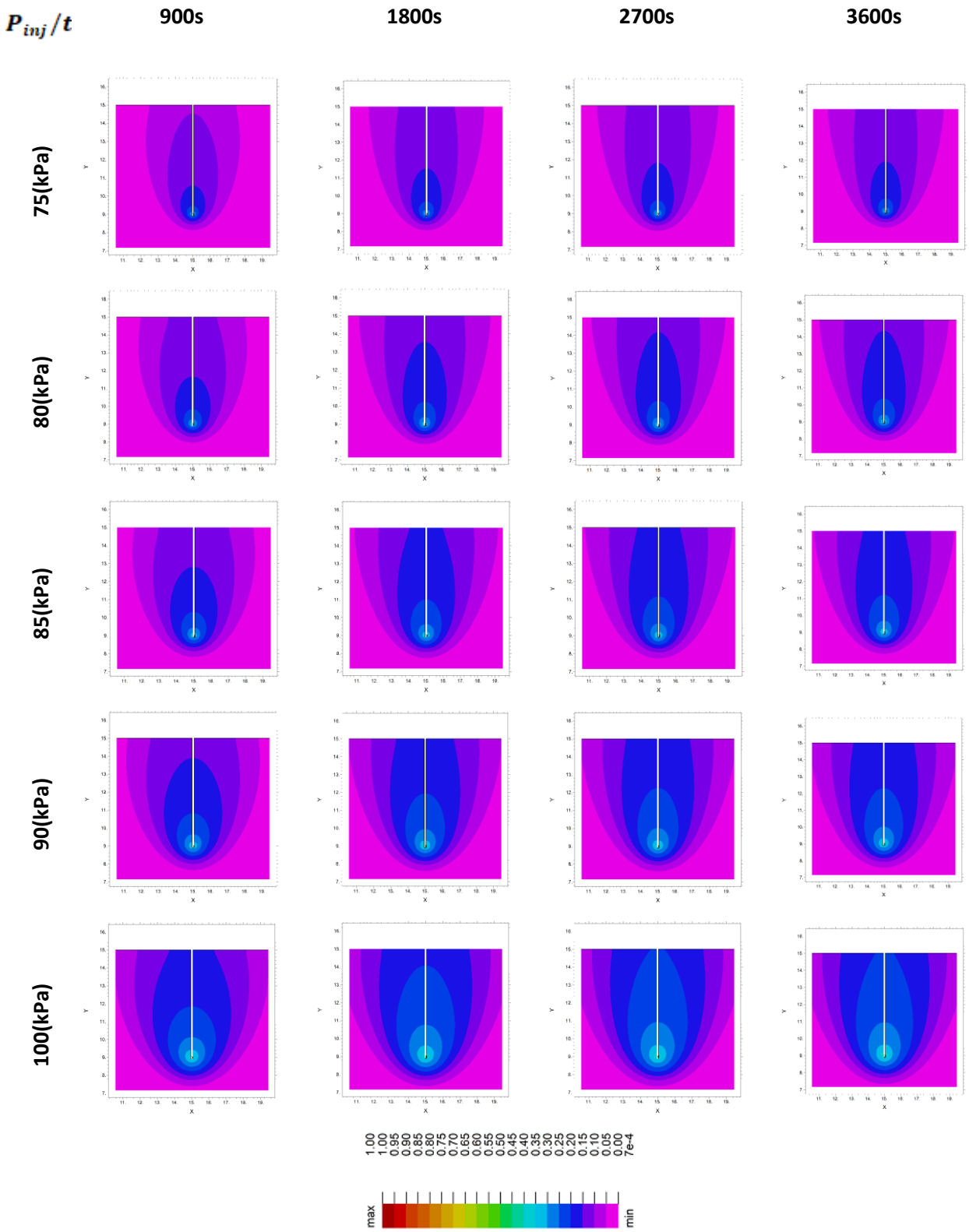

Figure 28 Temporal change in the non-wetting phase degree of saturation induced by air injection .Isocontours-distribution of plume expansion, taken from the corresponding injection pressures $(P_{nw,inj} = 70, 75, 80, 85, 90\ and\ 100kPa)$, for the soil number 3 ($k_{int} = 5.55x10^{-11}m^2$) in Table 2 and injection times equal to 900s, 1800s, 2700s, and 3600s. Distance in meters.

In Figure 28 it is observed that for soils with relatively high permeabilities, fast flows of the non-wetting phase injected are given. Fast flows for injections of 900s of duration typically reach the surface of the ground and begins to leave even for the lowest pressures of injection of the non-wetting phase. It is observed that for injection times of 1800s or greater the non-wetting phase area affected by the desaturation plume does not extend or does not change significantly in form (length). However, internally the isocontours associated with the magnitudes of the non-wetting phase saturation degree increases in magnitudes mainly in areas near the injector and these plumes tend to maintain mainly vertical flow. This in some way represents certain ease to flow from the non-wetting phase in the vicinity of the injector, because in those plumes the observed contents of the non-wetting phase as pore fluid are more significant for injection times of up to 3600s.

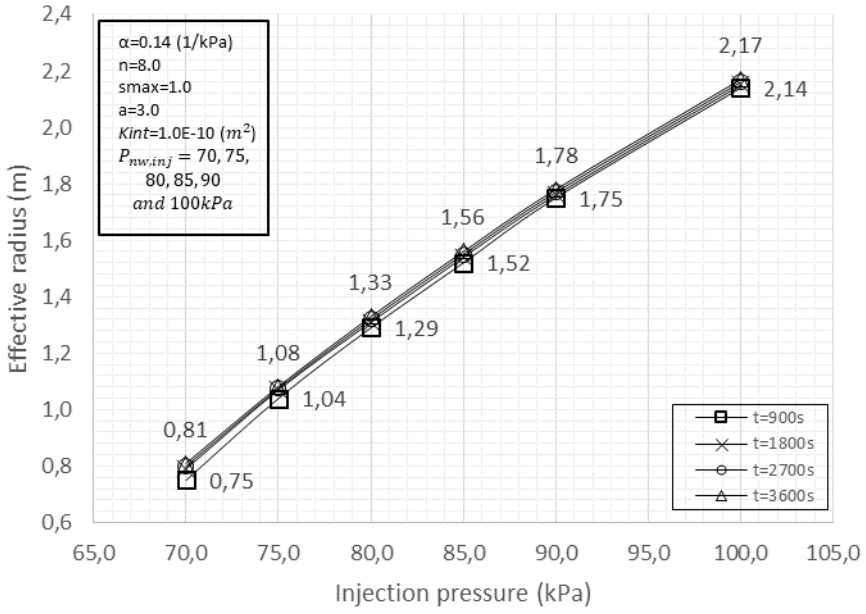

Figure 29 Plume effective radius or advance length, taken from the isocontour corresponding to $S_{nw} = 0.1$, for injection pressures $\left(P_{nw,inj} = 70, 75, 80, 85, 90\ and\ 100kPa\right)$, for Soil number 4 in Table 2 and injection times equal to 900s, 1800s, 2700s, and 3600s.

From Figure 29, it is possible to see one response in the injected pressures and the effective desaturation radius along the surface. In generally when results after 900s, 1800s, 2700s, and 3600s are plotted the effective desaturation radius increase with large pressures during the injection time, but at four cases reaching or generating the same non-wetting saturation degree at the surface. The previous result that can be explained or related to values of high permeabilities that control the injection phenomena. This trend for large permeabilities shows that the non-wetting phase flow in this kind of soils is mainly developed by a vertical gradient generating a defined upward trend in the flow. Isocontours of predictions of the evolution in the non-wetting phase saturation degree for the variation of the non-wetting injection pressures $\left(P_{nw,inj} = 70, 75, 80, 85, 90\ and\ 100kPa\right)$, for the soil number 4 ($k_{int} = 1.0x10^{-10}m^2$), employing the ground model and parameters constrained as is explained in the Table 2 is shown in Figure 30.

P_{inj}/t	900s	1800s	2700s	3600s
70(kPa)	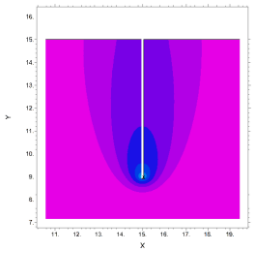	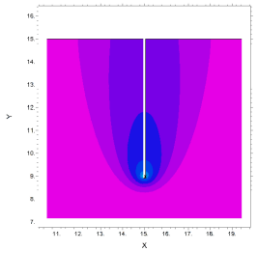	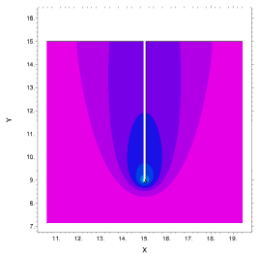	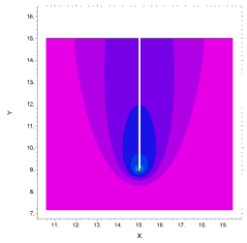
75(kPa)	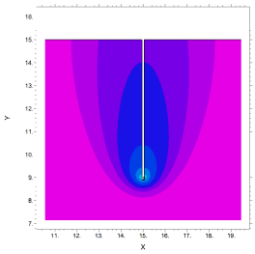	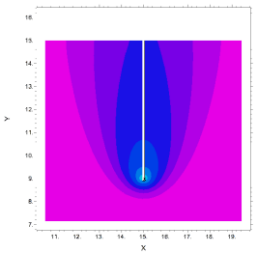	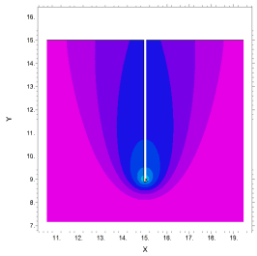	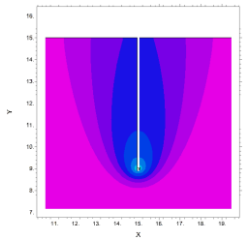
80(kPa)	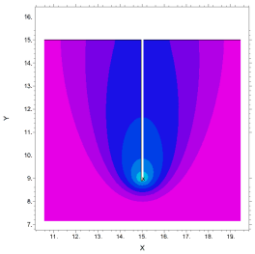	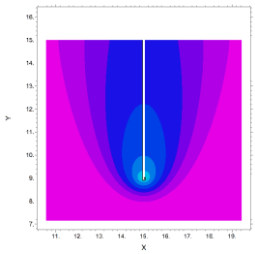	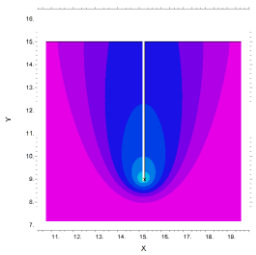	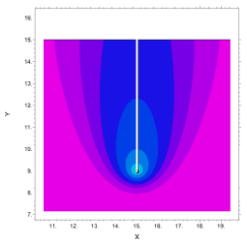
85(kPa)	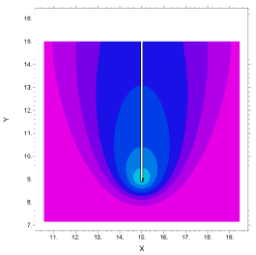	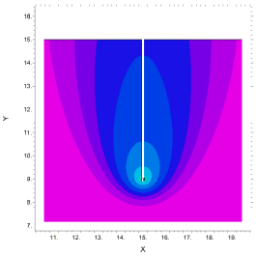	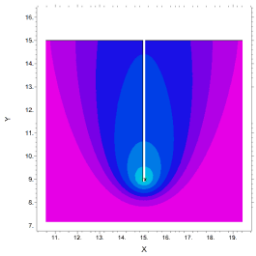	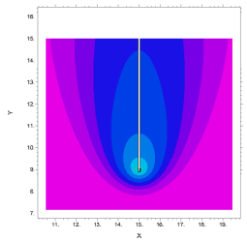
90(kPa)	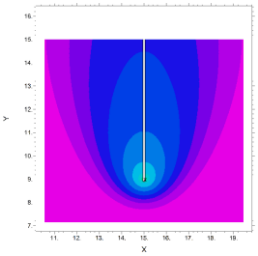	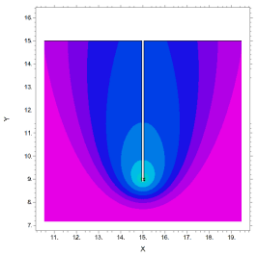	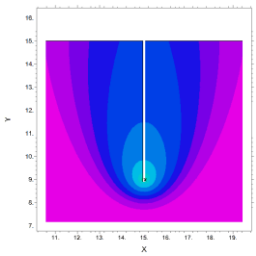	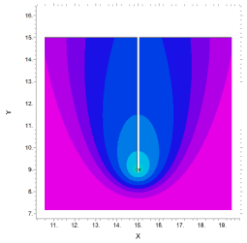
100(kPa)	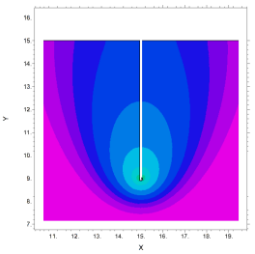	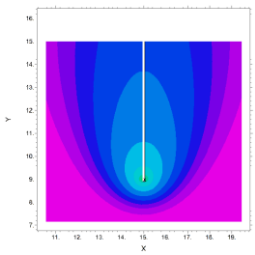	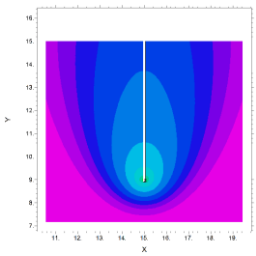	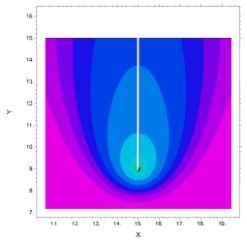

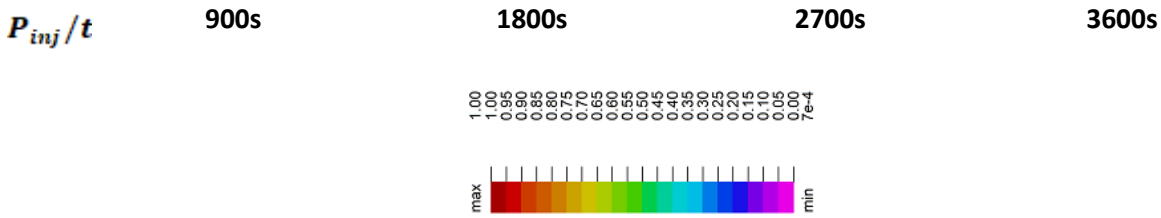

Figure 30 Temporal change in the non-wetting phase degree of saturation induced by air injection .Isocontours-distribution of plume expansion, taken from the corresponding injection pressures $\left(P_{nw,inj} = 70, 75, 80, 85, 90\ and\ 100kPa\right)$, for the soil number 4 ($k_{int} = \ 1.0x10^{-10}m^2$) in Table 2 and injection times equal to 900s, 1800s, 2700s, and 3600s. Distance in meters.

In Figure 30 it is observed that for soils with high permeabilities, fast flows of the non-wetting phase injected are given. Fast flows for injections of 900s of duration typically reach the surface of the ground and begins to leave even for the lowest pressures of injection of the non-wetting phase. It is observed that for injection times of 900s or greater the non-wetting phase area affected by the desaturation plume does not extend or does not change significantly in form(length). However, internally the isocontours associated with the magnitudes of the non-wetting phase saturation degree increases in magnitudes mainly in areas near the injector and these plumes tend to maintain mainly vertical flow. This in some way represents certain ease to flow from the non-wetting phase in the vicinity of the injector, because in those plumes the observed contents of the non-wetting phase as pore fluid are more significant for injection times of up to 3600s.

To observe the impact of the permeabilities on non-wetting phase flow and the effective desaturation radius, diverse conditions are predicted. The predicted cases are presented in Table 2. The predicted cases contain some diverse mixtures of intrinsic permeabilities and hydraulic parameters for the typical soils. In Figure 31 four different desaturation trends are included to present the impact of the injection pressure on the non-wetting phase infiltration problem into saturated and partially saturated different soils.

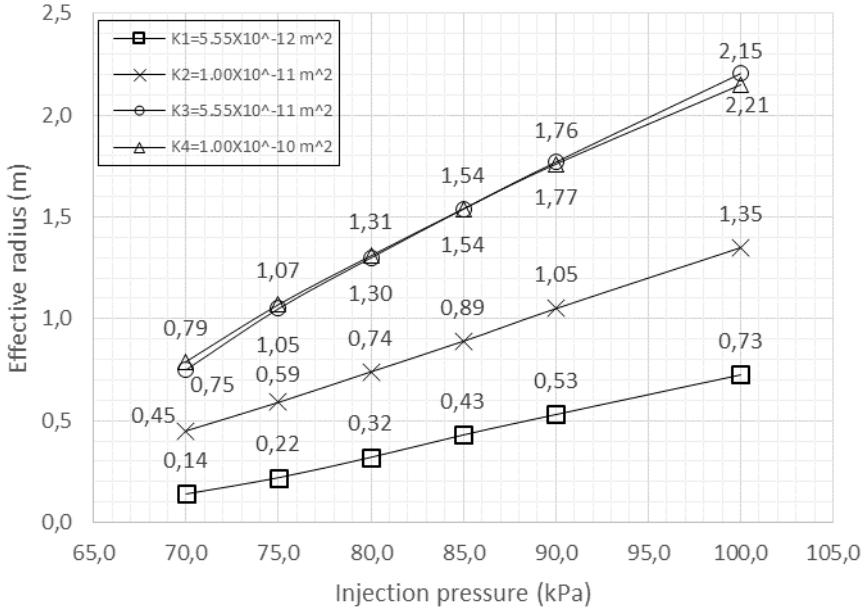

Figure 31 Plume effective radius or advance length, taken from the isocontour corresponding to $S_{nw} = 0.1$, for injection pressure $(P_{nw,inj} = 70, 75, 80, 85, 90\ and\ 100kPa)$, for four different Soils in Table 2, and injection time equal to 1800s.

Figure 31 shows the contrast of the injection pressure profiles at the end of the diverse injection configurations and for intrinsic permeabilities, namely, ($k_{int} = 5.55x10^{-12}m^2, 1.0x10^{-11}m^2, 5.55x10^{-11}m^2\ and\ 1.0x10^{-10}m^2$). After this figure, it is probable to see two different reactions in the injected pressures and the effective desaturation radius along the surface. In the cases when the injection pressures are large and the permeability, i.e. ($k_{int} = 5.55x10^{-12}m^2\ and\ 1.0x10^{-11}m^2$), the effective desaturation radius are clearly defined, since it increases with the increase of injection pressures and during time injection. For the cases of permeabilities, i.e., $(k_{int} = 5.55x10^{-11}m^2\ and\ 1.0x10^{-11}m^2)$ the effective desaturation radius increase with large pressures during the injection time, but almost both reaching or generating the same non-wetting saturation degree at the surface. The previous result of that can be explained or related to values of high permeabilities that control the injection phenomena. This trend for large permeabilities shows that the non-wetting phase flow in this kind of soils is mainly developed by a vertical gradient generating a defined upward trend in the flow. Isocontours of predictions of the evolution in the non-wetting phase saturation degree for the variation of the non-wetting injection pressures $(P_{nw,inj} = 70, 75, 80, 85, 90\ and\ 100kPa)$, and for intrinsic permeabilities, namely, ($k_{int} = 5.55x10^{-12}m^2, 1.0x10^{-11}m^2, 5.55x10^{-11}m^2\ and\ 1.0x10^{-10}m^2$), employing the ground model and parameters constrained as is explained in the Table 2 is shown in Figure 32.

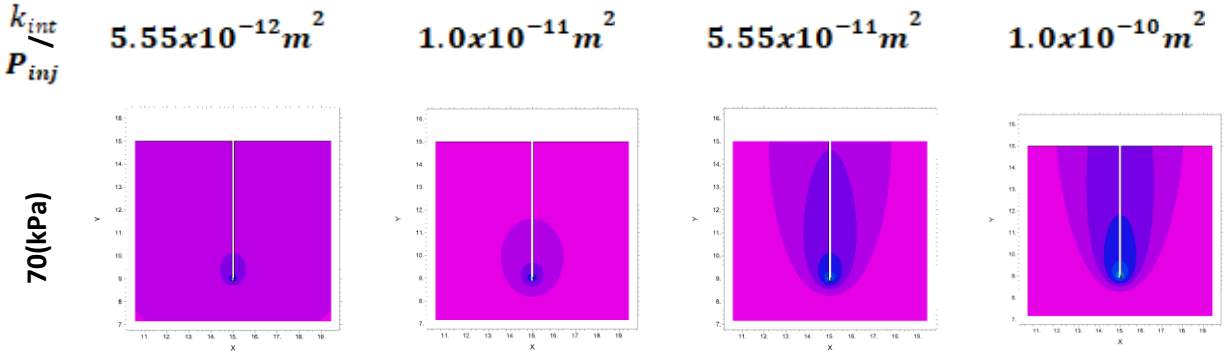

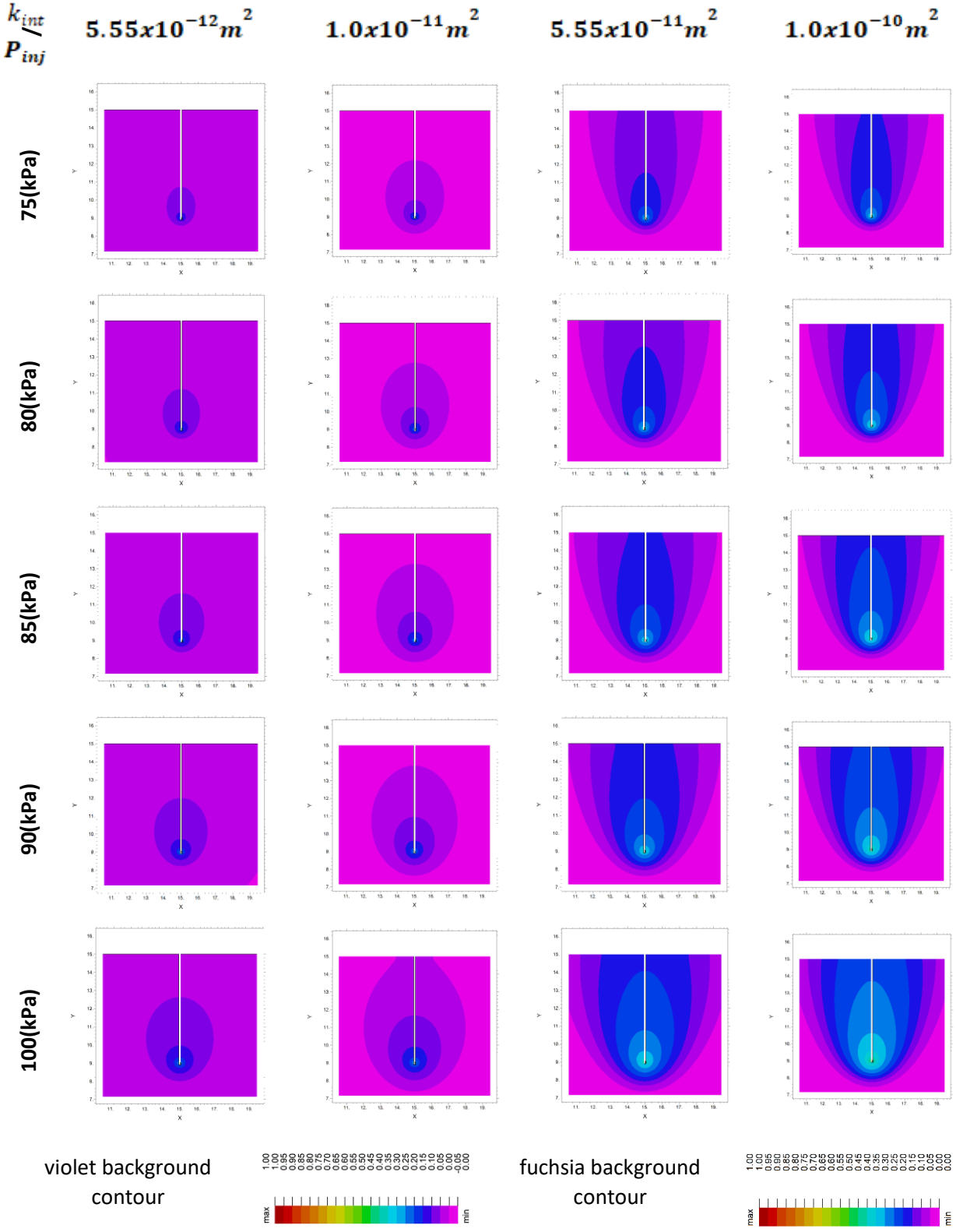

Figure 32 Change in the non-wetting phase degree of saturation induced by air injection. Isocontours-distribution of plume expansion, taken from the corresponding injection pressures $(P_{nw,inj} = 70, 75, 80, 85, 90\ and\ 100kPa)$, for intrinsic permeabilities, namely, ($k_{int} = 5.55x10^{-12}m^2, 1.0x10^{-11}m^2, 5.55x10^{-11}m^2\ and\ 1.0x10^{-10}m^2$) in Table 2 and injection time equal to 1800s. Distance in meters.

In the cases where the injection pressure was varied, an injection duration of 1800s was set, and the intrinsic permeability was changed for the prediction of the plumes for four different soils, it was possible to observe the importance of this last parameter for the processes of injection by the desaturation method proposed by Okamura. The graphs shown (See Figure 32) that this property provides the soil with the ability to transmit fluids within it and according to the results obtained, the more permeable the soil to which the injection is made, the higher the filtration; or in this case, the advance of the desaturation plumes within its structure. Typically, the shape of the desaturation plume in the predictions was approximated to a cone-shaped zone as is presented by Nyer and Sutherson [216] or a by a parabolically shaped zone as is presented by Reddy et al. [164] and by Chen et al.[244]. Additionally, it is perceived that the dimensions of the desaturation plume are substantially dependent on soil features, injection pressure, and depth of injector as Reddy et al., [164]stated.

Moreover, the predictions are similar to Elder and Benson [245] work that described that desaturation plumes have a tendency to develop in soil with a V-shaped form at low non-wetting phase injection pressures and have a tendency to develop in soil with a U-shaped form at high non-wetting phase injection pressures. The researchers proposed that the variation in plume geometry at high non-wetting phase pressures specify that desaturation plumes increase as the non-wetting phase is injected from the tip since the proportion of pneumatic to buoyant forces rises. Also, predictions results are consequent with Reddy and Adams [169] that described desaturation plumes with parabolic shapes for coarse-grained materials as uniform and homogenous sands, soils typically associated to be susceptible to liquefaction. The extent of the desaturation plume in the predictions shows an increasing response with reducing the intrinsic permeability and increasing tortuosity. Tighter desaturation plumes were perceived for high intrinsic permeability, in relation to the low resistance to be developed the non-wetting phase flow as is presented by Reddy and Adams [169].

It is crucial to relate isocontours of temporal variations in desaturation plumes showed in Figure 15, Figure 25, Figure 28 and Figure 30 with the work of Lundegard and Andersen [246] that observed from the desaturation plume that changes through the development of non-wetting phase injection occurs. Researchers defined three crucial stages during the method implementation. The first is called the expansion stage, described by a preliminary transitory interval where the desaturation plume associated with the evolution of the non-wetting phase in together vertical and horizontal ways. The second a collapsed stage that besides transitory through a decrease of the lateral extent of non-wetting phase ways happens it is more clear to be defined from soils with high intrinsic permeability. Also, the third that is a steady-state stage, stage defined by behavior that remains practically stationary, if non-wetting phase injection features are set as invariant.

4.1.3 Comparison with experimental results

Experimental information developed at scale level in a laboratory or in-situ test of air injection into saturated soils are unusual, expensive, relevant, and can be used as input information for numerical models analysis. These kinds of data let the adjustment and corroboration of numerical models employed to examine the behavior of saturated and partially saturated soils during multiphasic flow. Okamura et al. [126] executed a remarkable laboratory study and generated measurements of nominal rates, magnitudes of the soil desaturation induced by air injection developed with two types of soil boxes (small and large). Furthermore, the distributions of the desaturated zones within the soil, immediately and constantly throughout the air injection process were determined. The recorded information shows that, even though there is a visible relation on the physical characteristics of selected materials, the advancement of the non-wetting phase front is intensely restricted by the air pressures at the injector, and the material ability to allow fluids to pass through it.

In addition, numerical predictions were developed via multiphase flow software to characterize the advance of the desaturation front, and to explore the availability of the formulation in the tool

(biphasic model in TOUGH2 [167]), allowing the prediction of the advance of the non-wetting phase at a particular place in situ to be monitored in time and space. Predictions showed by Okamura demonstrate a reasonably good adjustment with laboratory experimentation concerning the rates, magnitudes, and distribution of the non-wetting phase especially for the small-box tests, while simulations of the non-wetting phase front somewhat exaggerate the quantities associated to the large-box tests. Therefore, Okamura et al. research shows that the predictive model defined is appropriate to explore some field analysis when the soil characteristics concerning flow transport are well-represented.

Some of the experimental results of air injection into a fully saturated model (small and large box) ground that was created with Toyoura sand are adopted. Large box experimental results are used to compare among numerical predictions achieved by a biphasic flow defined in this dissertation, and solutions by means of the finite element analysis method.

The laboratory test results were achieved by Okamura et al. [126] by executing fully saturated homogeneous column (small and larger) tests of coarser soil exposed to air injection. Tests were developed under conditions of allowed flow of water and air at the top of the column, initial wetting phase hydrostatic distribution for pressure, and air injection into the ground with inlet ports situated on the center-bottom of the box. The injection tests were piloted in a two different soil column apparatus characterized by Okamura et al. [126]. The large apparatus contained a transparent acrylic cylinder 0.9 m high, 1.72 m width and 0.60 m depth for retaining the soil, as shown in Figure 33. Time domain reflectometry (TDR) probes were introduced inside the box and used in the tests to define local and temporal variations on wetting phase saturation degree. Injection process at a defined pressure and duration were executed to the model ground at the injector. A wetting phase pressure instrument is placed above the model ground to continually define the behavior of the water level modified by the advance of the non-wetting phase front.

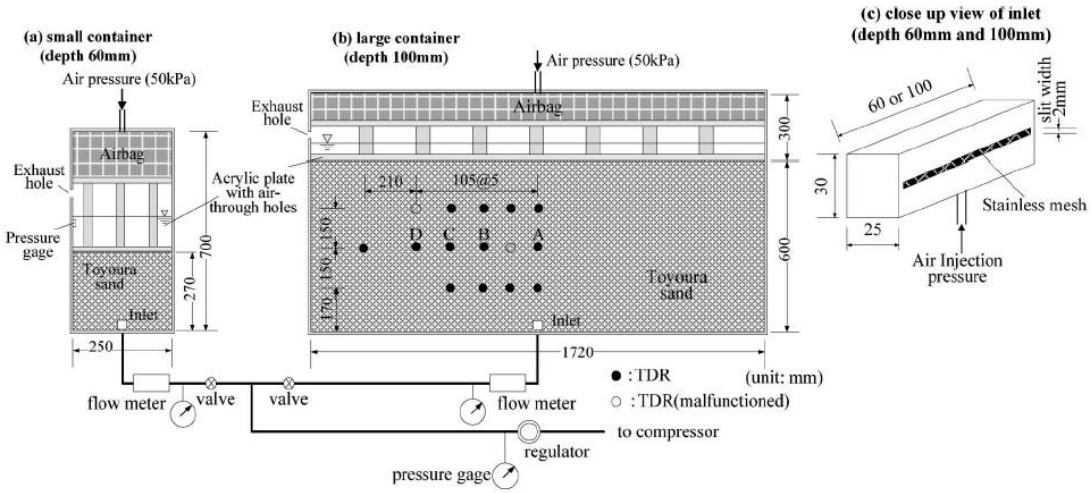

Figure 33 Sketch of the injection apparatus (a) small, (b) large, and (c) focused view of the inlet for air injection: for the large one, local wetting phase saturation degrees are measured by TDR probes (presented by black circles) and additionally at the locations (A)–(D), temporal changes in saturation are continuously measured. Taken from Okamura et al. [126].

Results of large soil column constructed with Toyoura sand are showed at this point. Laboratory experimentation was defined from a wetting phase hydrostatic condition with the water level situated at the top of the soil column. Tests are piloted at periodically incremented non-wetting phase pressures, variating from 10 to 15 kPa, and TDR probes measure time-dependent developments with spatial distributions of the saturation degree. Air injection is applied to the column for 5500 seconds; the results of the experiments are shown in Figure 34. Furthermore,

variations in air injection pressure, airflow rate per unit depth, and saturation degree at the positions (A), (B), (C), and (D), defined in the Figure 33, are showed in Figure 34. Flow rates at (A), (B), (C), and (D) are measured by the flow meter connected in injection conduct near and before the injection ports and presented in Figure 35

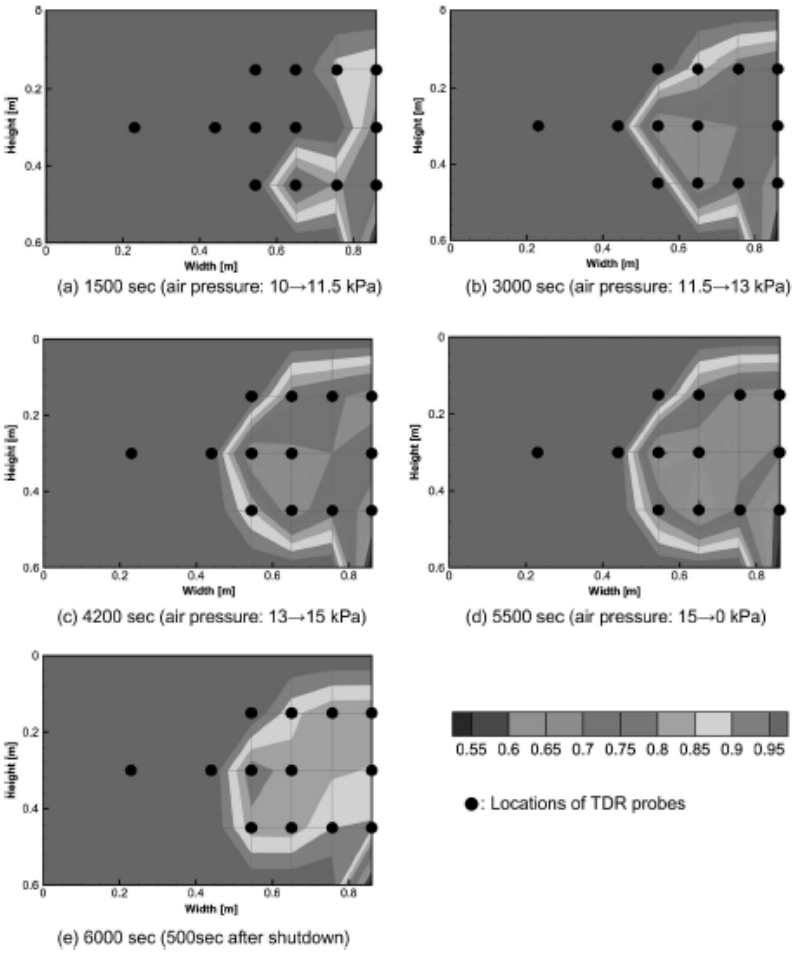

Figure 34 Distributions of saturation evaluated by TDR probes within the large-container ground at (a) 1500, (b) 3000, (c) 4200, (d) 5500 and (e) 6000 seconds (note that one half domain is shown). Taken from Okamura et al. [126].

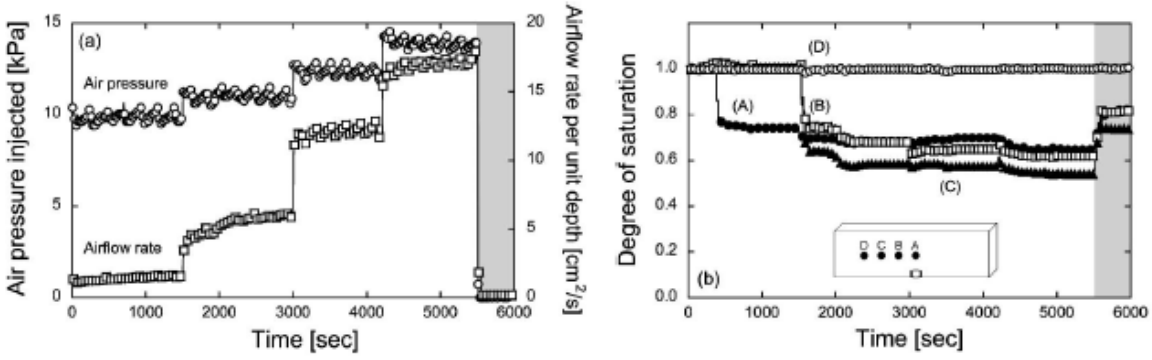

Figure 35 Changes in (a) air pressure injected and air-flow rate per unit depth and (b) degree of saturation with time for the large-container experiments under air pressured 10–15 kPa. Taken from Okamura et al. [126].

4.1.3.1 Simulation of a homogenous soil column

Equivalent boundary values as the implemented in the laboratory test and simulations presented in Okamura et al. [126] are adopted for the numerical predictions in this analysis. A triangular element column (0.6 m high and 1.72 m) mesh with one homogenous layer, and a drained boundary at the top is applied as the analysis domain. The depth dimension of the column is not included in this analysis because the non-wetting phase pattern can be studied in a two-dimensional domain with a transversal section crossing the injector. Soil column finite element mesh is shown in Figure 36. The required soil particles parameters for the material behavior, wetting and non-wetting phase essential for the numerical model in addition to the constitutive expression that describes the suction-saturation characteristics that are included in the predictions are listed in Table 4.

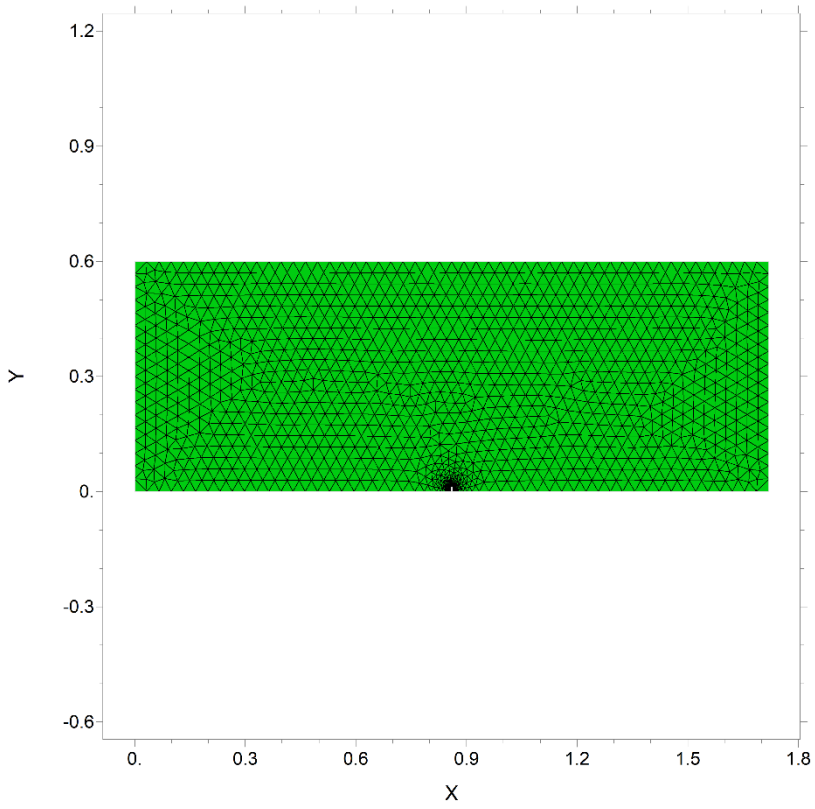

Figure 36 Finite element mesh and boundary conditions.

Table 4 Material and hydraulic parameters used for the numerical simulations.

Variable	Expression	Description
ρ_w	$1000\ kg/m^3$	Fluid density, wetting phase
μ_w	$1x10^{-3}\ Pa\,s$	Dynamic viscosity, wetting phase
ρ_{nw}	$1.28\ \ kg/m^3$	Fluid density, non-wetting phase
μ_{nw}	$1.81x10^{-5}\ Pa\,s$	Dynamic viscosity, non-wetting phase
θ	0.421	Porosity
$S_{w,max}$	1.0	Maximum wetting phase saturation degree
$S_{w,irr}$	0.155	Residual wetting phase saturation degree
α	$2.237 \times 10^{-4}\ \ 1/kPa$	Van Genuchten Alpha parameter
n	8.696	Van Genuchten n material parameter

Variable	Expression	Description
a	0.50	Parameter of coefficient of wetting phase permeability
b	0.33	Parameter of coefficient of non-wetting phase permeability
k_{int}	$2.04 \times 10^{-11}\ m^2$	Intrinsic permeability

4.1.3.2 Results of the simulations

The predicted wetting phase saturation degree isocontours achieved in the numerical simulation at defined injection pressures as presented in the laboratory test results are exposed in Figure 37. Isocontours represent the wetting phase front distribution with the time. Predictions of the distributions of the wetting phase saturation degree at times (a) 1500, (b) 3000, (c) 4200, (d) 5500 and (e) 6000 seconds (note that one-half domain is shown) are presented. When air injection starts the wetting phase saturation degree decreases for the sand notably in depths relatively close to the injector; this tendency progressively growths upward through the sand layer as the non-wetting front increases.

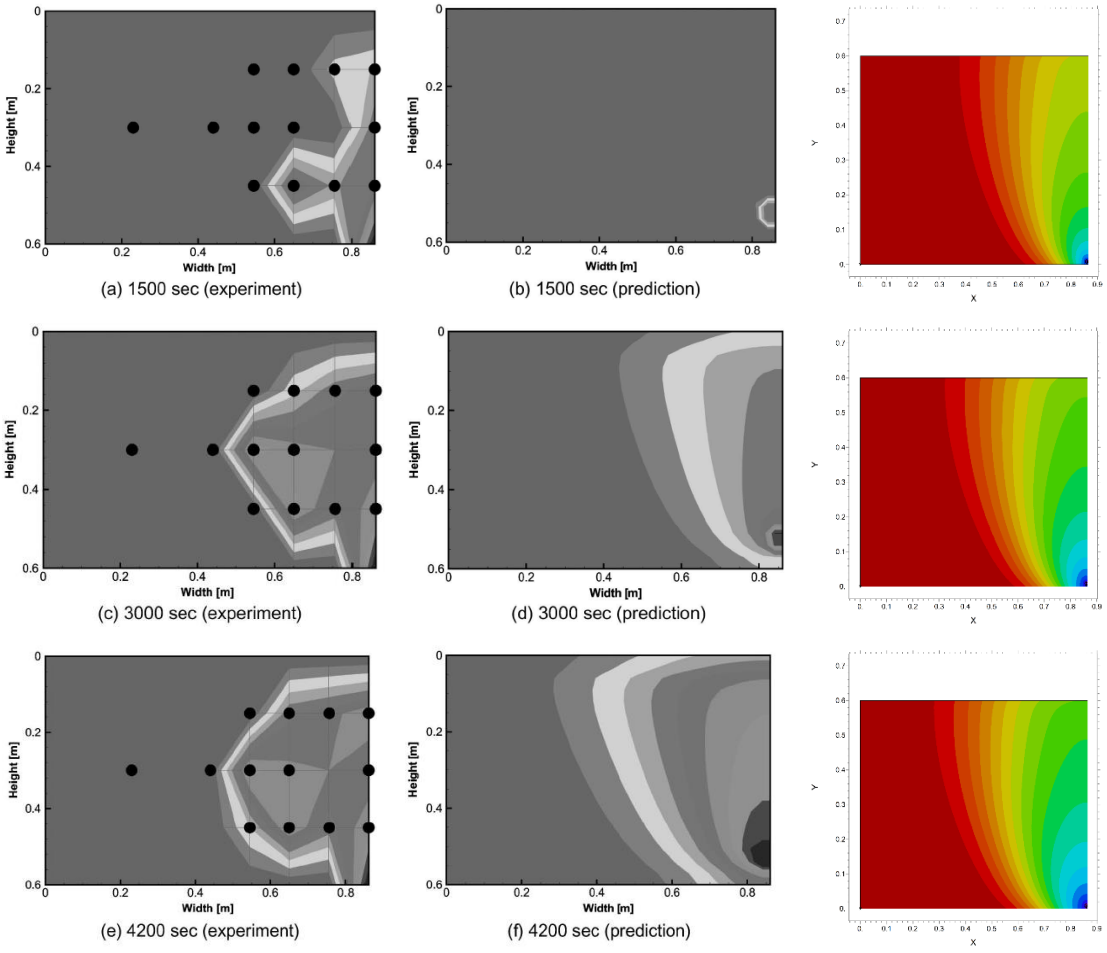

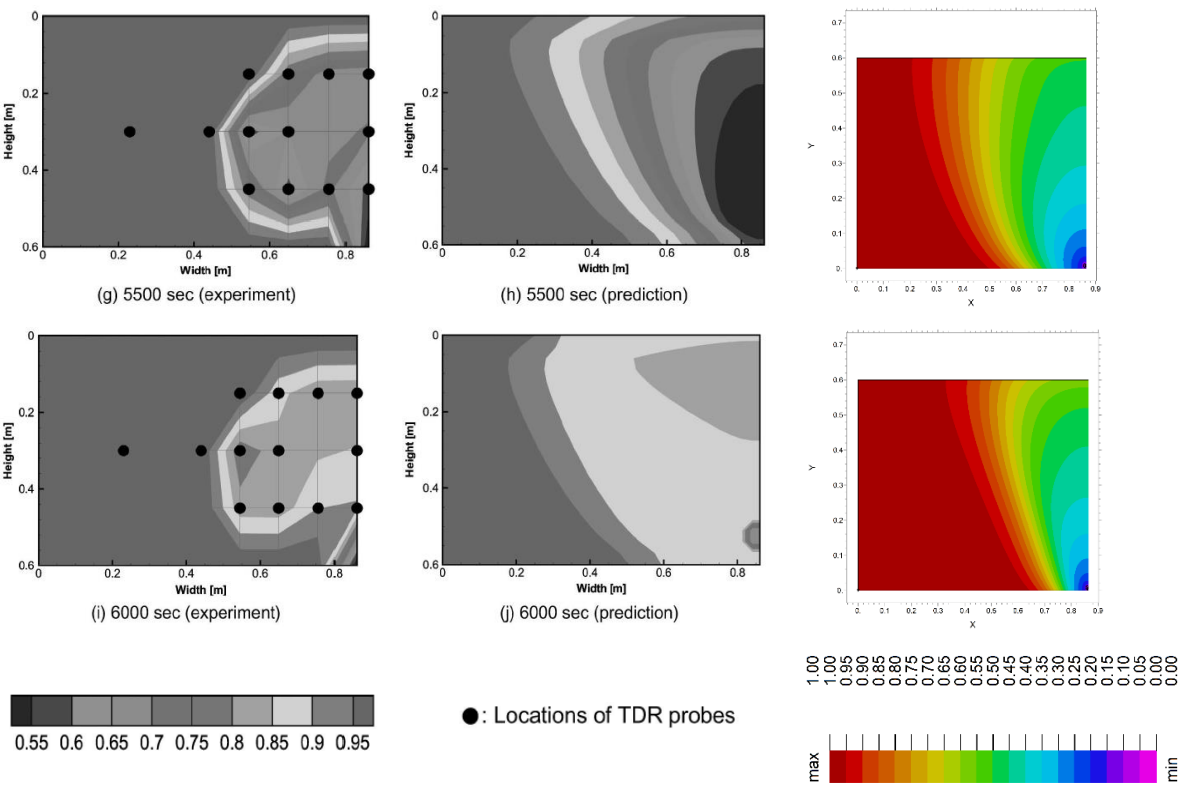

Figure 37 Comparisons of magnitude and distribution of desaturated zones among measurements and predictions. Taken from Okamura et al. [126], and complemented with predictions developed in this thesis.

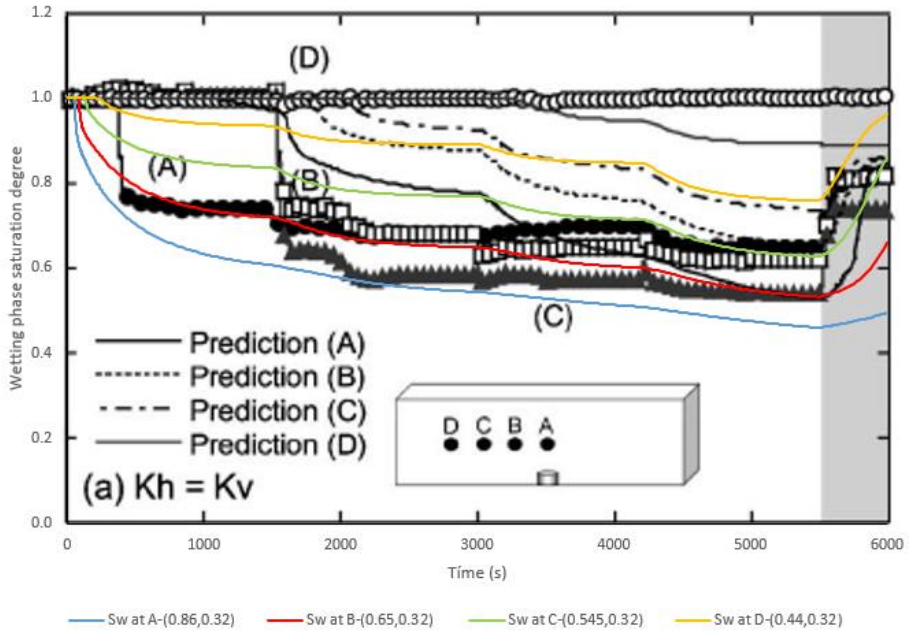

Figure 38 Comparisons of the wetting phase saturation degree among measurements and predictions with one-fold horizontal permeability against vertical value developed by Okamura et al. [126], and predictions developed in this thesis.

When laboratory test and simulation results taken from Okamura et al. [126] are compared with these thesis predicted results, it is exhibited that the numerical analysis captures the subsequent features perceived in the laboratory test and predictions developed with TOUGH2: (1) wetting phase

saturation degree decreases primarily near the injector and progressively decreases upward in the soil column while the air infiltrates by generated gradients in the non-wetting phase pressure, and buoyancy; (2) wetting phase saturation degree is lower and the non-wetting phase flow is faster when the injection pressure of the air is higher; (3) wetting phase saturation degree decreases and represents the advance of the non-wetting phase front that even after 5500 seconds of air injection did not reach the vertical walls inside the domain; (4) even though the air flow throughout the prediction was fast in comparison with the registered in the laboratory test, the closing results were near to the state measured at the laboratory.

Although the same pressures, permeabilities, and soil water characteristic curves comparable to the informed on the laboratory test were implemented for the prediction, a time delay during the advance of the non-wetting front in the laboratory test compared with air injection prediction developed in this work. This lag in advance of the non-wetting phase front can be described primarily by the uncertainty associated with the soil water characteristic curve and permeabilities that are significantly related to the void ratio. Additional precise data related to the soil water characteristic curve and permeabilities are essential to generate more rigorously predictions. In the future, it is essential to take in to account the importance of the laboratory measures connected to phase flow and deformation associated to the saturated-unsaturated behavior of the soils in the development of the predictive models with the purpose of comprehending the non-linear behavior of the partially saturated soils.

From the information achieved with the predictions, it is perceived that the suggested biphasic flow finite element model presented in this work can represent the general behavior detected throughout the laboratory test of the three-dimensional air-water flow into one homogenous layer soil column. The numerical model is valuable for the analysis of the saturated-unsaturated behavior of soils that are usually found in applied geotechnical problems associated to air injection such as partial induction of the wetting phase saturation degree in liquefiable soil improvement. In the future, it is crucial for the complete justification of the biphasic flow models to execute experimentation on air injection in saturated-unsaturated soils with rigorous estimation of the hydraulic and deformation responses.

On the other hand, some divergences in the input parameters can partially explain the variance in results concerning the numerical model established in the course of this research, and laboratory test results presented by Okamura et al. [126]. However, it is clear that these differences are not the essential discrepancy, and will not consequently take into account the more substantial dissimilarities among the results.

Two main conceptual dissimilarities are involved in the numerical model established in the course of this research, compared with the work of Okamura et al. [126]. The first of the differences is the way that capillary pressure-saturation relationships are implemented to simulate pressure distributions inside the plume. In this work it is assumed that the capillary pressure only depends on wetting phase saturation degree, the capillary term is reformulated as $\boldsymbol{\nabla} p_c\left(Se_{w;p_c}\right) = \frac{\partial p_c}{\partial S_w}\boldsymbol{\nabla} S_w$. Numerical results of air front advance are controlled only by hydraulic factors, and especially by the amount of pore fluid flow crossing the medium by the generated non-wetting phase pressure gradients associated to the diffusion (conduction) through the porous media, and not by the transport of dissolved air by advection and dispersion, each of them produces a mass flow of phase per unit area of the medium and per unit of time, because the last two are not in the formulation implemented in this thesis. The permeability that is an intrinsic soil characteristic turn into the primary material parameter that defines the development of the non-wetting phase front.

The second main dissimilarity among this numerical model and the work of Okamura et al. [126] is that the numerical model developed in this research did not take into account the impacts of non-wetting phase compressibility. Volume alterations associated with the propagation of the non-

wetting phase front across the soil and the resultant pressure changes are significant to the definitive form of air injected plumes. The magnitude of lateral propagation of the non-wetting phase is highly dependent on the pressure in the plume associated with the pore fluid pressure. In the future, a rigorous numerical analysis of the changes of non-wetting phase pressures as the non-wetting phase front plume increases is then essential in defining its definitive shape.

5 CONCLUSIONS AND FUTURE WORK

5.1 CONCLUDING REMARKS

An implementation for the prediction of biphasic flow in soil has been established by means of the criterions (standards) of an isothermal, incompressible and immiscible biphasic flow with matric suction impacts. This formulation includes porous models for relative permeability, matric suction, phase model and particular boundary conditions for porous media. A traditional software tool FLEX-PDE has been used to solve the provided partial differential equations (from the mathematical model to the numerical solution and graphical generation), and it is based on the Finite Element Method. The presented implementation demonstrate an adequate speedup, and it is equipped to aboard a complex and huge engineering topic. The implementation can work as a starting point to advance in other attributes; for example, innovative three-phasic or upgrade two-phase mathematical models. Furthermore, the simply changeable environment of the FLEX-PDE software can be conveniently used for novel numerical techniques or solution procedures.

The magnitude of the extension of a non-wetting phase plume after the injection process is predominantly controlled by the injection pressure of the non-wetting phase, and consequently by the pressure gradients that result as non-wetting phase propagates across the soil. If the injection pressure is too high, then a large effective desaturation radius is obtained, but if the injection pressure is higher than the maximum injection pressure defined in the literature, then fracturing of the soil will occur. On the other hand, if the injection pressure is too low, a narrow plume will be generated given that lateral spread will not have an opportunity to occur relative to the vertical propagation. The operation of the injection method must consequently safeguard that the injection pressure at the injector is as significant as conceivable given soil stability limitations, in order to let, as much the expansion of the non-wetting phase plume as possible.

The magnitude of the pressure gradient generating non-wetting phase flow is of great relevance to the magnitude of desaturation plume. Non-wetting phase pressures at the initial times of process determine, to a great amount, the magnitude of the region of influence of a specified non-wetting phase entry. The lateral propagation of the non-wetting phase happens until the non-wetting phase pressure in the plume at a particular point is higher than the pore entry pressure. Horizontal gradients are lower than vertical gradients after a defined quantity of flow has occurred, at which point horizontal plume flow is considerably reduced, and almost all the non-wetting phase expansion is in the upward trend. When a favorite upward trend of non-wetting phase flow is recognized, expansion in the horizontal trend never matches the flow rate of expansion of the upward trend, since the horizontal and vertical gradients increase at different rates.

Another variable that controls the magnitude of the extension of a non-wetting phase plume after the injection process is the permeability of the soil. In the analyzed cases, the magnitude of expansion of the desaturated zone is directly related to the relationship between the pressure and the permeability. For maximum desaturation plume, the non-wetting phase injected must be consequent to the advancement of the non-wetting phase front across the soil, and consequently by the rate of flow of pore fluid out of the medium.

It can be observed that after parameter α rises, the effective desaturation radius increases for the same time and the same assumed initial capillary pressure and the same material parameter n. The previous results mean that soils with large magnitudes for material parameter α, as soils like sands, are estimated to be a reduced amount of wetting phase saturated than soils with small α values, as soils like silts and clays, at the same capillary pressure and the same non-wetting phase injection time. As a result, for the same injection pressure and permeability at the same time, faster non-

wetting phase infiltrations can be expected for coarse-grained soils, as soils like sands, where parameter α is large. Although it is perceived that variations of the parameter α for fixed permeability values, constant injection pressures, and variable injection times generate relatively significant increases in the advance lengths of the non-wetting phase, it is observed that the magnitudes of the penetration radius do not vary significantly with variations of the parameter α for fixed times.

It is shown that for variations of material parameter n a non-linear reaction in the profiles is perceived. For minor n magnitudes, the predicted results of effective desaturation radius stay practically invariant, at the same injection pressure, and at any time when $(n = 1.3)$, but when n increases $(\mathrm{n} = 1.3 \text{ to } 2.0)$ the predicted results of effective desaturation radius start grow rapidly for the same time and with time increases. For larger n values, however, the response is less different or less reversed since predicted results of effective desaturation radius increase slowly when n increases$(\mathrm{n} = 2.0 \text{ to } 4.0)$. A comparable tendency is perceived in the predicted results of effective desaturation radius profiles when n increases $(\mathrm{n} = 4.0 \text{ to } 8.0)$, in which the predicted results of effective desaturation radius increase slowly but with a tendency to be approximately constant when n increases $(\mathrm{n} = 6.0 \text{ to } 8.0)$. These diverse reactions can be clarified by the primary wetting phase saturation degree $(S_w = 1)$ at the start of the injection process, specifically, $t = 0s$. Additionally, the desaturation proportion is fast for materials with the small n magnitude where the primary saturation disposition along the column is high; as a consequence, the wetting phase pressure inside the pores is high.

It is perceived that once material parameter a rises, the effective non-wetting phase saturation degree radius decreases along the column. Although it is perceived that variations of the parameter a for fixed permeability values, constant injection pressures, and variable injection times generate decreases in the advance lengths of the non-wetting phase, it is perceived that the magnitudes of the penetration radius do not vary significantly with variations of the parameter a for fixed times.

Predictions show that once material parameter b rises, the effective non-wetting phase saturation degree radius slowly increases along the column, when b increases $(\mathrm{b} = 0.33 \text{ to } 0.8)$. Although it is perceived that variations of the parameter b for fixed permeability values, constant injection pressures, and variable injection times generate decreases in the advance lengths of the non-wetting phase when b increases $(\mathrm{b} = 0.8 \text{ to } 1.0)$, it is perceived that the magnitudes of the penetration radius do not vary significantly with variations of the parameter b for fixed times.

The restrictive behavior of a saturated porous soil to the flow of a non-wetting phase injected front is applied by the permeability of the soil, through the intrinsic permeability of the soil and the viscosity of the pore fluid; and by the capillary resistance of the soil applied mostly by the size of its pore spaces. However, the Van Genuchten model requires input parameters that, in a non-intuitive mode, define the microscopic performance of the injected non-wetting phase in the pore spaces of the porous media, rather than its macroscopic performance. These input parameters on which this model is strongly dependent, are problematic to calculate, since it can take different magnitudes broadly within a specified soil type, and it may not be feasible to measure. Consequently, the problems using the existing model limits their effectiveness and their use as a tool for the potential efficiency of non-wetting phase injection as a remediation method for a defined zone.

Numerical predictions by a biphasic flow model implemented in this work show acceptable agreements with the laboratory test measurements developed by Okamura et al. of the non-wetting phase front (changes in the wetting phase saturation degree) advance and non-wetting phase flow rates for the large-container experiments. Although discrepancy on the rates and wetting phase saturation degree values during the non-wetting phase injection process were observed in predictions for the large container, simulation ilustrate the non-wetting phase front for the residual condition after non-wetting phase-injection had concluded. The entire numerical analysis results

indicate that this simplified bi-phasic flow model may be pertinent to analyze desaturation phenomena in situ to be tracked transitory in a particular domain as material flow characteristics are well recognized previously.

5.2 RECOMENDATIONS FOR FUTURE WORK

Additional research on the injection features of saturated and partially saturated soil is necessary, with the purpose of understanding the intricate non-linear correlation between the constitutive parameters. As well as the hydraulic parameters in the injection-infiltration-deformation phenomena in the saturated and partially saturated soil. The themes of experimentation and research that have to be investigated in future works are mentioned next.

There is the possibility of implementing air injection as a method of liquefiable soil improvement. Moreover, considering that air infiltration in saturated soils, desaturation and deformation are processes occur simultaneously (the latter two entirely depending on the first one), the study of the processes of air infiltration into the soil is made necessary by coupled methodologies of infiltration-strain that reflect variations of safety factors over time. Additionally, numerically examination have to be performed to study the plumes expansion of the degree of saturation of the soil improved by air injection since this parameter is critical in liquefaction studies and minor variations thereof will have significant effects on the soil resistance to liquefaction. A full parametric analysis has to be done counting the main hydraulic features that govern the performance of partially saturated soils (characteristic soil-water and permeability functions), injectability of air in the soil, pressures required during injection, injection duration, injection rates, desaturation radio and volumetric strains associated to the phenomena. The material parameters that actively control soil desaturation process by injecting air have to be studied.

While recent studies have provided useful qualitative information on the mechanisms of partial desaturation methods, there is a gap in the presentation of recommendations that could be implemented to improve the effectiveness of a desaturation technique at a location of given features. The correlation between operation features, such as injection flow rate and pressure, and site features, such as soil type and permeability is not well understood, and therefore no procedures exist to improve the operation of a partial desaturation method by air injection. The design and use of air injection methods as a remediation technology are therefore restricted to academic research. It is essential to do some in situ research with experienced operators who follow pilot studies and determine the optimal operative features of each specific scheme. It is clear that propend for providing guidelines to increase system efficiency would significantly improve the usefulness of air injection methods, converting it into a more widely applicable remediation technology.

The properties of the pore fluid have a significant effect on the magnitude of non-wetting phase plumes, mainly since can modify the permeability of the soil and thus change the expansion of the non-wetting phase plume. The permeability of a material is inversely proportional to the viscosity of the pore fluid, and consequently, increasing the viscosity of the pore fluid rises the resistance of the soil to the non-wetting phase flow. The study of the non-wetting phase plumes in different pore fluids has to be done.

It is essential to study the impact of the primary capillary pressure and the specific moisture capacity on the behavior and stability of the saturated and partially saturated material exposed to a non-wetting phase injection procedure. The instability of saturated and partially saturated soil is not a simple theme, and it is necessary for some complementary examination. As a result, it is required to expand the revision to the impacts of the constitutive parameters and the wetting phase and non-wetting phase permeability functions on the instability of the saturated and partially saturated material. Also, the experimental, theoretical and numerical instability of the saturated and partially saturated material in the triaxial state have to be studied.

An important and problematic theme connected to the prediction of the field and experimental studies in desaturation methods is limited the obtainable data related to the constitutive parameters of soils, the wetting phase saturation degree and capillary pressure connection and the relative permeability expressions implemented for partially saturated materials. Scale experimental models and in-situ field methods information let the full calibration, adjustment, and corroboration of mathematical models implemented to examine the performance of partially saturated materials. Consequently, it is essential for the full corroboration of the coupled mathematical models to develop experiments on injection-desaturation in materials with the entire and rigorously estimation of the hydraulic and the strain features.

In this research, predictions of materials exposed to non-wetting phase injection and desaturation process have been executed. But these numerical evaluations are simply just a humble approximation of the geotechnical topics concerning the biphasic flow in partially saturated materials. Consequently, it is essential to execute mathematical examinations including additional circumstances, diverse geometries and boundary conditions, and diverse initial conditions, e.g., road, coastal and river embankments, earth dams, excavations, the foundation of light-weight structures, overloaded soils, and so on. Also, the mixed impact of injection-desaturation in a material and the cyclic behavior is an exciting theme that has to be researched.

It is reasonable to mention that for the in situ behavior of the method the desaturation plumes not always are going to be generated perfectly symmetric concerning the different axis as in the predictions, in relation to the heterogeneities and singularities of the soil profile in situ. For that reason, predictions of desaturation plume are a good primary approach and it has to be complemented with models that include de behavior of biphasic flow in heterogeneous soils. However, if the problem of the homogeneity of the soils is discussed from its geological origin, it will be discovered that there are no homogeneous soils, mainly from hydraulic behavior.

In the injection infiltration mathematical model, a Van Genuchten model was assumed. Typically it is supposed that the wetting phase saturation-capillary pressure connection was identical for the wetting and non-wetting tracks. But the model is at the mercy of the void ratio, the stress conditions, and it tracks diverse routes for the wetting and non-wetting phenomena throughout the desaturation, for example, the material shows hysteretic behavior. So, it is important to contemplate these characteristics of soil water retention model in the examination of desaturation of soil, particularly in the circumstance where the material is exposed to numerous wetting and non-wetting phenomena.

REFERENCES

[1] I. M. Idriss and R. W. Boulanger, *Soil liquefaction during earthquakes*. Earthquake engineering research institute, 2008.

[2] M. Jefferies and K. Been, *Soil Liquefaction*. Abingdon, UK: Taylor & Francis, 2006.

[3] D. Ural, "Liquefaction Analysis: A Probabilistic Approach," 1996.

[4] R. B. Seed *et al.*, "Recent Advances in Soil Liquefaction Engineering : a Unified and Consistent Framework," in *Report no.EERC 2003-06, Earthquake Engineering Research Center*, 2003, pp. 1–72.

[5] T. Khodadadi and H. Bilsel, "Application of microorganisms for improvement of liquefiable sand," in *3rd international conference on new development in soil mechanics and geotechnical engineering. Near East University, Nicosia, North Cyprus*, 2012, pp. 857–863.

[6] P. M. Gallagher, A. Pamuk, and T. Abdoun, "Stabilization of liquefiable soils using colloidal silica grout," *J. Mater. Civ. Eng.*, vol. 19, no. 1, pp. 33–40, 2007.

[7] J. T. DeJong, B. M. Mortensen, B. C. Martinez, and D. C. Nelson, "Bio-mediated soil improvement," *Ecol. Eng.*, vol. 36, no. 2, pp. 197–210, 2010.

[8] M. K. Yegian, E. Eseller-Bayat, A. Alshawabkeh, and S. Ali, "Induced-partial saturation for liquefaction mitigation: experimental investigation," *J. Geotech. Geoenvironmental Eng.*, vol. 133, no. 4, pp. 372–380, 2007.

[9] M. Ishihara, M. Okamura, and T. Oshita, "Desaturating sand deposit by air injection for reducing liquefaction potential," in *Proc. 2003 Pacific Conference on Earthquake Engineering*, 2003.

[10] M. Okamura, M. Ishihara, and K. Tamura, "Liquefaction resistances and degree of saturation of sand improved with sand compaction piles," in *13 th World Conference on Earthquake Engineering. Paper*, 2004, no. 3484.

[11] Y. Okamura, Mitsu y Soga, "Effects of pore fluid compressibility on liquefaction resistance of partially saturated sand," *Soils Found.*, vol. 46, pp. 695–700, 2006.

[12] J. C. Santamarina, K. A. Klein, and M. A. Fam, *Soils and waves*. J. Wiley & Sons, 2001.

[13] E. Eseller-bayat, M. K. Yegian, and A. Alshawabkeh, "Liquefaction Response of Partially Saturated Sands. I : Experimental Results," *J. Geotech. Geoenvironmental Eng.*, vol. 139, no. 6, pp. 863–871, 2013.

[14] J. HE, J. CHU, and V. IVANOV, "Mitigation of liquefaction of saturated sand using biogas," *Géotechnique*, vol. 63, no. 4, pp. 267–275, Mar. 2013.

[15] J. He, J. Chu, H.-L. Liu, and Y.-F. Gao, "Microbial soil desaturation for the mitigation of earthquake liquefaction," *Japanese Geotech. Soc. Spec. Publ.*, vol. 2, no. 21, pp. 784–787, 2016.

[16] A. Zeybek and S. P. G. Madabhushi, "Centrifuge testing to evaluate the liquefaction response of air-injected partially saturated soils beneath shallow foundations," *Bull. Earthq. Eng.*, vol. 15, no. 1, pp. 339–356, 2017.

[17] N. P. Marasini and M. Okamura, "Air injection to mitigate liquefaction under light structures," *Int. J. Phys. Model. Geotech.*, vol. 15, no. 3, pp. 129–140, Sep. 2015.

[18] D. G. Fredlund and H. Rahardjo, *Soil mechanics for unsaturated soils*. John Wiley & Sons, 1993.

[19] S. Gokyer, "Numerical Simulation of Partial Saturation in Sands Induced by Flow and Chemical Reactivity," Northeastern University, 2015.

[20] N. Lu and W. J. Likos, *Unsaturated Soil Mechanics*. Wiley, 2004.

[21] S. Pietruszczak and G. N. Pande, "Constitutive relations for partially saturated soils containing gas inclusions," *J. Geotech. Eng.*, vol. 122, no. 1, pp. 50–59, 1996.

[22] J. L. H. Grozic, S. M. R. Imam, P. K. Robertson, and N. R. Morgenstern, "Constitutive modeling of gassy sand behaviour," *Can. Geotech. J.*, vol. 42, no. 3, pp. 812–829, 2005.

[23] J. L. H. Grozic, F. Nadim, and T. J. Kvalstad, "On the undrained shear strength of gassy clays," *Comput. Geotech.*, vol. 32, no. 7, pp. 483–490, 2005.

[24] J. L. Grozic, P. K. Robertson, and N. R. Morgenstern, "The behavior of loose gassy sand," *Can. Geotech. J.*, vol. 36, no. 3, pp. 482–492, 1999.

[25] J. L. H. Grozic, P. K. Robertson, and N. R. Morgenstern, "Cyclic liquefaction of loose gassy sand," *Can. Geotech. J.*, vol. 37, no. 4, pp. 843–856, 2000.

[26] S. J. Wheeler, "A conceptual model for soils containing large gas bubbles," *Geotechnique*, vol. 38, no. 3, pp. 389–397, 1988.

[27] D. Fredlund, "Prediction of unsaturated soil functions using the soil-water characteristic curve," *Geotech. Eng.*, vol. 13, p. 16, 1995.

[28] A. W. Bishop and G. Eldin, "Undrained triaxial tests on saturated sands and their significance in the general theory of shear strength," *Geotechnique*, vol. 2, no. 1, pp. 13–32, 1950.

[29] S. L. Kramer, *Geotechnical earthquake engineering*. Pearson Education India, 1996.

[30] I. Towhata, *Geotechnical earthquake engineering*. Springer Science & Business Media, 2008.

[31] Y. Yoshimi and K. Tokimatsu, "Settlement of buildings on saturated sand during earthquakes," *Soils Found.*, vol. 17, no. 1, pp. 23–38, 1977.

[32] Y. OHSAKI, "Effects of sand compaction on liquefaction during the Tokachioki earthquake," *Soils Found.*, vol. 10, no. 2, pp. 112–128, 1970.

[33] B. R. Cox *et al.*, "Liquefaction at strong motion stations and in Urayasu City during the 2011 Tohoku-Oki earthquake," *Earthq. Spectra*, vol. 29, no. s1, pp. S55–S80, 2013.

[34] E. (Earthquake E. R. Institute), "Preliminary Observations on the Tokachi-Oki, Japan, Earthquake of September 26, 2003. EERI Special Earthquake Report," 2003.

[35] E. (Earthquake E. R. Institute), "Loma Prieta Earthquake October 17, 1989. EERI Preliminary Reconnaissance Report," 1989.

[36] E. (Earthquake E. F. I. Team), "The Loma Prieta Earthquake of 17 October 1989. A Field Report by EEFIT," London, 1993.

[37] et al. Seed, R.B., Dickenson, M.F., Riemer, M.F., Bray, J.D., Sitar, N., Mitchell, J.K., Idriss, I.M., "Preliminary Report on the Principal Geotechnical Aspects of the October 17, 1989 Loma Prieta Earthquake. Report No. UCB/EERC-90/05 Earthquake," 1990.

[38] T. L. Holzer, M. J. Bennett, D. J. Ponti, and J. C. Tinsley III, "Liquefaction and soil failure during 1994 Northridge earthquake," *J. Geotech. Geoenvironmental Eng.*, vol. 125, no. 6, pp. 438–

452, 1999.

[39] M. Yasui, “Settlement and inclination of reinforced concrete buildings in Dagupan City due to liquefaction during the 1990 Philippine earthquake,” 1992.

[40] A. A. Acacio, Y. Kobayashi, I. Towhata, R. T. Bautista, and K. Ishihara, “Subsidence of building foundation resting upon liquefied subsoil: case studies and assessment,” *Soils Found.*, vol. 41, no. 6, pp. 111–128, 2001.

[41] K. Tokimatsu, H. Kojima, S. Kuwayama, A. Abe, and S. Midorikawa, “Liquefaction-induced damage to buildings in 1990 Luzon earthquake,” *J. Geotech. Eng.*, vol. 120, no. 2, pp. 290–307, 1994.

[42] E. (Earthquake E. F. I. Team), “The Hyogo-Ken Nanbu (Kobe) Earthquake of 17 January 1995. A Field Report by EEFIT.,” London, 1997.

[43] E. A. Hausler, *Influence of ground improvement on settlement and liquefaction: A study based on field case history evidence and dynamic geotechnical centrifuge tests*. 2002.

[44] R. Sancio, J. D. Bray, T. Durgunoglu, and A. Onalp, “Performance of buildings over liquefiable ground in Adapazari, Turkey,” in *Proc., 13th World Conf. on Earthquake Engineering*, 2004.

[45] J. D. Bray *et al.*, “Damage patterns and foundation performance in Adapazari,” *Earthq. Spectra*, vol. 16, no. S1, pp. 163–189, 2000.

[46] J. F. Bird and J. J. Bommer, “Earthquake losses due to ground failure,” *Eng. Geol.*, vol. 75, no. 2, pp. 147–179, 2004.

[47] E. (Earthquake E. R. Institute), “The Izmit (Kocaeli), Turkey Earthquake of August 17, 1999. EERI Special Earthquake Report.,” 1999.

[48] E. (Earthquake E. F. I. Team), “The Kocaeli, Turkey Earthquake of 17 August 1999. A Field Report by EEFIT,” London, 2003.

[49] E. (Earthquake E. R. Institute), “The Chi-Chi, Taiwan Earthquake of Sepetember 21, 1999. EERI Special Earthquake Report,” 1999.

[50] D.-H. Lee, C. H. Juang, and C.-S. Ku, “Liquefaction performance of soils at the site of a partially completed ground improvement project during the 1999 Chi-Chi earthquake in Taiwan,” *Can. Geotech. J.*, vol. 38, no. 6, pp. 1241–1253, 2001.

[51] R. DesRoches, M. Comerio, M. Eberhard, W. Mooney, and G. J. Rix, “Overview of the 2010 Haiti earthquake,” *Earthq. Spectra*, vol. 27, no. S1, pp. S1–S21, 2011.

[52] and U. (U. S. G. S. EERI (Earthquake Engineering Research Institute), “The Mw 7.0 Haiti Earthquake of January 12, 2010. USGS/EERI Advance Reconnaissance Team Report V1.1.,” 2010.

[53] M. Cubrinovski *et al.*, “Geotechnical reconnaissance of the 2010 Darfield (New Zealand) earthquake,” 2010.

[54] E. (Earthquake E. R. Institute), “Learning from Earthquakes, The Mw 7.1 Darfield (Canterbury), New Zealand Earthquake of September 4, 2010. EERI Special Earthquake Report,” 2010.

[55] M. Cubrinovski and I. McCahon, “Short term recovery project 7: CBD foundation damage,” *Nat. Hazards Res. Platform, Univ. Canterbury, Christchurch, New Zeal.*, 2012.

[56] K. Tokimatsu, H. Suzuki, K. Katsumata, and S. Tamura, “Geotechnical Problems in the 2011

Tohoku Pacific Earthquakes," 2013.

[57] A. Rollins, K., Franke, K., Luna, R., Rocco, N., Avila, D., and Climent, *Geotechnical Aspects of Sept. 5, 2012 M7.6 Samara, Costa Rica Earthquake.*, vol. Version 1. 2013, p. 1–57.

[58] and A. (Applied T. C. GEER (Geotechnical Extreme Events Reconnaissance), EERI (Earthquake Engineering Research Institute), "Geotechnical Observations. GEER/EERI/ATC Cephalonia, Greece 2014. Report Version 1.," 2014.

[59] F. Lanning *et al.*, "EERI Earthquake Reconnaissance Team Report: M7. 8 Muisne, Ecuador Earthquake on April 16, 2016," 2016.

[60] S. Nikolaou, X. Vera-Grunauer, and R. Gilsanz, "GEER-ATC Earthquake Reconnaissance: April 16 2016," *Muisne, Ecuador, Geotech. Extrem. Events Reconnaiss. Assoc. Rep. GEER-049, Version 1b. doi*, vol. 10, p. G6F30N, 2016.

[61] R. E. Kayen *et al.*, "Geotechnical aspects of the 2016 MW 6.2, MW 6.0, and MW 7.0 Kumamoto earthquakes," Geotechnical Extreme Events Reconnaissance Association, 2017.

[62] D. Stewart and R. Knox, "What is the Maximum Depth Liquefaction Can Occur?," 1995.

[63] S. Prakash, *Soil dynamics*. McGraw-Hill, 1981.

[64] H. B. Seed, "Landslides during earthquakes due to soil liquefaction," *J. Geotech. Engrg. Div.*, vol. 94, no. 5, pp. 1055–1122, 1968.

[65] H. B. Seed and I. M. Idriss, "Simplified procedure for evaluating soil liquefaction potential," *J. Soil Mech. Found. Div*, 1971.

[66] R. Dobry, R. S. Ladd, F. Y. Yokel, R. M. Chung, and D. Powell, *Prediction of pore water pressure buildup and liquefaction of sands during earthquakes by the cyclic strain method*, vol. 138. National Bureau of Standards Gaithersburg, MD, 1982.

[67] P. L. Florin, V.A, and Ivanov, "Liquefaction of Saturated Sandy Soils.," in *Proc of 5th Int. Conf. Soil Mech. and Found.*, 1961.

[68] K. Ishihara, "Stability of natural deposits during earthquakes," *Proc. 11th ICSMFE, 1985*, vol. 1, pp. 321–376, 1985.

[69] D. Stewart and R. Knox, "The earthquake America forgot," *Gutenberg-Richter Publ. Marble Hill, MO*, 1995.

[70] H. B. Seed, "Evaluation of soil liquefaction potential during earthquakes," *Rep. EERC*, 1975.

[71] E. V Watts, "Some aspects of high pressures in the D-7 zone of the Ventura Avenue field," *Trans. AIME*, vol. 174, no. 01, pp. 191–205, 1948.

[72] P. A. Domenico and F. W. Schwartz, *Physical and chemical hydrogeology*, no. v. 1. Wiley, 1998.

[73] V. . . et al. Bogomolov, "Principles of Paleohydrological Reconstruction of Groundwater Formation," in *24th Int. Geol. Cong .. Proc. Sec. II,* 1978, p. 205–226.

[74] I. G. Kissen, "The principal distinctive features of the hydrodynamic regime of intensive earth crust downwarping areas," *Hydrogeol. Gt. Sediment. Basins, Publ. Int. Assoc. Hydrol. Sci.*, pp. 178–185, 1978.

[75] A. Haldar and W. H. Tang, "Probabilistic evaluation of liquefaction potential," in *ASCE J Geotech Eng Div*, 1979, pp. 145–163.

[76] C. H. Juang, H. Yuan, D.-H. Lee, and C.-S. Ku, “Assessing CPT-based methods for liquefaction evaluation with emphasis on the cases from the Chi-Chi, Taiwan, earthquake,” *Soil Dyn. Earthq. Eng.*, vol. 22, no. 3, pp. 241–258, 2002.

[77] A. T. C. Goh, “Probabilistic neural network for evaluating seismic liquefaction potential,” *Can. Geotech. J.*, vol. 39, no. 1, pp. 219–232, 2002.

[78] A. T. C. Goh, “Neural-network modeling of CPT seismic liquefaction data,” *J. Geotech. Eng.*, vol. 122, no. 1, pp. 70–73, 1996.

[79] A. T. C. Goh, “Seismic liquefaction potential assessed by neural networks,” *J. Geotech. Eng.*, vol. 120, no. 9, pp. 1467–1480, 1994.

[80] C. H. Juang, H. Yuan, D.-H. Lee, and P.-S. Lin, “Simplified cone penetration test-based method for evaluating liquefaction resistance of soils,” *J. Geotech. geoenvironmental Eng.*, vol. 129, no. 1, pp. 66–80, 2003.

[81] G. P. Ganapathy and A. S. Rajawat, “Evaluation of liquefaction potential hazard of Chennai city, India: using geological and geomorphological characteristics,” *Nat. hazards*, vol. 64, no. 2, pp. 1717–1729, 2012.

[82] B. T. Nhung, N. H. Phuong, and N. T. Nam, “Assessment of earthquake-induced ground liquefaction susceptibility for Hanoi city using geological and geomorphologic characteristics,” *VIETNAM J. EARTH Sci.*, vol. 39, no. 2, pp. 139–154, 2017.

[83] K. Kotoda, K. Wakamatsu, and O. Masahiko, “Mapping liquefaction potential based on geomorphological land classification,” in *Proceedings of Ninth World Conference on Earthquake Engineering*, 1988, pp. 195–200.

[84] M. Rico, G. Benito, A. R. Salgueiro, A. Díez-Herrero, and H. G. Pereira, “Reported tailings dam failures: a review of the European incidents in the worldwide context,” *J. Hazard. Mater.*, vol. 152, no. 2, pp. 846–852, 2008.

[85] S. Azam and Q. Li, “Tailings dam failures: a review of the last one hundred years,” *Geotech. news*, vol. 28, no. 4, pp. 50–54, 2010.

[86] M. Davies and T. Martin, “Static liquefaction of tailings–fundamentals and case histories,” 2002.

[87] G. R. Martin, H. B. Seed, and W. D. Finn, “Effects of system compliance on liquefaction tests,” *J. Geotech. Eng. Div.*, vol. 104, no. 4, pp. 463–479, 1978.

[88] K. Rocker, “The liquefaction behavior of sands subjected to cyclic loading.,” Massachusetts Institute of Technology, 1968.

[89] R. C. Chaney, “Saturation effects on the cyclic strength of sands,” in *From Volume I of Earthquake Engineering and Soil Dynamics--Proceedings of the ASCE Geotechnical Engineering Division Specialty Conference, June 19-21, 1978, Pasadena, California. Sponsored by Geotechnical Engineering Division of ASCE in cooperation with:*, 1978, no. Proceeding.

[90] M. A. Sherif, C. Tsuchiya, and I. Ishibashi, “Saturation effects on initial soil liquefaction,” *J. Geotech. Eng. Div.*, vol. 103, no. 8, pp. 914–917, 1977.

[91] H. Xia and T. Hu, “Effects of saturation and back pressure on sand liquefaction,” *J. Geotech. Eng.*, vol. 117, no. 9, pp. 1347–1362, 1991.

[92] Y. Yoshimi, K. Tanaka, and K. Tokimatsu, “Liquefaction resistance of a partially saturated sand.,” *Soils Found.*, vol. 29, no. 3, pp. 157–162, 1989.

[93] K. Ishihara, H. Tsuchiya, Y. Huang, and K. Kamada, “Recent studies on liquefaction resistance of sand effect of saturation,” in *Proc. 4th Conf. Recent Advances in Geotech. Earth. Engg., Keynote Lecture*, 2001.

[94] Y. TSUKAMOTO, K. ISHIHARA, H. NAKAZAWA, K. KAMADA, and Y. HUANG, “Resistance of Partly Saturated Sand to Liquefaction with Reference to Longitudinal and Shear Wave Velocities.,” *SOILS Found.*, vol. 42, no. 6, pp. 93–104, 2002.

[95] S. Pietruszczak, G. N. Pande, and M. Oulapour, “A hypothesis for mitigation of risk of liquefaction,” *Geotechnique*, vol. 53, no. 9, pp. 833–838, 2003.

[96] J. Yang, S. Savidis, T. Sato, and X. S. Li, “Influence of vertical acceleration on soil liquefaction: new findings and implications,” *Proceeding soil rock Am.*, vol. 1, 2003.

[97] H. Nakazawa, K. Ishihara, Y. Tsukamoto, and T. Kamata, “Case studies on evaluation of liquefaction resistance of imperfectly saturated soil deposits,” in *Proceedings of International Conference on Cyclic Behaviour of Soils and Liquefaction Phenomena, Bochum, Germany*, 2004, vol. 31, pp. 295–304.

[98] J. Yang, S. Savidis, and M. Roemer, “Evaluating liquefaction strength of partially saturated sand,” *J. Geotech. Geoenvironmental Eng.*, vol. 130, no. 9, pp. 975–979, 2004.

[99] J. Yang, S. Savidis, and M. Roemer, “Evaluating liquefaction strength of partially saturated sand,” *J. Geotech. Eng. Div.*, vol. 130, no. 9, pp. 975–979, 2004.

[100] K. Ishihara, Y. Tsukamoto, and K. Kamada, “Undrained behavior of near-saturated sand in cyclic and monotonic loading,” in *Proc. Conf., Cyclic Behavior of Soils and Liquefaction Phenomena*, 2004, pp. 27–39.

[101] K. Ishihara and Y. Tsukamoto, “Cyclic strength of imperfectly saturated sands and analysis of liquefaction,” *Proc. Japan Acad. Ser. B*, vol. 80, no. 8, pp. 372–391, 2004.

[102] M. Okamura and Y. Soga, “Effects of pore fluid compressibility on liquefaction resistance of partially saturated sand,” *Soils Found.*, vol. 46, no. 5, pp. 695–700, 2006.

[103] M. Kazama, H. Takamura, T. Unno, N. Sento, and R. Uzuoka, “Liquefaction mechanism of unsaturated volcanic sandy soils,” *J. Geotech. Eng. Japan Soc. Civ. Eng.*, vol. 62, no. 2, pp. 546–561, 2006.

[104] R. Bouferra, N. Benseddiq, and I. Shahrour, “Saturation and preloading effects on the cyclic behavior of sand,” *Int. J. Geomech.*, vol. 7, no. 5, pp. 396–401, 2007.

[105] A. Jafari-Mehrabadi, M. Abedinzadegan Abdi, and R. Popescu, “Analysis of liquefaction susceptibility of nearly saturated sands,” *Int. J. Numer. Anal. methods Geomech.*, vol. 31, no. 5, pp. 691–714, 2007.

[106] G. N. Pande and S. Pietruszczak, “Assessment of risk of liquefaction in granular materials and its mitigation,” in *Proc. 12th Int. Conf. Int. Assoc. Comput. Methods Adv. Geomech.(IACMAG), Goa, India*, 2008, pp. 2619–2627.

[107] T. Unno, M. Kazama, R. Uzuoka, and N. Sento, “Liquefaction of unsaturated sand considering the pore air pressure and volume compressibility of the soil particle skeleton,” *Soils Found.*, vol. 48, no. 1, pp. 87–99, 2008.

[108] A. Amaratunga and J. L. H. Grozic, “On the undrained unloading behaviour of gassy sands,” *Can. Geotech. J.*, vol. 46, no. 11, pp. 1267–1276, 2009.

[109] N. Delia, “Laboratory testing of the Monotonic behavior of partially saturated sandy soil,”

Earth Sci. Res. J., vol. 14, no. 2, pp. 181–186, 2010.

[110] A. Arab, I. Shahrour, and L. Lancelot, "A laboratory study of liquefaction of partially saturated sand," *J. Iber. Geol.*, vol. 37, no. 1, pp. 29–36, 2011.

[111] M. E. Raghunandan and A. Juneja, "A study on the liquefaction resistance and dynamic properties of De-saturated sand," *EJGE*, vol. 16, pp. 109–122, 2011.

[112] R. P. Orense, N. Yoshimoto, and M. Hyodo, "Cyclic shear behavior and seismic response of partially saturated slopes," *Soil Dyn. Earthq. Eng.*, vol. 42, pp. 71–79, 2012.

[113] K. Ishihara, "Liquefaction and flow failure during earthquakes," *Geotechnique*, vol. 43, no. 3, pp. 351–451, 1993.

[114] Y. Tsukamoto, S. Kawabe, J. Matsumoto, and S. Hagiwara, "Cyclic resistance of two unsaturated silty sands against soil liquefaction," *Soils Found.*, vol. 54, no. 6, pp. 1094–1103, 2014.

[115] N. S. Rad, A. J. D. Vianna, and T. Berre, "Gas in soils. II: Effect of gas on undrained static and cyclic strength of sand," *J. Geotech. Eng.*, vol. 120, no. 4, pp. 716–736, 1994.

[116] K. Ishihara, Y. Huang, and H. Tsuchiya, "Liquefaction resistance of nearly saturated sand as correlated with longitudinal wave velocity," *Poromechanics A Tribut. to Maurice A. Biot, Balkema*, pp. 583–586, 1998.

[117] S. Yasuda, T. Kobayashi, Y. Fukushima, M. Kohari, and T. Simazaki, "Effect of degree of saturation on the liquefaction strength of Masa," in *Proc. 34th Jpn. Nat. Conf. Geotech. Engrg*, 1999, pp. 2071–2072.

[118] Y. Huang, H. Tsuchiya, and K. Ishihara, "Estimation of partial saturation effect on liquefaction resistance of sand using P-wave velocity," in *Proc. JGS Symposium*, 1999, vol. 113, pp. 431–434.

[119] T. KOKUSHO, "Correlation of pore-pressure B-value with P-wave velocity and Poisson's ratio for imperfectly saturated sand or gravel," *Soils Found.*, vol. 40, no. 4, pp. 95–102, 2000.

[120] J. Yang and T. Sato, "Analytical study of saturation effects on seismic vertical amplification of a soil layer," *Geotechnique*, vol. 51, no. 2, pp. 161–165, 2001.

[121] N. P. Marasini, "Investigation of Soil Liquefaction in Kathmandu Valley and Remediation on Existing Structures Using Desaturation By Air-injection Technique," Ehime University, 2016.

[122] M. Okamura *et al.*, "In-Situ Desaturation Test by Air Injection and Its Evaluation through Field Monitoring and Multiphase Flow Simulation," *J. Geotech. Geoenvironmental Eng.*, vol. 137, no. 7, pp. 643–652, Jul. 2011.

[123] M. Okamura, M. Ishihara, and K. Tamura, "Degree of saturation and liquefaction resistances of sand improved with sand compaction pile," *J. Geotech. geoenvironmental Eng.*, vol. 132, no. 2, pp. 258–264, 2006.

[124] M. Okamura, M. Ishihara, and K. Tamura, "Liquefaction Resistances and Degree of Saturation of Sand Improved with Sand Compaction Piles," *Soils Found.*, vol. 43, no. 5, pp. 175–187, 2003.

[125] M. Okamura and T. Teraoka, "Shaking Table Tests to Investigate Soil Desaturation as a Liquefaction Countermeasure," in *Seismic Performance and Simulation of Pile Foundations in Liquefied and Laterally Spreading Ground*, 2005, pp. 282–293.

[126] H. Yasuhara, M. Okamura, and Y. Kochi, “Experiments and predictions of soil desaturation by air-injection technique and the implications mediated by multiphase flow simulation,” *Soils Found.*, vol. 48, no. 6, pp. 791–804, 2008.

[127] M. Okamura and T. Teraoka, “Shaking table tests to investigate soil desaturation as a liquefaction countermeasure,” *Seism. Perform. Simul. Pile Found. Liq. Laterally Spreading Gr.*, pp. 282–293, 2006.

[128] Y. Tomida and M. Okamura, “Verification of Desaturation Technique as a Liquefaction Countermeasure for Existing Embankments,” *Int. J. Landslide Enviroment*, vol. 1, no. 1, pp. 111–112, 2013.

[129] K. T. y K. T. Yoshiaki Yoshimi, “Liquefaction resistance of a partially saturated sand,” vol. 29, pp. 157–162, 1989.

[130] K. Okamura, M y Tamura, “Prediction method for liquefaction-induced settlement of embankment with remedial measure by deep mixing method,” *Soils Found.*, vol. 44, no. 4, pp. 53–65, 2004.

[131] M. Okamura *et al.*, “In-situ test on desaturation by air injection and its monitoring,” *Japanese.) J. Jpn. Soc. Civ. Eng. C*, vol. 65, pp. 756–766, 2009.

[132] A. Zeybek and G. S. P. Madabhushi, “Durability of partial saturation to counteract liquefaction,” *Proc. Inst. Civ. Eng. Improv.*, vol. 170, no. 2, pp. 102–111, 2017.

[133] K. R. Reddy and J. A. Adams, “Effects of soil heterogeneity on airflow patterns and hydrocarbon removal during in situ air sparging,” *J. Geotech. Geoenvironmental Eng.*, vol. 127, no. 3, pp. 234–247, 2001.

[134] I. Kohno and M. Nishigaki, “Some aspects of laboratory permeability test,” *Soils Found.*, vol. 22, no. 4, pp. 181–190, 1982.

[135] W. M. Camp, H. C. Camp, and R. D. Andrus, “Liquefaction Mitigation Using Air Injection,” in *International Conferences on Recent Advances in Geotechnical Earthquake Engineering and Soil Dynamics*, 2010.

[136] C. Marulanda, P. J. Culligan, and J. T. Germaine, “Centrifuge modeling of air sparging — a study of air flow through saturated porous media,” *J. Hazard. Mater.*, vol. 72, no. 2–3, pp. 179–215, Feb. 2000.

[137] J. Takemura, R. Igarashi, J. Izawa, M. Okamura, and M. Masuda, “Centrifuge model tests on soil desaturation as a liquefaction countermeasure,” in *Proceedings of the 17th International Conference on Soil Mechanics and Geotechnical Engineering: The Academia and Practice of Geotechnical Engineering*, 2009, vol. 1, pp. 502–505.

[138] A. Zeybek and S. P. G. Madabhushi, “Influence of air injection on the liquefaction-induced deformation mechanisms beneath shallow foundations,” *Soil Dyn. Earthq. Eng.*, vol. 97, pp. 266–276, 2017.

[139] H. Yasuhara, M. Okamura, and Y. Kochi, “Experiments and Predictions of Soil Desaturation By Air-Injection Technique and the Implications Mediated By Multiphase Flow Simulation,” *Soils Found.*, vol. 48, no. 6, pp. 791–804, 2008.

[140] N. P. Marasini and M. Okamura, “Numerical simulation of centrifuge tests to evaluate the performance of desaturation by air injection on liquefiable foundation soil of light structures,” *Soils Found.*, vol. 55, no. 6, pp. 1388–1399, Dec. 2015.

[141] K. Mitsuji, “Numerical simulations for development of liquefaction countermeasures by use of partially saturated sand,” in *Proceedings of the 14th World Conference on Earthquake Engineering October*, 2008, pp. 12–17.

[142] Q. Gao, Z. Liu, and X. (Bill) Yu, “Computer Simulations on the Effects of Desaturation on Soil Liquefaction Resistance,” in *IACGE 2013*, 2013, pp. 786–795.

[143] M. A. Biot, “Mechanics of deformation and acoustic propagation in porous media,” *J. Appl. Phys.*, vol. 33, no. 4, pp. 1482–1498, 1962.

[144] M. A. Biot, “General theory of three-dimensional consolidation,” *J. Appl. Phys.*, vol. 12, no. 2, pp. 155–164, 1941.

[145] A. Yashima, F. Oka, Y. Taguchi, and A. Tateishi, “Three dimensional liquefaction analysis considering the compressibility of fluid phase,” in *Proceedings 40th JGS Symposium*, 1995, pp. 257–264.

[146] F. Oka, A. Yashima, T. Shibata, M. Kato, and R. Uzuoka, “FEM-FDM coupled liquefaction analysis of a porous soil using an elasto-plastic model,” *Appl. Sci. Res.*, vol. 52, no. 3, pp. 209–245, 1994.

[147] F. Oka, A. Yashima, A. Tateishi, Y. Taguchi, and A. Yamashita, “A cyclic elasto-plastic constitutive model for sand considering a plastic-strain dependence of the shear modulus,” *Geotechnique*, vol. 49, no. 5, pp. 661–680, 1999.

[148] Y.-J. Tsai, “Air flow paths and porosity/permeability change in a saturated zone during in situ air sparging,” *J. Hazard. Mater.*, vol. 142, no. 1, pp. 315–323, 2007.

[149] J. E. McCray, “Mathematical modeling of air sparging for subsurface remediation: state of the art,” *J. Hazard. Mater.*, vol. 72, no. 2, pp. 237–263, 2000.

[150] P. D. Lundegard and G. Andersen, “Multiphase numerical simulation of air sparging performance,” *Ground Water*, vol. 34, no. 3, pp. 451–460, 1996.

[151] J. E. McCray and R. W. Falta, “Numerical simulation of air sparging for remediation of NAPL contamination,” *Ground Water*, vol. 35, no. 1, pp. 99–110, 1997.

[152] D. J. Wilson, C. Gómez-Lahoz, and J. M. Rodríguez-Maroto, “Groundwater cleanup by in-situ sparging. VIII. Effect of air channeling on dissolved volatile organic compounds removal efficiency,” *Sep. Sci. Technol.*, vol. 29, no. 18, pp. 2387–2418, 1994.

[153] D. J. Wilson, J. M. Rodríguez-Maroto, and C. Gómez-Lahoz, “Groundwater Cleanup by In-Situ Sparging. VI. A Solution/Distributed Diffusion Model for Nonaqueous Phase Liquid Removal,” *Sep. Sci. Technol.*, vol. 29, no. 11, pp. 1401–1432, 1994.

[154] D. J. Wilson and R. D. Norris, “Sparging and biosparging: Insights through mathematical modeling,” in *Proceedings of the Fourth International Symposium on In Situ and On-Site Bioremediation*, 1997, vol. 1, pp. 147–152.

[155] A. J. Rabideau and J. M. Blayden, “Analytical model for contaminant mass removal by air sparging,” *Groundw. Monit. Remediat.*, vol. 18, no. 4, pp. 120–130, 1998.

[156] E. L. Wipfler, M. I. J. Van Dijke, and S. Van der Zee, “Three-phase flow analysis of dense nonaqueous phase liquid infiltration in horizontally layered porous media,” *Water Resour. Res.*, vol. 40, no. 10, 2004.

[157] M. I. J. Dijke and S. Zee, “Correction to ‘Modeling of air sparging in a layered soil: Numerical and analytical approximations,’” *Water Resour. Res.*, vol. 34, no. 8, p. 2073, 1998.

[158] M. C. Marley, F. Li, and S. Magee, “The application of a 3-D model in the design of air sparging systems,” in *Proc. Petroleum Hydrocarbons Organ. Chem. Groundwater: Prevention, Detection, Restoration*, 1992.

[159] K. L. Sellers and R. P. Schreiber, “Air sparging model for predicting groundwater clean up rate,” *Proc. Conf. Pet. Hydrocarb. Org. Chem. Gr. Water Prev. Detect. Restoration, East. Reg. Gr. Water Issues*, pp. 365–376, 1992.

[160] D. J. Wilson, “Groundwater Cleanup by in-situ Sparging. II. Modeling of Dissolved Volatile Organic Compound Removal,” *Sep. Sci. Technol.*, vol. 27, no. 13, pp. 1675–1690, 1992.

[161] S. D. Burchfield and D. J. Wilson, “Groundwater Cleanup by in-situ Sparging. IV. Removal of Dense Nonaqueous Phase Liquid by Sparging Pipes,” *Sep. Sci. Technol.*, vol. 28, no. 17–18, pp. 2529–2551, 1993.

[162] L. A. Roberts and D. J. Wilson, “Groundwater cleanup by in-situ sparging. III. Modeling of dense nonaqueous phase liquid droplet removal,” *Sep. Sci. Technol.*, vol. 28, no. 5, pp. 1127–1143, 1993.

[163] C. Gomez-Lahoz, J. M. Rodriguez-Maroto, and D. J. WILSON∗, “Groundwater cleanup by in-situ sparging. VII. Volatile organic compounds concentration rebound caused by diffusion after shutdown,” *Sep. Sci. Technol.*, vol. 29, no. 12, pp. 1509–1528, 1994.

[164] K. R. REDDY, S. KOSGI, and J. Zhou, “A review of in-situ air sparging for the remediation of VOC-contaminated saturated soils and groundwater,” *Hazard. Waste Hazard. Mater.*, vol. 12, no. 2, pp. 97–118, 1995.

[165] K. R. Reddy and J. Zhou, “Finite element modeling of in situ air sparging for ground water remediation,” in *Proceedings of the 2nd International Congress on Environmental Geotechnics*, 1996, pp. 299–304.

[166] A. Zeybek and G. S. P. Madabhushi, “Physical modelling of air injection to remediate liquefaction,” *Int. J. Phys. Model. Geotech.*, pp. 1–13, 2017.

[167] K. Pruess, “TOUGH2: A general-purpose numerical simulator for multiphase nonisothermal flows,” Berkeley, CA, Jun. 1991.

[168] Y. Tomida, “A Study on Soil Desaturation as a LiquefactionCounter- measure for Highway Embankmens,” Ehime University, Japan, 2014.

[169] K. R. Reddy and J. A. Adams, “Cleanup of Chemical Spills Using Air Sparging,” in *Chapter*, vol. 14, 2001, p. 14.1-14.29.

[170] P. D. Lundegard and D. LaBrecque, “Air sparging in a sandy aquifer (Florence, Oregon, U.S.A.): Actual and apparent radius of influence,” *J. Contam. Hydrol.*, vol. 19, no. 1, pp. 1–27, 1995.

[171] H. Ogata and M. Okamura, “Experimental study on air behaviour in saturated soil under air injection,” in *Proc. Symp. On Natural Disaster Prevention, JSCE, Tokushima, Japan*, 2006, pp. 89–90.

[172] M. Okamura and K. Noguchi, “Liquefaction resistances of unsaturated non-plastic silt,” *Soils Found.*, vol. 49, no. 2, pp. 221–229, 2009.

[173] USEPA, “A Technology Assessment of Soil Vapor Extraction and Air Sparging. EPA/600/R-92/173.,” Cincinnati, OH, 1992.

[174] Wisconsin DNR, “Updated information and errata regarding guidance on design, installation and operation of in situ air sparging systems. File Ref. 4440.,” Madison, WI, 1995.

[175] Wisconsin DNR, “Guidance for design, installation, and operation of in situ air sparging systems. Publ-SW186-93,” Madison, WI, 1993.

[176] E. Holbrook, T.B., Bass, D., Boersma, P., DiGiulio, D.C., Eisenbeis, J., Hutzler, N.J., Roberts, “Vapor Extraction and Air Sparging Design and Application,” Annapolis, MD, 1998.

[177] S. S. Suthersan, J. Horst, M. Schnobrich, N. Welty, and J. McDonough, *Remediation Engineering: Design Concepts, Second Edition*. 2016.

[178] M. Okamura *et al.*, “In-situ desaturation test by air injection and its evaluation through field monitoring and multiphase flow simulation,” *J. Geotech. Geoenvironmental Eng.*, vol. 137, no. 7, pp. 643–652, 2010.

[179] M. Okamura and Y. Tomida, “Full scale test on cost effective liquefaction countermeasure for highway embankment,” in *Proceedings of Sixth Internal Geotechnical Symposium on Disaster Mitigation in Special Geoenvironment Conditions*, 2015.

[180] R. L. Johnson, P. C. Johnson, D. B. McWhorter, R. E. Hinchee, and I. Goodman, “An overview of in situ air sparging,” *Groundw. Monit. Remediat.*, vol. 13, no. 4, pp. 127–135, 1993.

[181] H. Bian, Y. Jia, I. Shahrour, A. Santini, and N. Moraci, “A potential cost effective liquefaction mitigation countermeasure: induced partial saturation,” in *AIP Conference Proceedings*, 2008, vol. 1020, no. 1, pp. 427–433.

[182] E. E. Bayat, M. K. Yegian, A. Alshawabkeh, and S. Gokyer, “A NEW mitigation technique for preventing liquefaction-induced building Damages during earthquakes,” 2009.

[183] E. Eseller-Bayat, M. K. Yegian, A. Alshawabkeh, and S. Gokyer, “Prevention of liquefaction during earthquakes through Induced partial saturation in sands,” *Geotech. Eng. - New Horizons 21st Eur. young Geotech. Eng. Conf.*, vol. 188, no. Figure 1, pp. 188–194, 2012.

[184] M. K. Yegian, E. Eseller, and A. Alshawabkeh, “Preparation and Cyclic Testing of Partially Saturated Sands,” in *Unsaturated Soils 2006*, 2006, pp. 508–518.

[185] J. Chu, “Solutions to sustainability in construction: some examples,” *Procedia Eng.*, vol. 145, pp. 1127–1134, 2016.

[186] Y. Huang and Z. Wen, “Recent developments of soil improvement methods for seismic liquefaction mitigation,” *Nat. Hazards*, vol. 76, no. 3, pp. 1927–1938, 2015.

[187] J. T. DeJong *et al.*, “Biogeochemical processes and geotechnical applications: progress, opportunities and challenges,” *Geotechnique*, vol. 63, no. 4, p. 287, 2013.

[188] J. Chu, V. Ivanov, H. Jia, G. Chenghong, M. Naeimi, and P. Tkalich, “Microbial geotechnical engineering for disaster mitigation and coastal management,” in *WCCE-ECCE-TCCE Joint Conference: Earthquake & Tsunami. Istanbul Turkey*, 2009.

[189] V. Rebata-Landa and J. C. Santamarina, “Mechanical effects of biogenic nitrogen gas bubbles in soils,” *J. Geotech. Geoenvironmental Eng.*, vol. 138, no. 2, pp. 128–137, 2012.

[190] V. Ivanov and V. Stabnikov, *Construction Biotechnology: Biogeochemistry, Microbiology and Biotechnology of Construction Materials and Processes*. Springer, 2016.

[191] J. He, “Mitigation of liquefaction of sand using microbial methods.,” 2013.

[192] N. Hamdan, E. Kavazanjian Jr, B. E. Rittmann, and I. Karatas, “Carbonate mineral precipitation for soil improvement through microbial denitrification,” *Geomicrobiol. J.*, vol. 34, no. 2, pp. 139–146, 2017.

[193] J. He, J. Chu, and V. Ivanov, “Remediation of liquefaction potential of sand using the biogas method,” in *Geo-Congress 2013: Stability and Performance of Slopes and Embankments III*, 2013, pp. 879–887.

[194] B. M. Montoya *et al.*, “Liquefaction mitigation using microbial induced calcite precipitation,” in *GeoCongress 2012: State of the Art and Practice in Geotechnical Engineering*, 2012, pp. 1918–1927.

[195] M. H. Weil, J. T. DeJong, B. C. Martinez, and B. M. Mortensen, “Seismic and resistivity measurements for real-time monitoring of microbially induced calcite precipitation in sand,” 2011.

[196] J. Chu, V. Ivanov, J. He, M. Naeimi, B. Li, and V. Stabnikov, “Development of microbial geotechnology in Singapore,” in *Geo-Frontiers 2011: Advances in Geotechnical Engineering*, 2011, pp. 4070–4078.

[197] E. A. Seagren and A. H. Aydilek, “Biomediated geomechanical processes,” *Environ. Microbiol. 2nd edn (eds R. Mitchell J.-D. Gu)*, pp. 319–348, 2010.

[198] J. He, J. Chu, and H. Liu, “Undrained shear strength of desaturated loose sand under monotonic shearing,” *Soils Found.*, vol. 54, no. 4, pp. 910–916, 2014.

[199] J. He and J. Chu, “Undrained responses of microbially desaturated sand under monotonic loading,” *J. Geotech. Geoenvironmental Eng.*, vol. 140, no. 5, p. 4014003, 2014.

[200] J. He, J. Chu, and L. Xin, “Undrained Behavior of Desaturated Sand under Static Loading,” in *Soil Behavior and Geomechanics*, 2014, pp. 34–42.

[201] E. Kavazanjian Jr and S. T. O’Donnell, “Mitigation of Earthquake-Induced Liquefaction via Microbial Denitrification: A Two-Phase Process,” in *IFCEE 2015*, 2015, pp. 2286–2295.

[202] J. He, J. Chu, S. Wu, and J. Peng, “Mitigation of soil liquefaction using microbially induced desaturation,” *J. Zhejiang Univ. A*, vol. 17, no. 7, pp. 577–588, 2016.

[203] E. Peng and D. Zhang, “Prevention of Liquefaction of Saturated Sand Using Biogas Produced by Pseudomonas stutzeri,” *DEStech Trans. Mater. Sci. Eng.*, no. ictim, 2017.

[204] S. O’Donnell, *Mitigation of earthquake-induced soil liquefaction via microbial denitrification: A two-stage process*. Arizona State University, 2016.

[205] Y. Li, “Mitigation of sand liquefaction using in situ production of biogas with biosealing,” pp. 1–48, 2014.

[206] J. Chu, “Innovation in disaster mitigation technologies,” in *Geotechnical Predictions and Practice in Dealing with Geohazards*, Springer, 2013, pp. 375–384.

[207] L. A. Van Paassen, C. M. Daza, M. Staal, D. Y. Sorokin, W. van der Zon, and M. C. M. van Loosdrecht, “Potential soil reinforcement by biological denitrification,” *Ecol. Eng.*, vol. 36, no. 2, pp. 168–175, 2010.

[208] S. Saleh-Lakha *et al.*, “Effect of pH and temperature on denitrification gene expression and activity in Pseudomonas mandelii,” *Appl. Environ. Microbiol.*, vol. 75, no. 12, pp. 3903–3911, 2009.

[209] G. Stanford, S. Dzienia, and R. A. Vander Pol, “Effect of temperature on denitrification rate in soils,” *Soil Sci. Soc. Am. J.*, vol. 39, no. 5, pp. 867–870, 1975.

[210] V. Stabnikov, V. Ivanov, and J. Chu, “Construction Biotechnology: a new area of

biotechnological research and applications," *World J. Microbiol. Biotechnol.*, vol. 31, no. 9, pp. 1303–1314, 2015.

[211] S. J. Vesper, L. C. Murdoch, S. Hayes, and W. J. Davis-Hoover, "Solid oxygen source for bioremediation in subsurface soils," *J. Hazard. Mater.*, vol. 36, no. 3, pp. 265–274, 1994.

[212] E. E. Eseller-Bayat, "Seismic response and prevention of liquefaction failure of sands partially saturated through introduction of gas bubbles," 2009.

[213] P. Horgue, C. Soulaine, J. Franc, R. Guibert, and G. Debenest, "An open-source toolbox for multiphase flow in porous media," *Comput. Phys. Commun.*, vol. 187, pp. 217–226, Feb. 2015.

[214] P. Forchheimer, "Wasserbewegung durch boden," *Z. Ver. Deutsch, Ing.*, vol. 45, pp. 1782–1788, 1901.

[215] M. I. J. van Dijke and S. E. A. T. M. van der Zee, "Multi-phase flow modeling of air sparging," *Adv. Water Resour.*, vol. 18, no. 6, pp. 319–333, 1995.

[216] J. P. Ziagos, R. J. Gelinas, S. K. Doss, and R. G. Nelson, "Adaptive forward-inverse modeling of reservoir fluids away from wellbores," Lawrence Livermore National Lab., CA (US), 1999.

[217] G. F. Pinder and W. G. Gray, *Essentials of Multiphase Flow in Porous Media*. Wiley, 2008.

[218] K. Aziz, K. Aziz, and A. Settari, *Petroleum reservoir simulation*. Applied Science Publishers, 1979.

[219] M. G. Gerritsen and L. J. Durlofsky, "Modeling fluid flow in oil reservoirs," *Annu. Rev. Fluid Mech.*, vol. 37, pp. 211–238, 2005.

[220] Z. Chen, G. Huan, and Y. Ma, *Computational methods for multiphase flows in porous media*, vol. 2. Siam, 2006.

[221] J. Bear, *Hydraulics of groundwater*. McGraw-Hill International Book Co., 1979.

[222] A. H. Demond and P. V Roberts, "An examination of relative permeability relations for two-phase flow in porous media 1," *JAWRA J. Am. Water Resour. Assoc.*, vol. 23, no. 4, pp. 617–628, 1987.

[223] J. Bear, "Dynamics of Fluids in Porous Media Elsevier New York Google Scholar," 1972.

[224] C. Marulanda, "A study of air flow through saturated porous media and its applications to in-situ air sparging," Massachusetts Institute of Technology, 2001.

[225] P. A. C. Raats and A. Klute, "Transport in Soils: The Balance of Momentum 1," *Soil Sci. Soc. Am. J.*, vol. 32, no. 4, pp. 452–456, 1968.

[226] P. Baveye and G. Sposito, "The operational significance of the continuum hypothesis in the theory of water movement through soils and aquifers," *Water Resour. Res.*, vol. 20, no. 5, pp. 521–530, 1984.

[227] A. LLoret and E. E. Alonso, "Consolidation of unsaturated soils including swelling and collapse behaviour," *Géotechnique*, vol. 30, no. 4, pp. 449–477, 1980.

[228] T. W. Lambe and R. V Whitman, "Soil Mechanics, 553 pp." John Wiley, New York, 1969.

[229] M. T. Van Genuchten, "A closed-form equation for predicting the hydraulic conductivity of unsaturated soils," *Soil Sci. Soc. Am. J.*, vol. 44, no. 5, pp. 892–898, 1980.

[230] A. Corey, "Pore - size distribution , in Indirect Methods for Estimating the Hydraulic Properties

of Unsaturated Soils (M.Th. van Genuchten et al., eds.),” *Univ. Calif.*, pp. 37–43, 1992.

[231] Y. Mualem, “Hydraulic conductivity of unsaturated porous media: generalized macroscopic approach,” *Water Resour. Res.*, vol. 14, no. 2, pp. 325–334, 1978.

[232] D. R. Nielsen, L. Luckner, M. T. van Genuchten, F. J. Leij, and L. J. Lund, “Theoretical aspects to estimate reasonable initial parameters and range limits in identification procedures for soil hydraulic properties,” in *Proc. Intl. Workshop on Indirect Methods for Estimating the Hydraulic Properties of Unsaturated Soils, edited by M. Th van Genuchten, FJ Leij, and LJ Lund, University of California, Riverside*, 1992, pp. 147–160.

[233] S. A. Jonasson, *Estimation of soil water retention for natural sediments from grain size distribution and bulk density.* 1991.

[234] J. W. Hopmans, M. E. Grismer, J. Chen, Y. P. Liu, C. Agreement, and B. K. Lien, “Parameter estimation of two-fluid capillary pressure saturation and permeability functions,” *Natl. Risk Manag. Res. Lab. Off. Res. Dev. USEPA*, 1998.

[235] V. Navarro, “Modelo de comportamiento mecánico e hidráulico de suelos no saturados en condiciones no isotermas,” *Univ. Politécnica Cataluña*, 1997.

[236] R. Juncosa, “Modelos de flujo multifásico no isotermo y de transporte reactivo multicomponente en medios porosos,” Universidad Politécnica de Madrid, 1999.

[237] S. Olivella Pastallé, *Nomsothermal multiphase flow of brine and gas through saline media*. Universitat Politècnica de Catalunya, 1995.

[238] H. R. Thomas, “Model development and validation of the Thermo-hydraulic-mechanical and Geochemical code development and applications. Thermal- Hydraulic-Mechanical and Geochemical behaviour of the clay barrier. Final report Thermo-hydro-mechanical code development and a,” 1995.

[239] W. S. Clayton, “A field and laboratory investigation of air fingering during air sparging,” *Groundw. Monit. Remediat.*, vol. 18, no. 3, pp. 134–145, 1998.

[240] E. F. Garcia Aristizabal, “Numerical Analysis of the Rainfall Infiltration Problem in Unsaturated Soil,” Kyoto University, 2010.

[241] D. P. Ahlfeld, A. Dahmani, and W. Ji, “A conceptual model of field behavior of air sparging and its implications for application,” *Groundw. Monit. Remediat.*, vol. 14, no. 4, pp. 132–139, 1994.

[242] R. D. Norris, *Handbook of Bioremediation*. Taylor & Francis, 1993.

[243] M. C. Marley, D. J. Hazebrouck, and M. T. Walsh, “The application of in situ air sparging as an innovative soils and ground water remediation technology,” *Groundw. Monit. Remediat.*, vol. 12, no. 2, pp. 137–145, 1992.

[244] M. Chen, R. E. Hinkley, and J. E. Killough, “Computed tomography imaging of air sparging in porous media,” *Water Resour. Res.*, vol. 32, no. 10, pp. 3013–3024, 1996.

[245] C. R. Elder and C. H. Benson, “Air channel formation, size, spacing, and tortuosity during air sparging,” *Groundw. Monit. Remediat.*, vol. 19, no. 3, pp. 171–181, 1999.

[246] P. D. Lundegard and G. Andersen, “Numerical simulation of air sparging performance,” *Proc. Pet. Hydrocarb. Org. Chem. Gr. Water Prev. Detect. Restor.*, pp. 461–476, 1993.